Comparison of Lumbar Disc Degeneration, Fusion and Disc Arthroplasty on Biomechanics of Adjacent Segment

BY

SITHICHAI CHAICHANAVITCHAKIJ
B.S., Chulalongkorn University, Thailand, 2011

THESIS

Submitted as partial fulfillment of the requirements
for degree of Master of Science in Bioengineering
in the Graduate College of the
University of Illinois at Chicago, 2015

Chicago, Illinois

Defense Committee:

Thomas J. Royston, Chair
Raghu N. Natarajan, Advisor
Susan Renner, University of St. Francis

ACKNOWLEDGEMENTS

I would like to sincerely express my gratefulness to Professor Raghu N. Natarajan for his continued supports in my academic study and related research, for his patience and motivation. I would also like to thank Dr. Thomas Royston and Dr. Susan Renner for their knowledge and expertise in their respective fields of specialty.

I also thank Ayushmita De, PhD candidate, my fellow labmate in for the simulating discussion and continuous encouragement and for all the fun we have had in the last two years.

Lastly, I would like to acknowledge the Department of Bioengineering at the University of Illinois at Chicago and the Department of Orthopedic Surgery at Rush University Medical Center for providing the resources I needed to achieve my goals.

TABLE OF CONTENTS

TABLE OF CONTENTS (continued)

LIST OF TABLES

LIST OF FIGURES

LIST OF FIGURES (continued)

FIGURE PAGE

SUMMARY

Back pain is an unavoidable discomfort that is very common in the United States. It happens naturally while aging and may be expedited for those who do laborious work or are smokers. In severe cases, surgical treatments are needed. Spinal fusion has been a "gold standard" for treating back pain. Spinal fusion is a procedure that involves fusing two vertebral discs by inserting bone graft where the intervertebral disc has deteriorated; this reduces motion at those vertebral levels. However, the adjacent vertebras may start to compensate for the loss in motion, potentially causing future problems. Another surgical treatment is disc arthroplasty, a surgical treatment that preserves motion at the problematic level by using an artificial disc.

In the experiment I designed, CAT Scan based-data on the anatomical structure of spine was applied. A three-dimensional finite element model of lumbar spine was created using the 3D finite element software called ADINA. Material properties were taken from literature and the model was validated against cadaveric results. The study included analysis of motion, facet forces and von Mises stress at the adjacent segments. This study started with a single level degeneration at L5S1 that caused the motions at the adjacent segment (L4L5) and also the skipped segment (L3L4) increased in motion. Increases in facet forces and von Mises stress at the adjacent segments were observed as the increase of grade of degeneration. However, stress at the degeneration disc reduced with the increase of degeneration. Consequently, a single level degeneration in a normal spine will lead to spinal fusion or disc replacement at the adjacent segments (and maybe at the skipped segments). The

two options of the surgical treatment, spinal fusion and disc replacement, were studied. A comparison of changes in adjacent segment motions in the lumbar spine with single level fusion and single level disc arthroplasty was studied. Both of these surgeries were assumed done at the same vertebral segment level. The rest of the intervertebral discs were assumed to be normal (grade II). The hybrid approach was used in this analysis.

Lower rotation at the adjacent segments was seen in the spine with disc arthroplasty under flexion and extension. Under torsion and lateral bending, the rotation of the adjacent segments slightly increased. However, the rotations at the adjacent segments in the spine with fusion increased under all tested loading conditions. In a presence of disc arthroplasty, facet forces and von Mises stress at the adjacent segments reduced respect to an intact model while increase of facet force at the adjacent segments was observed in the spine with fusion. The study was repeated on lumbar spine with disc arthroplasty (L4L5) with a single degeneration of adjacent segment (L5S1). Rotation at the adjacent segments did decrease under loading of flexion and extension. Facet forces and von Mises stress on the nucleus and annulus were decreased in grade II. However, the trends increased as the grades of degeneration increase. On the other hand, decrease in rotation under lateral bending and torsion was observed at the implant level and the lower segment while the rotation in the upper segment increased. The implant level showed the increase in rotation under flexion and extension. Especially, under extension moment, the rotation at the implant level increased twice as much as the normal disc. Stress of annulus and nucleus under lateral bending and torsion was higher respect to the spine with degeneration alone.

The following conclusions are achieved from the current study

1) A single-level degeneration disc leads to increase in motion, facet forces and von Mises stresses at the adjacent segments and the skipped segment.

2) Lower motion, facet forces and von Mises stresses at the adjacent segment was observed in a spine with disc arthroplasty while higher motion, facet forces and von Mises stresses at the adjacent segments were seen in a spine with fusion.

3) In the lumbar spine with disc arthroplasty and degenerated adjacent segment, as the increase of grade of degeneration, decreases in motion, facet forces and von Mises stress at the adjacent segment were observed under flexion and extension while increase in motion and von Mises stresses at the adjacent segments was seen under lateral bending and torsion.

1) Introduction

1) Anatomy of the Spine

The human spine has three very important roles. Firstly, it supports the weight of the upper body. Secondly, it provides flexibility in a variety of movements. Lastly and most importantly, it protects the spinal cord, which contain nerves from the brain and branches to different parts of the body. There are five regions of the spine (as shown in Figure 1-1): cervical, thoracic, lumbar, sacrum and coccyx. Each region has a different vertebral shape that is responsible for accommodating different motions.

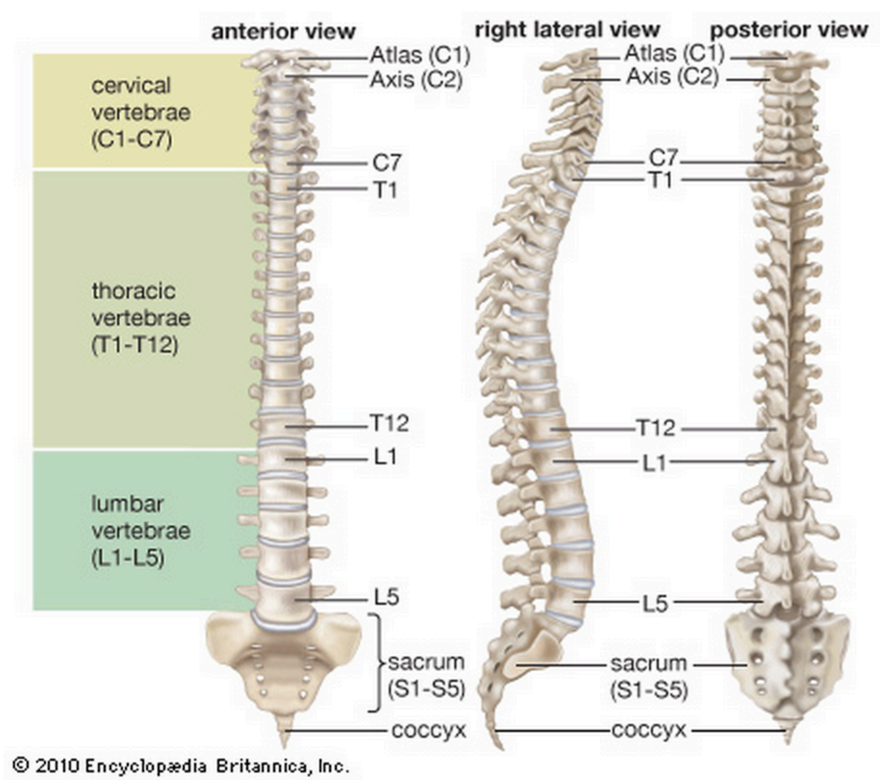

Figure 1-1 shows anterior, posterior and right lateral view of the spine (http://www.britannica.com)

Cervical region is the most superior and extends downward from the skull and contains 7 vertebrae. The cervical spine supports the head and the vertebral bodies are relatively small, except for C1, which does not have a ventral body. C1 is the first vertebra of the spinal column and is known as the Atlas. Ct and C2 (Axis) not only support the skull, but also attach the head to the neck. C2 to C6 (Figure 1-2), bifid spinous processes increase the surface area where the mucles and ligaments combine. C7 is a transition between cervical and thoracic region; therefore, C7 has characteristics of both the cervical and thoracic. The large vertebral foramen accommodates the spinal cord while the two transverse foramens do the same for the nerves, vertebral artery and vertebral vein.

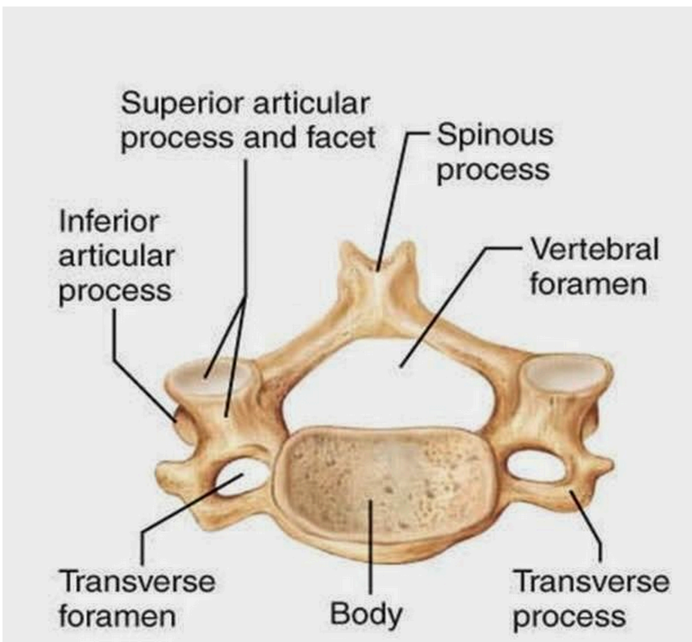

Figure 1-2 Cervical vertebra body (medicalfreakz.blogspot.com)

Thoracic region is inferior to the cervical region and superior to the lumbar region and consists of 12 segments. The smallest vertebra is T1 (the first vertebra in the thoracic region) while the largest vertebra is T12 (the last vertebra in the thoracic region). There is no transverse foramen in thoracic regions as the nerves pass through the intervertebral foramen. Spinal cord also passes through vertebral foramen, similar to the setup in the cervical region as shown in the Figure 1-3. There are costal facets (costovertebral joints) on each side of vertebral bodies connecting the ribs. The ribs provide space and protection to many vital organs, including the heart and lungs. This is one of the reasons why the thoracic region has limited flexibility.

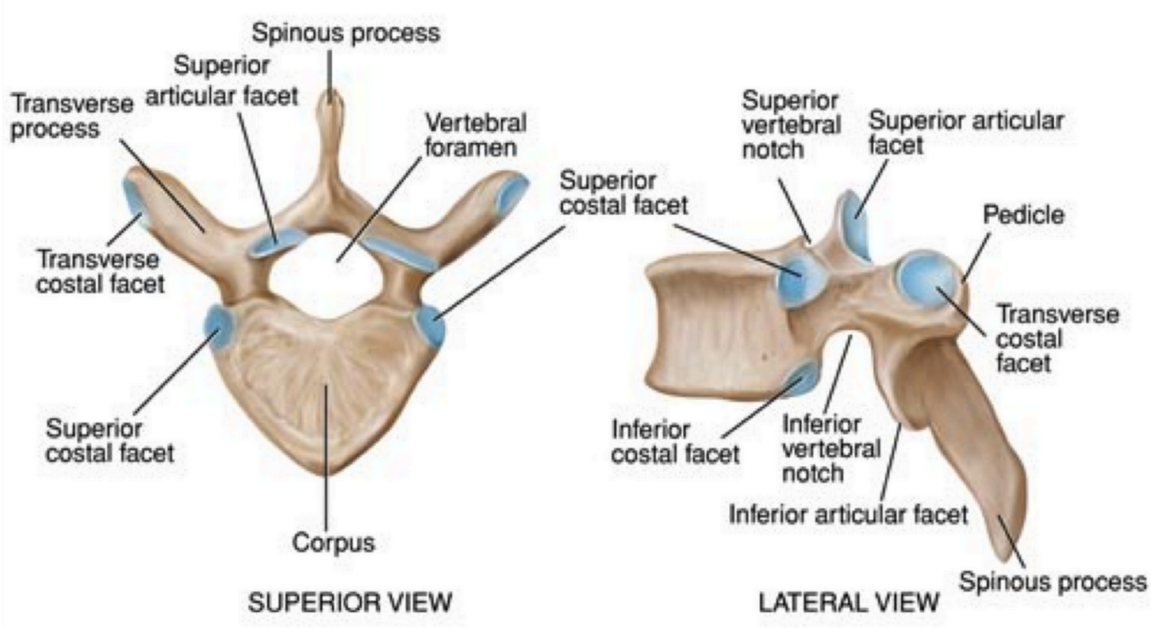

Figure 1-3 Thoracic vertebral body (medicalfreakz.blogspot.com)

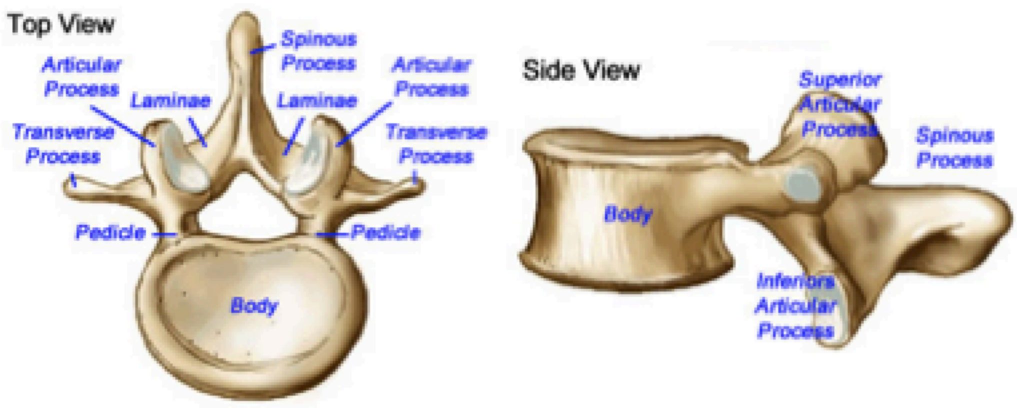

Figure 1-4 Lumbar Vertebral body (www.kidport.com)

Figure 1-4 shows schematic of a lumbar vertebra. The lumbar region consists of 5 vertebras and is located at the lower back. The vertebral bodies are larger and stronger compared to vertebras in other regions. They support the upper body weight and allow for twisting and bending movement. The bottom two segments, L4 and L5, bear the most body weight, and allow for a wide angle of rotation and is the reason why there is curvature in the spine. Therefore, these levels are more prone to injury and degradation (Moore, 2011). The nerves and spinal cord pass through the intervertebral foramen like they do in the thoracic region. This study is particularly focusing on the lumbar region.

Sacrum and Coccyx are the most inferior sections of the spine. As an adult, levels in the above two sections are fused together in one single bone. The sacrum is wedge shaped and supports the upper body weight and spread to the pelvis and legs. Coccyx, or tailbone is found in the tail of most mammals; however, in humans, there is no external tail and it anchors muscles in the pelvic region.

Intervertebral discs are located between the vertebral bodies and mainly allows for movement in the spine (Figure 1-5). Motions include flexion, extension, lateral bending, and torsion (twisting). The discs make up about 30% of the entire height of the spine. The smallest discs are found in the cervical region while the largest discs are found in the lumbar region. In general, intervertebral discs primarily support compressive force and act as shock absorbers. Therefore, the disc has higher elastic properties than any other material in the spine. The discs consist of two parts: annulus fibrosus and nucleus pulposus. The nucleus is located in the center and the annulus fibrosus surrounds it. Annulus fibrosus is ring-like and consists of type I and type II collagen. Numerous layers of fibrocartilage (mostly of type I collagen) are stacked horizontally, creating concentric rings called lamellae. This arrangement increases strength and withstands compressive loads. The nucleus pulposis, an inner gel-like, is rich in type II collagen and water (80% of the content). It acts as a hydrostatic unit providing uniform distribution of pressure throughout the disc. When there is a load on the disc, it creates a hydrostatic pressure inside the disc and squeezes water out to balance the stability of the spine. This process is reversible; in other words, water flows in and out of the disc. Yet, hydration of the discs will decrease the ability to withstand the load.

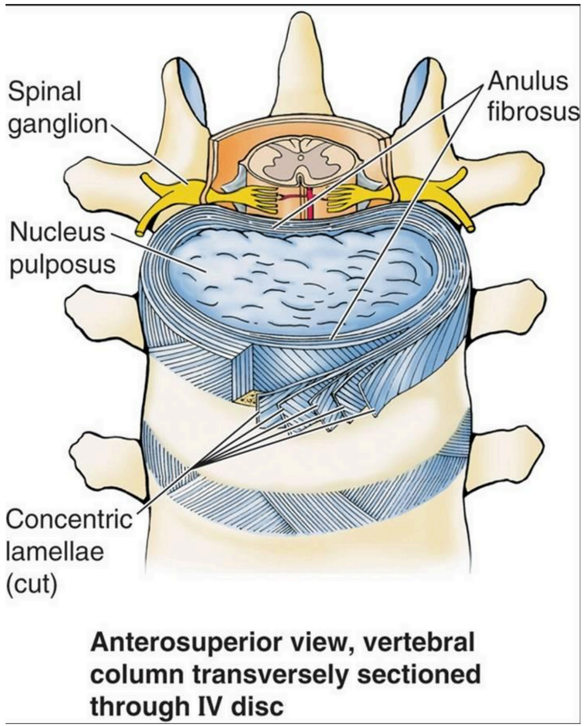

Figure 1-5 shows an intervertebral disc. The ring-like is annulus fibrosus and nucleus pulposus is located inside the ring. (www.studyblue.com)

Facet capsular joint consists of connective tissue connecting the superior and inferior facets of a vertebral pair. Each vertebra has four facet joints, two on the top and two on the bottom. The function of a facet joint is to limit spinal motion and transfer loads from the upper body to the lower body. Different regions of the spine have orientations that are distinct at each of facet joint (Figure 1-6)(Hamill & Knutzen, 2009). In the cervical region, the facet joints orient 45 degrees (with respect to the transverse plane and parallel to the frontal plane) and result in six possible motions (flexion, extension, left lateral bending, right lateral bending, left torsion and right torsion.) Facet joints in the thoracic region orient in 60 degrees (with respect to the transverse plane and 20 degree to the frontal plane) but limit movement to just lateral bending and torsion (there is no flexion or extension). Lastly, in the lumbar region, the facet joints angle perpendicular to the transverse plane and 45 degrees to the frontal plane, permitting motion in flexion, but not in extension or torsion.

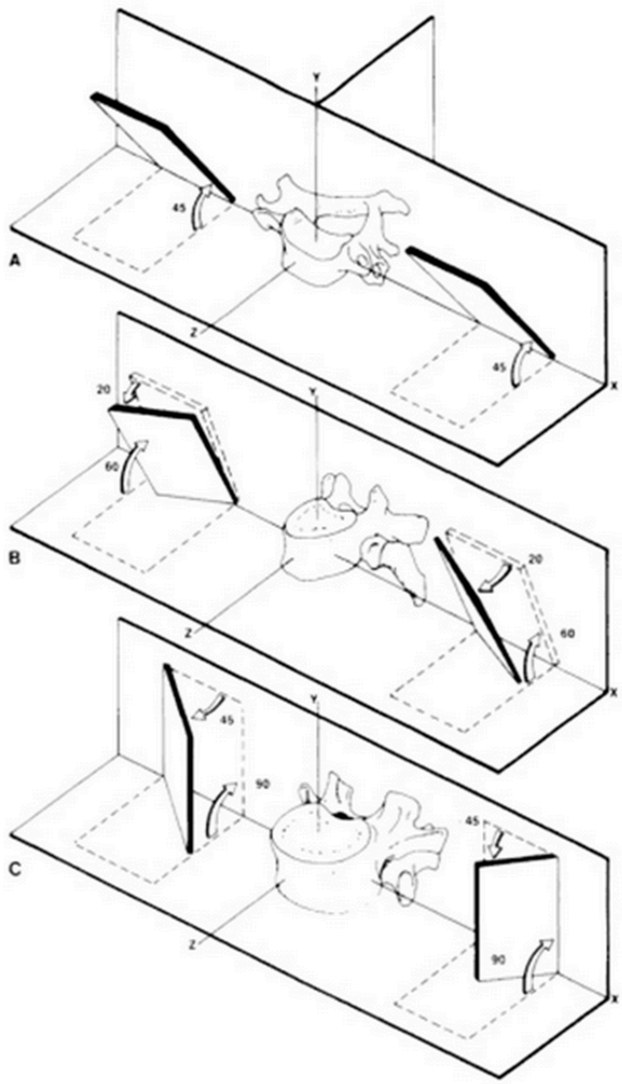

Figure 1-6 A) Facet joint orientation in vervical region. B) Facet joint orientation in thoracic region. C) Facet joint orientation in lumbar region. (http://www.wikiradiography.net)

2) Disc Degeneration

Due to wear and tear, material properties of the intervertebral disc in the spine worsen. Aging is one of the main inevitable factors that cause degeneration of the intervertebral discs (Ghosh, 1988). Unfortunately, everyone will face degeneration in the spinal disc; however, not everyone will suffer from its consequences. It occurs more often and sooner in people who consistently do heavy physical work or consume nicotine in one form or another (Oda, Matsuzaki, Tokuhashi, & Wakabayashi, 2004), (Fogelholm & (deceased), 2001). Degradation can take place throughout the spine. And even worse, the neighboring discs have to support unseen or irregular loading and unfamiliar rotations. Due to a wide range of motions and heavy loads, the lower lumbar region tends to have degenerative issues more frequently than other regions, specifically at L4L5 or L5S1 level (Moore, 2011). As a result of disc degeneration, intervertebral discs start thinning, the endplates are harder to locate in the MRIs, and annulus fibrosus and nucleus pulposus become less pliable (Naidich, 2011). This defines disc degenerative disease. Disc degenerative disease occurs when the disc's ability to distribute loads throughout the disc gradually deteriorates. Not only does it diminish the ability to act as a shock absorber, but it also increases stress at the facet joints; another problem that accumulates as a result of disc degeneration. Degeneration of intervertebral discs in lumbar spine is one of the most common reasons that cause lower back pain (Freemont, Watkins, Le Maitre, & Jeziorska, 2002).

3) Lower Back Pain

Back pain can be attributed to biological changes present in the intervertebral discs or other spinal disorders, including disc degeneration, disc herniation, facet arthroplasty, spinal stenosis, and spondylolisthesis (Figure 1-7). Naturally, the lumbar spine contains strong vertebras that are connected by facet capsular, ligaments, and muscles and is cushioned by the intervertebral disc. The lumbar spine supports the weight of the upper body and allows the spine to achieve a wide range of motion. However, lower back pain comes into the picture when the intervertebral discs experience heavy loads, abnormal ranges of movements and harmful chemicals. Thus, the lumbar spine is more prone to injuries as it bears much of the weight and movement. As mentioned above, one of the major roles of the spine is to guard the spinal cord. A bulging or herniated disc irritates the nerves in the spinal cord and could result in pain. Reoccuring pain will limit movement that is required to accomplish regular tasks. The severity of back pain can increase with time if it is not properly addressed. In addition, pain could spread down the leg as the sciatic nerve may be affected if the position of the spinal cord is compromised.

So far, there are two major strategies to treat degeneration; surgical and nonsurgical. To determine the right treatment, it is mandatory that patients get the correct diagnosis. A history of injuries, relevant complications, and symptoms are important data to analyze. Usually, physicians offer a traditional approach – noninvasive methods to treat pain. It could be as simple as physicians recommending limiting regular activities or consulting physical therapy. When noninvasive approaches fail, surgical treatment will be considered. In non-severe cases, dynamic stabilization devices are a popular alternative. Severe cases include spinal fusion and disc arthroplasty (Ghosh, 1988).

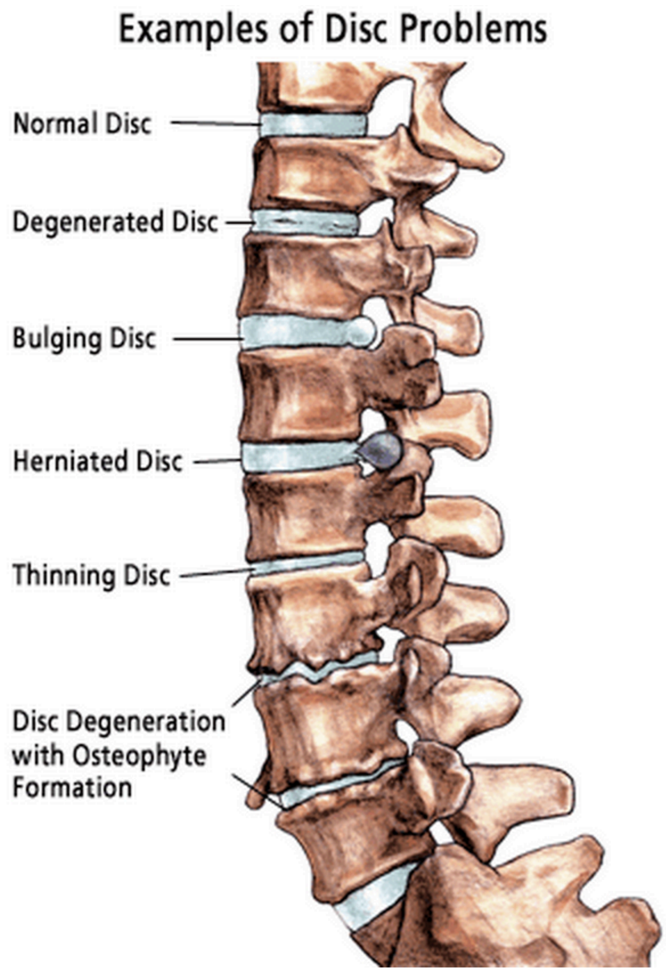

Figure 1-7 shows various types of disc problems.

(www.spineuniverse.com)

4) Lumbar Spinal Fusion

Lumbar spinal fusion is a surgical approach that aims to reduce the pain caused by irregular motion or instability of the lumbar disc, spinal deformity, correcting curvatures or fractured vertebrae. The idea of spinal fusion is to fuse one or more vertebrae together in order to freeze the motion in that particular level; this is known known as spondylodesis or spondylosyndesis (Figure 1-8). Lumbar spinal fusion has been reported to be a successful method that reduces pain (France, Yaszemski, Lauerman, & Cain, 1999).

Autografts and or allografts are be used in combination with the body's natural bone for re-growth. Autografts are harvested from the patient while allografts are harvested from a cadaver. Bone grafts are set in the body to form and fuse respective sections of the vertebrae. Both types of bone graft provide calcium scaffolding, which encourages bone growth. However, allografts are less often used in fusion because they are not living cells and may have biocompatibility issues. The graft can be placed anteriorly or posteriorly or in a combination of both.

However, there are some complications of spinal fusion. The segments that are adjacent to the fusion level will have to compensate for loss in movement since the total rotation of the spine will have to remain the same for every activity (Strömqvist, Johnsson, & Axelsson, 1997). Patients are most concerned with regaining the ability to return to regular activities after surgery. As a result, the rest of the discs have to compensate for movement to achieve the necessary rotation. Consequently, an increase in intradiscal pressure and motion at the adjacent levels are found(Weinhoffer, Guyer, & Herbert, 1995), (C. Lee & Langrana, 1984) (Luk, Lee, & Leong, 1987),(Lehmann, Spratt, & Tozzi, 1987). These finding suggest the coming of future problems due to this compensation.

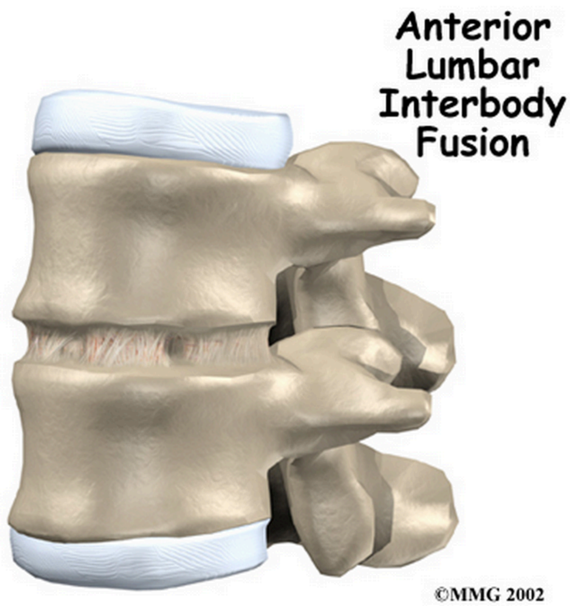

Figure 1-8 Lumbar Spinal Fusion

(http://www.orthogate.org/patient-education/lumbar-spine/anterior-lumbar-interbody-fusion)

5) Adjacent Segment Degeneration Disease (ASDD)

Once, degeneration takes place, an adjacent segment appears to degenerate whether the degeneration at the original level is treated or not. This is known as Adjacent Segment Degeneration Disease (ASDD.) Nonetheless, there is no clear conclusion whether the degeneration is a result of natural wear and tear or if it is associated with fusion (Hilibrand & Robbins, 2004).

There are several obvious disadvantages of spinal fusion. Increased stiffness and limited to no movement at the fused segment are some major concerns for the fusion approach. Because the fusion approach fuses two levels of vertebrae together, other levels, including the adjacent levels, of the spine have to compensate for the loss in movement from the fused levels. Consequently, the adjacent segments have to experience abnormal rotations. Many studies have implicated that fusion accelerates degeneration in the adjacent segments (K. Y. Ha, Schendel, Lewis, & Ogilvie, 1993; C. K. Lee, 1988; Park, Garton, Gala, & Hoff, 2004; Shono, Kaneda, Abumi, & McAfee, 1998).

There is follow-up data supporting the claim that fusion leads to adjacent segment degeneration (Pellise Ferran, Hernandez, Vidal, & Minguell, 2007). According to Ferran's group, they analyzed long-term (average of 7.5 years) radiographic changes in unfused lumbar segments after a posterolateral lumbar fusion. Total of 212 unfused segments from 62 patients were analyzed. The study showed that there was no change observed at the segment below the fusion; however, there was significant loss in disc height detected in all unfused segments above the fusion. They concluded that the major parameter that caused the decrease in disc height was the location of the adjacent unfused segments.

Shujie's group did finite element analysis on L3 to L5 model (Per, Hans, Adel, Yiang Xiao, & Rune, 2009). Three different grades of degeneration were varied at L4L5 level. They imitated the fusion procedure, specifically the anterior lumbar fusion approach. The result showed that the intradiscal pressure, intersegmental rotation range and Tresca stresses at the adjacent levels were higher than in the normal case. The conclusion advocated the claim that the adjacent upper segment was disturbed when fusion was done in the degenerated disc.

6) Disc Arthroplasty

One of the most promising results from artificial disc replacement or total disc replacement is to reduce or prevent the adjacent segment degeneration, also known as “motion sparing” (Cunningham et al., 2008). This is one of the surgical treatments (arthrodesis and disc arthroplasty) that attempt to cure back pain, besides spinal fusion and dynamic stabilization. The goal is to eliminate the pain caused by degenerative disc disease. Disc implantation will restore movement at the degenerated level in all planar directions. Therefore, the adjacent levels do not need to compensate for the operated levels. In other words, this procedure aims to overcome a shortcoming of fusion, including ASDD (K. Y. Ha et al., 1993; C. K. Lee, 1988; Park et al., 2004; Pellise Ferran et al., 2007; Shono et al., 1998).

Some research groups are trying to better design an artificial disc by adding edges and curves to constrain the rotation of the conventional artificial disc (Wang, Zhang, Sadeghipour, & Baran, 2013) (Noailly, Lacroix, & Planell, 2005). However, the most popular design of the artificial disc is similar to the mechanics of other joint replacements: a ball and socket. This research aims to find the affect of a ball and socket type implant.

Artificial disc replacements are mostly done in lumbar or cervical spine. Thoracic region do not allow for much movement; therefore, vertebrae and soft tissues do not degrade as fast as they do in the other two regions. In general, disc arthroplasty is done by anterior approach, which anterior longitudinal ligament at that particular level has to be scarified. Most of the disc content will be removed but the lateral and posterior annulus will be remained.

Most of the recent research experiments analyzed the motion, pressure and contact forces when an implant was inserted into the intervertebral space, while the rest of the intervertebral discs remained normal (grade2). This gives us an idea of how the implant behaves and helps physicians in solving future pain issues. In addition, we can compare the motion in the intact spine and estimate if the implant will hinder or support the adjacent level. However, this is not always the case in the practical world. As mentioned above, when one intervertebral disc level is degenerated, the adjacent levels tend to have degeneration problems much sooner than later. One of the most important indications is whether a patient has to return for an additional surgery. In other words, it is possible for two consecutive degenerated levels with varying severities. We would like to seek a way to estimate the outcome of disc arthroplasty and degenerated discs in one spine. Nevertheless, there is no research that is working on how disc arthroplasty behaves when there is degeneration and an implant present at the adjacent level.

7) Thesis Goals

To study the biomechanical responses of lumbar spine (L1S1), when there is a ball-and-socket implant present and studying the adjacent segments to by using a refined poro-elastic finite element model.

The following were objectives.

1) To determine the effect of disc degeneration on adjacent segments in a normal (grade II) spine.

2) To compare the effect of disc implant and fusion on adjacent segments in a normal (grade II) spine.

To determine the effect of disc arthroplasty on the adjacent segments in a lumbar spine with disc

2) Background and Related Literature

1) In Vitro Studies

A) Segments with Intervertebral Disc Arthroplasty

In-vitro intervertebral disc research was mainly done on cadavers. Generally, spines of human cadavers were fixed at the bottom while the loadings were applied at the top. The direction of the forces depends on loading conditions. Panjabi M. did an in-vitro biomechanical study, testing one- and two-level ProDisc-L VS one- and two-level fusions (M. Panjabi, Henderson, Abjornson, & Yue, 2007). The study was done on six fresh human cadaveric lumbar spines (T12 to S1). The loading conditions included flexion, extension, left and right lateral bending, and left and right axial rotation. All the loading conditions were tested on each of the 5 cadaveric constructs. The study concluded that one- and two- level disc arthroplasties produced negligible effects on the adjacent levels for all the loading conditions. However, one- and two- level fusions produced considerable changes in adjacent levels for all the loading conditions. Lastly, a one level disc arthroplasty and a one level fusion showed similar results

A semi-constrained Activ L (a ball and socket) artificial disc was tested on five human cadaveric spines (L2S2) by (S.-K. Ha, Kim, Kim, & Park, 2009). The study was tested in all 6 loading conditions of flexion, extension, lateral bending and rotation and a control loading was applied. The control loading is technique is applied when the same amount of moment is needed for both the intact and implanted models. The disc space between L4L5 was where the implant was placed. 400 N of follower load was applied throughout the loading. Results showed that the range of axial rotation decreased significantly after Activ L arthroplasty was inserted. In contrast, Activ L arthroplasty showed more ROM in flexion and lateral bending than the intact model did. Disc pressure of the inferior adjacent level decreased however, it remained the same for the superior adjacent level for all loading conditions when compared to values of the intact model.

Ha's group and Hitchon's group did an in vitro study on seven human cadaveric spines (L2S1) (Hitchon, Eichholz, Barry, & Rubenbauer, 2005). Maverick artificial disc is a ball and socket disc (Medtronic Sofamor-Danek, Memphis, TN) that was used in this study and inserted in L4L5 level. Pure moments were applied in flexion, extension, lateral bending, and axial rotation. They observed that the spine with the implanted Maverick artificial disc showed higher rigidity than the intact spine model. Similar to the above experiment, their group also applied the loading control approach to conduct the experiment. The result showed that increased forces were applied on cadavers with an implanted artificial disc than for cadavers without any implants in order to achieve the same rotations in each loading condition.

2) In Vivo Studies

A) Segments with Intervertebral Disc Arthroplasty

In vivo studies are mainly focused on patients who have had disc arthroplasty surgery in the lumbar spine. After surgery, patients are usually able to return to their normal daily activities without physical restrain. Most researchers have followed-up with patient data over an extended period of time. Oswestry Disability Index (ODI) scores and Visual Analogue Scale (VAS), pain scores were also used to evaluate the results.

Gregory G. Knapik et al., conducted a study comparing kinematics and biomechanical loadings of the lumbar spine between an intact spine and the same spine with a total disc replacement at L5S1(Knapik, Mendel, & Marras, 2012). Range of motion was observed while the subject executed bending and lifting during normal daily activities. The implant level showed larger range of motion than it did in the intact spine. In flexion and extension, the motion increased at the higher lumbar level; however, for lateral bending and twisting rotation, the motion was less than it was in the intact spine.

Delamarter R. et al. reported results from 53 patients, including 35 patients who had a disc replacement and 18 patients who had a spinal fusion (Delamarter, Fribourg, Kanim, & Bae, 2003). The improvement was evaluated based on VAS and ODI scores. Six weeks post-surgery, patients with disc replacements showed more improvement than patients with a spinal fusion did 6 to 12 weeks post-surgery. However, 6 months, post surgery, no signs of major distinction were apparent.

Tropiano P. et al. did a follow-up study on 64 patients who had either a single or multiple-level implantation for Total Disc Replacement, TDR, (Tropiano, Huang, Girardi, Cammisa, & Marnay, 2006). The average follow-up time was 8.7 years. The research shows significant improvements in back pain, disability, radiculopathy and Stauffer-Coventry scores. 60% of the patients had excellent results while only 25% had poor results. Gender or multi-level operations did not affect the results much, however patients younger than 45 years of age and had prior lumbar surgery experienced a worse outcome.

Putzier et al. reported clinical and radiographical results that studied average follow-up time of 17 years (Putzier et al., 2006). As Charité designed the first artificial disc, there was ample research over a long period of time studying their quality. 71 patients were treated with type I-III (of possible 84) Charité discs. The evaluation was based on ODI and VAS scores. Radiographs show that there were no major dissimilarities between the three types of implants. 11 percent of patients underwent reoperation. In the functional implants, there was no adjacent segment degeneration observed. However, there is still little knowledge on long-term usage of total disc replacement.

Post surgery follow-ups, comparing Charité and ProDisc showed interesting results (Shim, Lee, Shin, & Kang, 2007). This study compared data from 61 patients who had total disc replacements. There were 33 patients who had Charité replacements and 24 patients who had ProDisc replacements. They also compared ODI and VAS pain scores for both of the two discs. The result showed there was no significant difference between those scores. Also, there were no significant differences in the degradation of facets and adjacent levels above the index level.

In summary, there were some of researchers who claimed that disc arthroplasty helped solving back problems (Blumenthal, Ohnmeiss, Guyer, & Hochschuler, 2003; Delamarter et al., 2003; Lemaire et al., 1997; Shim et al., 2007; Tropiano et al., 2006); however, there were complications that surfaced after long-term implantation, including reoperation and facet-joint issues (Ross, Mirza, Norris, & Khatri, 2007). We still have insufficient knowledge on the kinematics and performance of the implants since in vivo follow-up studies with long-term time intervals are time consuming to execute. Therefore, an alternative study with finite element analysis is proposed.

3) Related Existing Finite Element Studies

Finite element analysis (FEM) a powerful alternative approach to predicting and analyzing information about spine biomechanics. It has been one of the most popular methods of understanding biomechanical problems. Unlike in vivo and in vitro studies, FEM circumvents the experimenting process and estimates outcomes of scenarios when applying different parameters or loading conditions. For example, Jonathan N. Grauer et al. compared a two-level Charité artificial disc replacement with a fusion with single-level disc replacement and analyzed the outcomes (Grauer, Biyani, Faizan, & Kiapour, 2006). A large number of factors can be controlled as well as varied. The analysis can become complicated, however FEM simplifies the procedures to produce real-life results. The results can be obtained and analyzed much faster than actually running an experiment with a fresh sample. However, FEM has its own complexities. Most of the FEM models are simplified versions of a real-life model. Therefore, the more realistic the quality of the FEM model is more accurate the results are. One of the best ways to produce an accurate model is to use a radiograph as a reference. Wang Z. proposed a method to combine CT and MRI based data to construct a 3D FEM (Li & Wang, 2006). He received raw radiographic data and CT scans. Then the data was constructed in CTK software and imported to an FEA program. Displacement and Von Mises stresses were obtained during post processing mode.

Jérôme N.'s group did a finite element study on L3L5 lumbar spine (Noailly et al., 2005). The study tried to find the biomechanical changes in L3L4 level after having an implant at L4L5 level. The artificial disc was modeled from Institute of

Composites and Biomedical Materials (National Research Council, Naples, Italy). Unlike all other available artificial discs that were ball and socket types, the one they were using in their research had the worked similarly to the “real” disc. The size of the implant was designed to perfectly fit the shape of the physiological disc. They have separated the implanted models into 2 categories. The first model has a small gap between the artificial disc and the vertebrae, which over time, is filled with osseous material called the noncoherent model. The endplate and artificial disc are completely bounded in the second model and no gap is present. In other words, right after surgery, it is expected to be the noncoherent model and after the bone grows, it is expected to be the coherent model. In this study, the changes were observed and compared between the implanted model and the intact model. Loading conditions included compression, flexion, extension and axial rotation. The analysis showed that the motion of L3L4 level was only slightly influenced by the existence of the implant at the L4L5 level. However, the mobility of the implant in flexion and extension decreased for both noncoherent and coherent models. However, the noncoherent model exhibited twice as much mobility as the coherent model.

One of the most common types of artificial discs is a ball and socket type. This is the most common joint type in the human body. However, the designs of the implants are dissimilar depending on their roles in the body.

Vijay K.’s group designed a finite element study to find the effects of charité artificial disc (ball and socket type) on the implanted and adjacent segments (Goel, Grauer, Patel, & Biyani, 2005). The study was on L3S1 spine model, and the artificial disc was inserted at L5S1 level. They observed and compared the mobility of both intact and implanted models by the hybrid approach and load control approach. The method of implant insertion mimicked the surgical method including removal of the anterior longitudinal ligament, nucleus, and anterior portion of the annulus at L5S1 level. Posterior and lateral portions of the annulus were left intact. The friction coefficient of the implant was estimated at 0.02. The implanted model was subjected to 400N of axial compression and 10.6Nm of the load control. In the hybrid approach, the models required just 9.6 Nm of moment in flexion and 7.3 Nm in extension to reach the rotation of the intact model at L3S1. In load control, at the artificial disc level, the motion in flexion and extension increased by 26% and 98%, respectively. The motion in L3L4 level and L4L5 slightly decreased for both flexion and extension. For the hybrid approach, the total rotation across L3S1 was the same in both intact model and implanted model. However, at the artificial disc level, the motion increased by 18.9% and 43.4% in flexion and extension, respectively. However, at the L3L4 level, flexion and extension decreased by 7% and 24%, and at L4L5 level, the motion was decreased by 12% and 28.6%, respectively.

Similarly to Vijay's group, Rohlmann A. conducted a study using 3D nonlinear finite element model (L1 to L5) (Rohlmann, Zander, & Bergmann, 2005). A ball-socket type of implant was put in L3L4 level. They were looking for the optimal location of the implant insertion and the need of lateral annulus. Loading conditions included compression (standing post), flexion, extension and axial rotation. In this study, he suggested that lateral annulus should be preserved in every possible way. It would help stabilize the spine in all motions. In addition, the position of the implant influenced rotation highly in flexion and standing position. Also, restoration of ALL has a huge influence when applying loading condition of extension and standing post. It also reduced the excessive posterior stress (pedicle stress and facet loads, which was a disadvantage of disc arthroplasty) (Dooris, Goel, Grosland, & Gilbertson, 2001).

One of the most concerns when putting implant into intervertebral space is type of the implant, whether it is a fixed-core (semi-constrained) or a mobile-core (unconstrained) intervertebral implant. Moumene has conducted FEM study comparing the effect of two type of artificial discs to facet joints and polyethylene core (Moumene & Geisler, 2007). In this study, both prosthesis are FDA-approved; the semi-constrained prosthesis was Prodisc-L while the unconstrained prosthesis was Charité. The FEM consisted of L4 and L5 vertebrae, and the implant was put into the L4L5 disc space with the height of 12.5 mm. Anterior approach implantation was the idea of how to insert the implant into the intervertebral space; however, the entire annulus was taken off (complete discectomy). The result showed that the unconstrained (Charité) arthroplasty has reduced the facet loading while the semi-constrained (Prodisc-L) has increased the facet loading. In addition, polyethylene core of the semi-constrained prosthesis was affected more sensitively in placement location than the unconstrained one. To be more specific, the semi-constrained core did not get any effect from the implant placement whereas the other one's stresses increased by up to 40%.

Shih-Hao C. et al. did finite element modeling on five levels of lumbar spine (from L1 to L5)(Chen, Chen, Chen, & Zhong, 2009). After validating the FEM of intact model, they compared range of motion, annulus stress and facet contact pressure at the surgical level (L4L5) and the adjacent level between the intact model, the model with disc arthroplasty and the model with posterior lumbar interbody fusion (PLIF) with a pedicle screw fixation system. A ball and socket type of implant was used. The model with disc arthroplasty showed higher range of motion, annulus stress and facet pressure at the implant level (L4L5). However, the adjacent levels presented similar range of motion, annulus stress and facet pressure to those of intact model. In contrast, the PLIF model displayed lower range of motion, annulus stress and no facet pressure at the fusion level. Logically, the adjacent levels visibly showed higher range of motion, annulus stress and facet pressure.

Another group of researchers also constructed FEM on a model with disc and arthroplasty and a model with fusion (Denozière & Ku, 2006). A ball and socket type of implant was used in this analysis. The range of motion and ligament tensions was compared. They have concluded that the model with disc arthroplasty expressed higher risk of instability due to excessive ligament tensions, high facet pressure and huge range of motion (increased 52% on average of flexion, extension, lateral bending and torsion). Moreover, the adjacent level presented increase of mobility and stresses. Conversely, the model with fusion pointed out the reduction of mobility of 44% on average at the fusion level while the adjacent level showed the increase in mobility just 11%.

Gregory G. et al. determined the effect of a ball and socket implant with a lifting test (Knapik et al., 2012). They have built a FEM of spine from T12 to S1 with the fixation at the bottom of S1. The implant was inserted at L5S1 level. The model with implant and the intact model showed significant difference in range of motion in the level above the implant level while doing lifting condition. The motion in sagittal plane (flexion and extension) were greater at the higher lumbar levels; in contrast, lateral bending and twisting motion showed less motion at the higher lumbar levels.

4) <u>Purpose of Study</u>

We are aware of the advantages and disadvantages of spinal fusion. Even though knowing that adjacent levels have to compensate for loss in motion due to a fused level, spinal fusion is still considered a "gold standard" for surgical treatment. Because disc arthroplasties have been an option more recently, there are insufficient publications to draw a deep understanding of its mechanisms in the human body and the long-term effects and material stability. Disc arthroplasty has been supported and disproved; there is no definitive conclusion stating disc arthroplasty is better than other surgical options. Most of the in vivo researches were follow-up studies, generally evaluating the success of disc arthroplasty surgeries by using ODI and VAS scores. Majority of the follow-up studies showed satisfactory results. However, there were some cases that needed reoperations. From a biomechanical perspective, the effects of disc arthroplasty were studied via in vitro and finite element analysis studies. The concept of follower load was employed. A lot of experiments were analyzed, fixed applied loadings to a normal spine and a spine with disc arthroplasty. Most FEM studies used hybrid approach, which fixes the rotation for each model, to analyze the results. Each research group has their own technique to develop models of the lumbar region. A variety of models have been investigated, including single level, two-level, three-level or five-level lumbar spine models. Noticeably, model geometries, material properties and other assumptions were different. A 3D poro-elastic model was proposed as a novel analytical modeling of the lumbar spine with disc degeneration.

In this study, three-dimensional poro-elastic model of the whole lumbar spine was built and validated with cadaver results. This model was used to

1) Study the effect of a single-level disc degeneration on the adjacent segments motion in the human lumbar spine
2) Compare the influences of a single-level spinal fusion with a single-level disc arthroplasty on the adjacent segment biomechanics in the human lumbar spine
3) Study the effect of disc arthroplasty with a degeneration disc on the adjacent segment motion

Motion, facet forces and von Mises stress at the segment adjacent to degenerated, fused, disc arthroplasty discs were studied in each condition of the lumbar spine under six moments.

Materials and Methods

1) Finite Element Intact Model Construction

A) Constructing a L1-S1 Model

The finite element program that has been used for this analysis is Automatic Dynamic Incremental Nonlinear Analysis (ADINA) version 8.8.3 (ADINA R-D Inc., Watertown, MA). Three-dimensional vertebral bodies (L1 to S1) were obtained from CT scan and Mimics. They are all rigid bodies generated under the same global coordinates. By using the vertebrae as a reference, endplates, annuluses and nucleuses were created in Solidworks (Student Edition 2014) in the same coordinate system. Every ”body” was saved as a parasolid (.X_T) file and imported into ADINA accordingly.

All the components were imported in ADINA separately, starting from L1 to S1. The endplates were imported next. Then, annuluses and nucleuses were imported in that order. The table below shows the number of each body component.

Components	Body number
Vertebrae (L1-S1)	1 to 6
Endplates	7 to 16
Annulus fibrosus	17 to 21
Nucleus pulposus	22 to 26

Table 3-1 shows the body number of each component in FEM.

B) Model Adjustment

Surfaces at facet joints were extruded five millimeters in order to mimic the function of zygapophysial joints. In the lumbar spine, the facet joints oppose excessive rotation and extension. A normal plane of each facet surface was calculated by using coordinates of three points of the surface. An average of the surfaces' planes was used as the direction of extrusion. Consequently, the extruded bodies will be attached to the original plane. The merging command in ADINA bonded the new bodies to the original vertebral bodies. Therefore, the extruded facets that are rigidly connected to the main vertebrae have the same properties as the vertebrae.

The height of the intervertebral discs in lumbar spine is about 13 millimeters (including the endplates.) All endplates have consistent heights of about 1.5 millimeters. The average distance between each vertebra is the height of the disc, a calculated average of the distance between the anterior and posterior parts of the vertebral bodies. The following table presents the adjusted height of intervertebral discs in each level.

Level of the Disc	Average (mm)	Anterior (mm)	Posterior (mm)
L1L2	11.9	12.8	11.0
L2L3	13.1	13.2	13.0
L3L4	12.35	14.0	10.7
L4L5	13.15	16.0	10.3
L5S1	13.0	18.0	8.0

Table 3-2 presents the adjusted height of intervertebral discs in each segment.

As a result of the global coordinates, the imported components aligned in their respective positions. Only the lumbar spine was analyzed starting from L1 to S1. Unfortunately, all soft materials, such as anterior longitudinal ligaments, posterior longitudinal ligaments, intertransverse ligaments, ligamentum flavum, interspinous ligaments, supraspinous ligaments and capsular ligaments could not be imported from CT information. To add ligaments, “line straights” were created to mimic the ligaments.

C) Assembling Soft Materials

Anterior longitudinal ligaments (ALL) are located at the anterior part of the vertebrae. Line straights, which mimic the ALL, were created to connect each level of vertebrae. The location of ALL starts from the middle anterior part and extends to the left and right sides. There are total of five elements representing ALL that connect each vertebra. The material properties were defined as a nonlinear- elastic material.

Posterior longitudinal ligaments (PLL) are located at the posterior part of the vertebrae. The ligaments are between the left and right pedicle. The location of the PLL begins at the middle of the posterior part and extends to the left and right sides. There are five PLL elements that connect at each level. The material properties were defined as a nonlinear-elastic material.

Ligamentum flavum (LF) connects between the laminae of adjacent vertebrae. There are a total of four elements representing ligamentum flavum that connects at each level of vertebrae two are on the left and the other two are on the right lamina. The material properties were defined as a nonlinear-elastic material.

Interspinous Ligaments connect the spinous processes of the vertebrae. In FEM, there are four elements for interspinous ligaments that attach at each level. Also, the material properties were defined as a nonlinear-elastic material.

Intertransverse ligaments connect between the transverse processes of the vertebrae. Two elements were created at the left transverse process and the other two were created at the right to connect the adjacent vertebra. The material properties were also defined as a nonlinear-elastic material.

Supraspinous ligaments locate at the same spot as interspinous ligaments, connecting the tips of the spinous processes. There are two elements generated for this ligament. The nonlinear-elastic material was set as the material properties.

Facet capsular ligaments surround the posterior of the facet joints in order to strengthen the joint and provide additional support. In the model, four elements represent capsular ligaments connecting each joint. The material properties were defined as a nonlinear-elastic material.

D) Material Properties

The table next page shows material properties of each component. Intervertebral discs were defined as poro-elastic materials (Natarajan, Williams, & Andersson, 2004).

Part	Notes	Material Constants
Cortical Bone	Rigid body	E = 12000 MPa, v = 0.30
Endplate	Poro-elastic material	E = 24 MPa, v = 0.40, Porosity = 0.80
Annulus fibrosus	Hyperelastic material Mooney-Rivlin	L1L2 – C1 = 0.20, C2 = 0.20 L2L3 – C1 = 0.25, C2 = 0.25 L3L4 – C1 = 0.13, C2 = 0.13 L4L5 – C1 = 0.20, C2 = 0.20 L5S1 – C1 = 0.15, C2 = 0.15
Nucleus pulposus	Poro-elastic material	L1L2 – E = 1.00, v = 0.49, Porosity = 0.83 L2L3 – E = 1.25, v = 0.49, Porosity = 0.83 L3L4 – E = 0.65, v = 0.49, Porosity = 0.83 L4L5 – E = 1.00, v = 0.49, Porosity = 0.83 L5S1 – E = 0.75, v = 0.49, Porosity = 0.83
Anterior ligament	Nonlinear elastic material	(Chazal et al., 1985)
Posterior ligament	Nonlinear elastic material	(Chazal et al., 1985)
Ligamentum flavum	Nonlinear elastic material	(Chazal et al., 1985)
Interspinous ligament	Nonlinear elastic material	(Chazal et al., 1985)
Intertransverse ligament	Nonlinear elastic material	(Chazal et al., 1985)
Supraspinous ligament	Nonlinear elastic material	(Chazal et al., 1985)
Facet capsular ligament	Nonlinear elastic material	(Chazal et al., 1985)

Table 3-3 shows material properties of each component in the intact spine.

E) Fixity and Boundary Conditions

The glue command in ADINA was used to connect all of the components. To use this command, the component that has the higher elastic modulus will be the ‘Master’ while the components with the lower elastic modulus will be the ‘Slave’. In other words, the ‘Slave’ will follow whatever the ‘Master’ does.

Component connection	Roles
Vertebra – Endplate	Master – Slave
Endplate – Annulus	Slave – Master
Endplate – Nucleus	Slave – Master
Annulus – Nucleus	Master – Slave

Table 3-4 shows master or slave roles of each component for the glue command.

The degrees of freedom for the entire model are 000111. The movement in xyz translation was allowed while the rotation in xyz was not allowed. Fixity was assigned to the bottom surface of S1 vertebra. So the bottom of S1 was completely fixed in space.

F) Element Groups and Mesh

To simplify, the number of an element groups were defined to match the number of geometry bodies. For example, body 1, which is L1 vertebra, is defined as element group 1. Each group of ligaments has their own element group and has two nodes. Creating a mesh for vertebrae, the annulus and nucleus were in length mode and the maximum length is 20 millimeters. Division mode was used for endplates with an ndiv equal to 1. Lastly, the implant was meshed by using length mode and the size was 1 millimeter. The model has a combination of 340,632 elements, 82,128 nodes and 61 element groups. The table below indicates element groups for each component.

Components	Mode	Element number
Vertebrae (L1 to S1)	Length	1 to 6
Endplates	Division	7 to 16
Annulus fibrosus	Length	17 to 21
Nucleus pulposus	Length	22 to 26
ALL	Truss	80 to 84
PLL	Truss	90 to 94
Ligamentum flavum	Truss	100 to 104
Interspinous ligament	Truss	110 to 104
Intertransverse ligament	Truss	120 to 124
Supraspinous ligament	Truss	130 to 134
Facet capsular ligament	Truss	140 to 144

Table 3-5 indicates element groups for each component in the intact spine.

G) Contact Groups

The contact command prevents any intersections in the model. It differentiates to the program, parts that cannot be penetrated. Therefore, the facet joints need the contact command. Each side of each vertebrae level of the facet has its own group. The facet at the left anterior of L1 was paired with the facet at the left posterior of L2. This was the first contact group. The second group was the facet at the right anterior of L1 and the facet at the left posterior of L2. And so on. The friction coefficient was assumed to be zero. In the intact model, there are total of 10 contact groups.

2) Formulating a Model with Disc Degeneration at L5S1 segment

A) Model Adjustment

According to (Moore, 2011), the levels are more prone to degeneration are L4L5 and L5S1. Therefore, the intervertebral disc at the L5S1 level was varied in four grades of degeneration. The normal condition of the spine is considered to be grade II. As the degeneration worsens, the material properties, dimensions and permeability factors also change (Natarajan, Williams, & Andersson, 2006). In this section, L5S1 intervertebral disc will be varied from grade II to grade V. The disc at L4L5 remains intact (grade II).

For grade III intervertebral disc at L5S1, the height of the annulus was reduced by 15% from the height at grade II. The size (diameter of eclipse) of the nucleus remained the same. The height of the nucleus was consistent with the height of annulus.

For grade IV intervertebral disc at L5S1, the height of the annulus was reduced by 33% from the height at grade II. The size (diameter of eclipse) of nucleus was also reduced by 42%. Material properties for both annulus and nucleus were changed. Again, the height of the nucleus was consistent with the height of the annulus.

For grade V intervertebral disc at L5S1, the height of the annulus was reduced by 70% from the normal condition. The size (diameter of eclipse) of nucleus was the same as the nucleus at grade IV. Annulus' material property were different while nucleus' material property remained unchanged from the nucleus at grade IV. The height of the nucleus was consistent with the height of the annulus.

In the degenerated model, the endplates at L5S1 level stayed the same as in the intact model.

B) Material Properties

The table below shows the material properties and all the changes in different conditions at the L5S1 intervertebral disc (Natarajan et al., 2006).

Degeneration	**Height of Annulus (A-P)**	**Diameter of Nucleus**	**Material Property of Annulus**	**Material Property of Nucleus**
Grade 2	15-5	a=16.33, b=29.81	C_1, C_2=0.15	E=0.75
Grade 3	12.75-4.25	a=16.33, b=29.81	C_1, C_2=0.18	E=0.875
Grade 4	10.05-3.35	a=9.43, b=17.20	C_1, C_2=0.18	E=0.875
Grade 5	4.5-1.5	a=9.43, b=17.20	C_1, C_2=0.075	E=0.875

Table 3-6 shows the material properties and the changes in different grades of degeneration.

C) Fixity and Boundary Conditions

Every boundary condition remained the same. The fixity at S1 was constrained in all six dimensions.

D) Element Groups and Mesh

All three models have total of 421,378 elements, 93,453 nodes and 64 element groups. The table below shows element groups for each component in Model with Implant at L4L5 Level and Degeneration at L5S1 Level.

Components	Mode	Element number
Vertebrae (L1 to S1)	Length	1 to 6
Endplates	Division	7 to 14
Annulus fibrosus	Length	15 to 18
Nucleus pulposus	Length	19 to 22
Implant at L4L5	Length	23 to 25
Lateral Annulus at L4L5	Length	26 to 27
ALL	Truss	80 to 84
PLL	Truss	90 to 94
Ligamentum flavum	Truss	100 to 104
Interspinous ligament	Truss	110 to 104
Intertransverse ligament	Truss	120 to 124
Supraspinous ligament	Truss	130 to 134
Facet capsular ligament	Truss	140 to 144

Table 3-7 presents mode of subdivision of each element groups in the intact spine.

E) Contact Groups

Contact groups at the facet capsular remained the same as well as the contact groups between the implant parts. The fiction coefficient between the implant components was 0.1.

3) Formulating a Model with Implant at L4L5 Segment

A) Model Adjustment

The implant has a height of 11.5 millimeter, diameter of 33 millimeter. The implant is fully fit to the intervertebral space in the sagittal plane (anterior to posterior.) the top and bottom surface of the implant were smooth and rigidly connected to the L4 and L5 vertebrae. The implant is a ball and socket type.

According to the surgical approach, anterior part of annulus at L4L5 was cut off along with ALL at L4L5 level. Only lateral side of L4L5 annulus was left because the size of the implant reached anterior and posterior of vertebral (fully fit in sagittal plane). Endplate at L4L5 level was also removed. Due to the difference in dimension between the implant and the original intervertebral disc, the bottom surface of L4 and the top surface of L5 vertebrae were adjusted to the correct fit.

Other vertebrae, intervertebral disc and the facet were remained the same. The model with implant at L4L5 level is very similar to the intact model.

B) Assembling Soft Materials

Most of the ligaments, facet contact remained the same. However, L5 vertebra was cut differently from the one in the intact model, resulting in the absence of some points that used to create ligaments. To solve the problem, nearby points were chosen to construct the ligaments. In this analysis, ALL at the L4L5 level were entirely removed in order to imitate the actual surgery procedure.

C) Material Properties

The implant consists of 3 parts. The top part and bottom part is Chrome-Cobalt. The middle part is polyethylene. The table below shows the material properties of the implant.

Parts	Young's Modulus	Material Constant
Chrome-Cobalt	Nonlinear elastic material	E = 300000 MPa, v = 0.27
Polyethylene	Nonlinear elastic material	E = 2000 MPa, v = 0.3

Table 3-8 shows material properties of a ball-and-socket artificial disc.

Material properties of vertebral body, endplates, nucleus, annulus and ligaments remained the same.

D) Fixity and Boundary Conditions

Every boundary condition remained the same. The bottom of S1 was fixed in all six dimensions.

E) Element Groups and Mesh

The model with implant has 411,054 elements, 95,578 nodes and 64 element groups. The table next page shows the element groups for each component.

Components	Mode	Element number
Vertebrae (L1 to S1)	Length	1 to 6
Endplates	Division	7 to 14
Annulus fibrosus	Length	15 to 18
Nucleus pulposus	Length	19 to 22
Implant at L4L5	Length	23 to 25
Lateral Annulus at L4L5	Length	26 to 27
ALL	Truss	80 to 84
PLL	Truss	90 to 94
Ligamentum flavum	Truss	100 to 104
Interspinous ligament	Truss	110 to 104
Intertransverse ligament	Truss	120 to 124
Supraspinous ligament	Truss	130 to 134
Facet capsular ligament	Truss	140 to 144

Table 3-9 shows the element groups for each component in the spine with disc arthroplasty.

F) Contact Groups

In addition to contact groups of the facet joint, two more contact groups were created for the implant. First contact group was for the top and middle part of the implant. The second one was for the middle and the bottom part of the implant. The contact groups of the implant has friction coefficient of 0.1.

4) Formulating a Model with Implant at L4L5 Segment and Disc Degeneration at L5S1 Segment

A) Model Adjustment

This model has similar structure as the model with only degeneration at L5S1 level. However, at L4L5 intervertebral disc was substituted with a ball and socket artificial disc. Level of degeneration at L5S1 was varied to four grades, such as grade II, grade III, grade IV and grade V. The intact condition was considered to be grade II.

B) Material Properties

The implant had material properties similar to the ones in the previous model. The material properties of the disc degeneration and the implant are the same as Table 3-6 and Table 3-8, respectively.

C) Fixity and Boundary Conditions

Every boundary condition remained the same. The fixity at S1 was constrained in all six dimensions.

D) Element Groups and Mesh

All three models have a total of 421,378 elements, 93,453 nodes and 64 element groups. Element groups for each component in the spine with an implant at L4L5 Level and degeneration at L5S1 Level are similar to Table 3-9.

E) Contact Groups

Contact groups at the facet capsular and contact groups between the implant parts remained the same. The fiction coefficient between the implant components was 0.1.

5) Formulating a Model with Spinal Fusion at L4L5 Segment

A) Model Adjustment

Most parts of the model remained the same. However, the annulus fibrosus at L4L5 was removed, and the nucleus' property was altered so it was as rigid as cortical bone in order to imitate the fusion approach. In this model, soft materials, element groups, contact groups, boundary conditions and fixity conditions stayed the same.

B) Material Properties

The table shows the material properties of the changes in the fusion model.

Part	Note	Material Constant
Annulus at L4L5 level	Removed	None
Nucleus at L4L5 level	Nonlinear elastic material	E = 12000 MPa, v = 0.30

Table 3-10 shows the material properties of the changes in the spine with spinal fusion.

C) Fixity and Boundary Conditions

Every boundary condition remained the same. The fixity at S1 was constrained in all six dimensions.

D) Element Groups and Mesh

The model has total of 302,255 elements, 73,351 nodes and 60 element groups.

E) Contact Groups

Contact groups at the facet capsular remained the same.

6) Loading Conditions

The concept of follower load was employed in the implant level (Shirazi-Adl & M, 2000). To imitate the surgical approach, the intervertebral space is supposed to be a little smaller than the height of the implant. This small gap squeezed and held the implant in place without having any effect on the movement. In addition, thermal rods were constructed in order to mimic the pressure at the implant level. A rod was created at the center of the implant that connected the top and bottom parts of the implant. High temperatures were applied so that the rod would uniformly contract along the line and apply pressure on the implant. In this case that pressure was 800 N.

The effect of the implant will be studied using a hybrid method (M. M. Panjabi, 2007). Specifically, the total range of motion of the implanted model remained in the same as the intact model in every loading condition.

For each model, the moments applied on the model were different in each case. Since this experiment employed the hybrid method, the total rotation was iteratively calculated in order to get the same rotation.

7) Calculation of Rotation

After the moments were applied, the rotations were calculated. The following calculation is for flexion. The same method was employed for all other rotations.

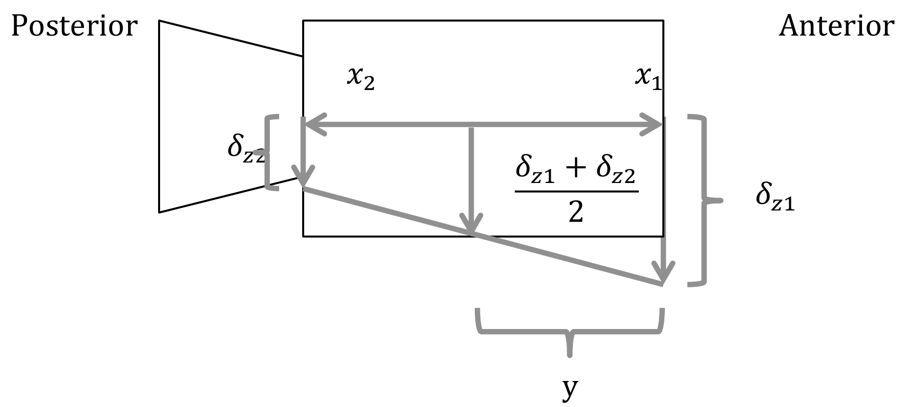

Find **θ**

$$x = \delta_{z1} - \left(\frac{\delta_{z1}+\delta_{z2}}{2}\right) mm$$

$$x = \frac{\delta_{z1}}{2} - \frac{\delta_{z2}}{2}\ mm$$

$$x = \frac{\delta_{z1}-\delta_{z2}}{2}\ mm$$

$\tan\theta = \frac{x}{y}$;

$$\frac{x}{y} = \frac{\frac{\delta_{z1}-\delta_{z2}}{2}}{y}$$

$$\tan\theta = \frac{\frac{\delta_{z1}-\delta_{z2}}{2}}{\frac{x_1-x_2}{2}}$$

For small θ ; $\tan\ \theta\ =\ \theta$ (rad)

$$\theta\ (degree) = \frac{\delta_{z1}-\delta_{z2}}{x_1-x_2}\ x\ (\frac{180}{\pi})$$

A graph was plotted for each loading condition. Then, rotation of each segment was analyzed and compared against the results of a cadaver.

4) Intact Model Validation

The model validation process ensures that the results of the experiment that were done using finite element models are accurate. Under the same conditions of external forces, the finite element model should behave the same way as it does in life. The external forces include flexion, extension, left and right lateral bending and left and right torsion. Consequently, the finite element model can be used to predict the behavior of the spine in many other conditions, which have not been done.

For flexion and extension, Vertical moments of 8 Nm and 6 Nm were applied at the anterior and posterior parts of L1. Two points were picked at the symmetrically sagittal plane of L1 vertebral body. A vector length from the anterior point and posterior point was calculated. Then the moment was divided by the length of the vector to get the couple forces that are needed to oppose the forces those two points. The loads were applied at L1 vertically.

Left torsion and right torsion: A horizontal moment of 4Nm was applied also at the anterior and posterior part of L1 to verify the torsional motion. In this step, it is similar to the verification of the flexion and extension because the locations of forces acting on the anterior and posterior parts are the same. Therefore, the couple force was calculated from the horizontal loading moment of 4Nm divided by the length of the vector. These couple forces were applied horizontally.

Lastly, for left and right lateral bending: a vertical moment of 6Nm was applied at the right and left lateral side of L1 to verify the motion in lateral bending. Two points were picked at the symmetrically frontal plane of the vertebral body. A vector length from the left most and right most points was calculated. The loading moment was divided by the length of the vector to get the couple forces. These couple forces were applied vertically.

The time step function was employed for every loading condition. The moments were distributed into 20 steps.

To get the motion information at each level, four points were picked from each vertebra, one from the anterior, one from the posterior, one from the left side of the vertebra and one from the right side of the vertebra as show in Figure 4-1. Locations of the four points at each level were obtained at the initial step and the last step of loading. The initial and last locations of these points were calculated to get the rotation at each level.

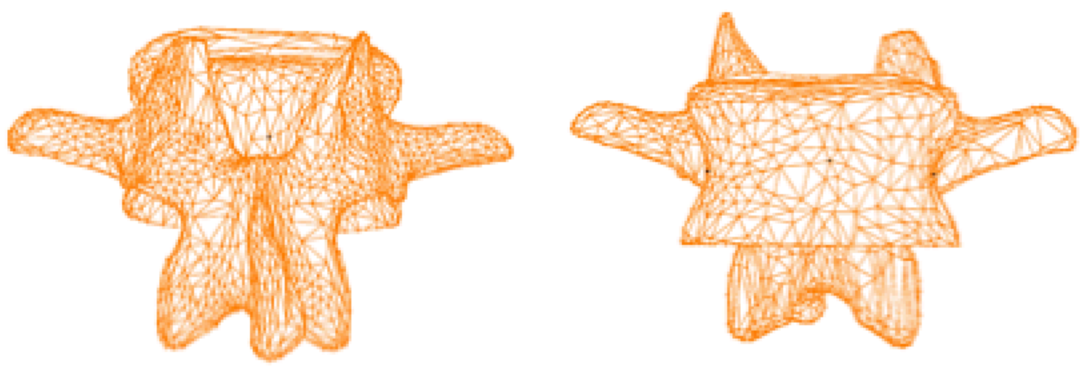

Figure 4-1 Posterior and anterior views of L1 vertebra with four points.

Primary rotation of the L1S1 spine was validated with motion data from the cadaver; if the maximum motion from each loading condition fell between the rotation of the FEM and the cadaver, then the model was deemed.

5) Results

1. Intact Model Validation

Rotation from each individual segment and plane was calculated. In other words, the rotation in the sagittal plane, such as flexion and extension, was added; the rotation in the frontal plane, left and right lateral bending, was combined; lastly, the rotation in the transverse plane, left and right torsion, was also summed. All of the summed rotations in each plane were compared with rotations of the cadaver. The calculations of the intact finite element model mostly fell within one standard deviation; however L1L2, L2L3 and L3L4 in lateral bending did not. Figure 5-1 compares rotation of each segment at each loading condition. The following graphs at every loading condition will refer to total rotation of the intact spine from L1 to S1. Flexion, extension, lateral bending and torsion each have a total rotation of 25.6 degrees, 18.9 degrees, 22.5 degrees and13 degrees, respectively.

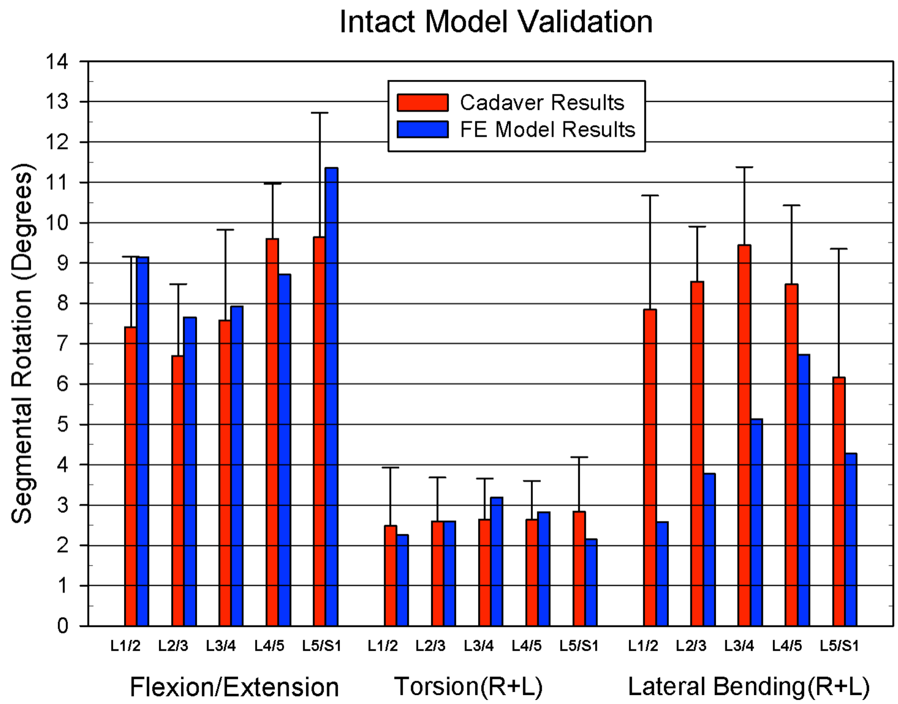

Figure 5-1 Comparison of rotation in each segment of each loading condition between the cadaver results and finite element modeling result.

2. Finite Element Modeling of L1 to S1 Spine with Degeneration at L5S1 Level

Figure 5-2 presents rotation (in degrees) of four cases of degeneration at L5S1, namely grade II, III, IV and V. The hybrid method was employed to analyze the effect of degeneration of the intervertebral disc (M. M. Panjabi, 2007). Figure 5-2 (A), (B), (C) and (D) show loading conditions in flexion, extension, lateral bending and torsion, respectively. With degeneration of intervertebral disc at L5S1, besides the loading condition of lateral bending, L5S1 disc represented in flexion, extension and torsion became stiffer more abruptly in grade III and gradually becomes stiffer as grade increase from IV and V; therefore, the rotation at L5S1 segment decreased while the overall rotations at all other levels compensated for the loss in motion. For lateral bending, motion at L5S1 gradually decreases as degeneration worsens; however, for grade III, IV and V, the motion at L2L3, L3L4 and L4L5 were in about the same level but they were higher than grade II. At L5S1's motion, the big drop of rotation was observed between grade II and grade III in flexion, extension, lateral bending and torsion, ranging from 6 to 3 degrees, 5 to 3 degrees, 4 to 2 degrees and 2 to 1 degrees, respectively.

According to Figure 5-2 (A) and (B), intervertebral disc degeneration at L5S1 impacts the motion when grades become worse from II to V. The motion suddenly dropped at L5S1 while the motion at L4L5 and L3L4 were raised, accordingly. Conversely, under lateral bending and torsion, motion at L5S1 gradually decreases as the grades of degeneration increases.

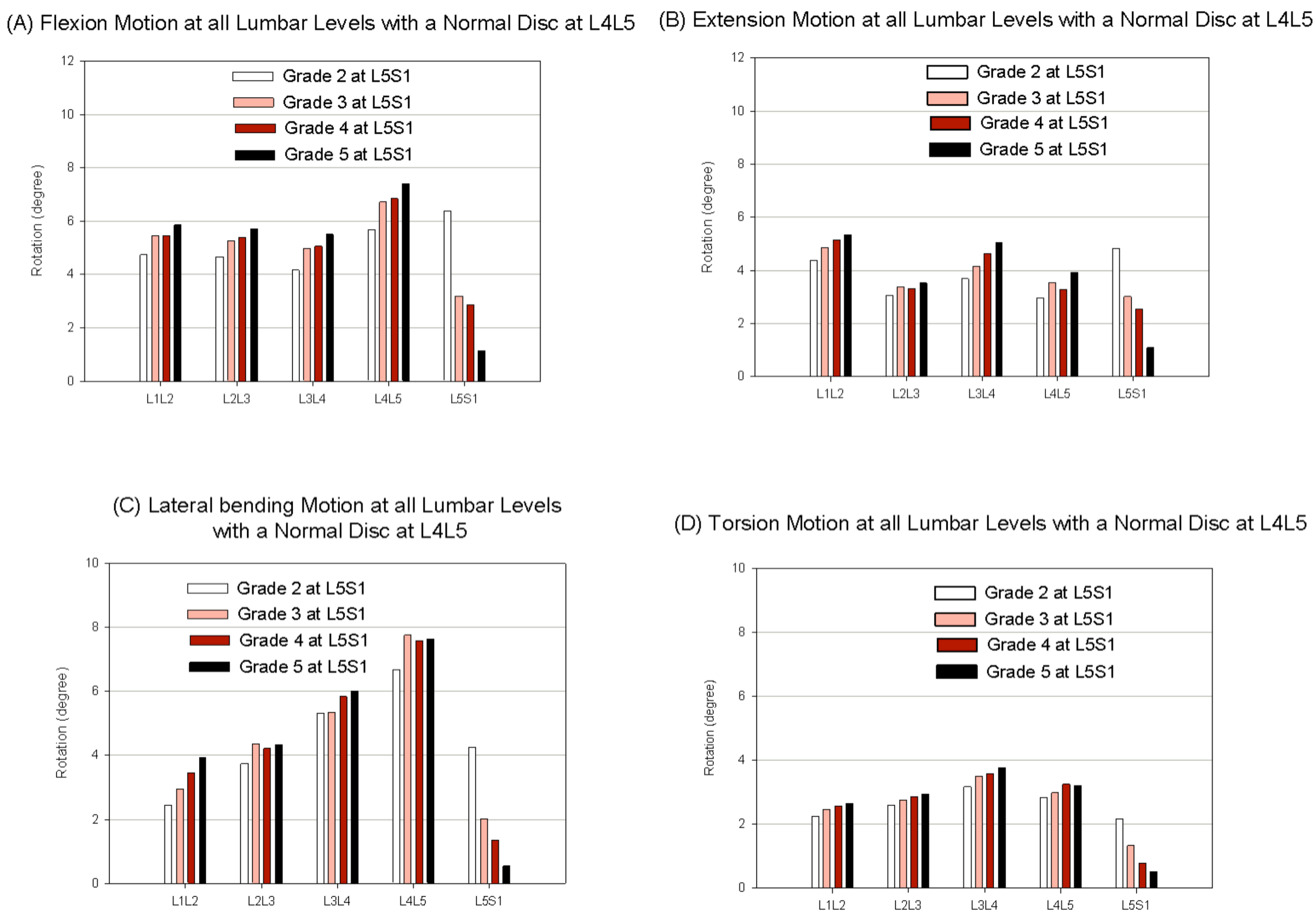

Figure 5-2 shows rotation under loading condition of (A) flexion, (B) extension, (C) lateral bending and (D) torsion.

Rotation of the intact spine and the rotation of the spine with degeneration at L5S1 were calculated and presented with percentages. Figure 5-3 (A), (B), (C) and (D) show the percentage change in rotation for flexion, extension, lateral bending and torsion in all grades of degeneration, respectively. Grade of degeneration is represented in the x-axis while the level of intervertebral disc was in y-axis, and percentage change was along the z-axis. All loading conditions in different grades of degeneration at L5S1 have similar trends. The motion at L5S1 decreased when comparing to the motion of L5S1 in the intact spine while the motion at L3L4 and L4L5 were larger than both models. To be more specific, the motion in flexion (Figure 5-3(A)) at L5S1 was abruptly reduced by -50% for grade III and then gradually decreased as the grades increased. For adjacent levels, the rotation of L4L5 increased progressively due to the degeneration at L5S1. Moreover, the rotation at the skipped level at L3L4's also increased compared to the motion at L3L4 in an intact spine. The motion at L5S1 in lateral bending acted similar to the motion in flexion, which decreased in grade III decreased further from IV- V. However, the adjacent level's and the skipped level's motion increased (but less in Flexion). Under extension and torsion moments, the model with degeneration also produced similar results. The degeneration level has decreased motion from -40% to -80% while the adjacent level has increase by 5% to 30%. Clearly, as the result of degeneration at L5S1, degenerated disc is much stiffer reducing motion at L5S1. The adjacent level's motion increased.

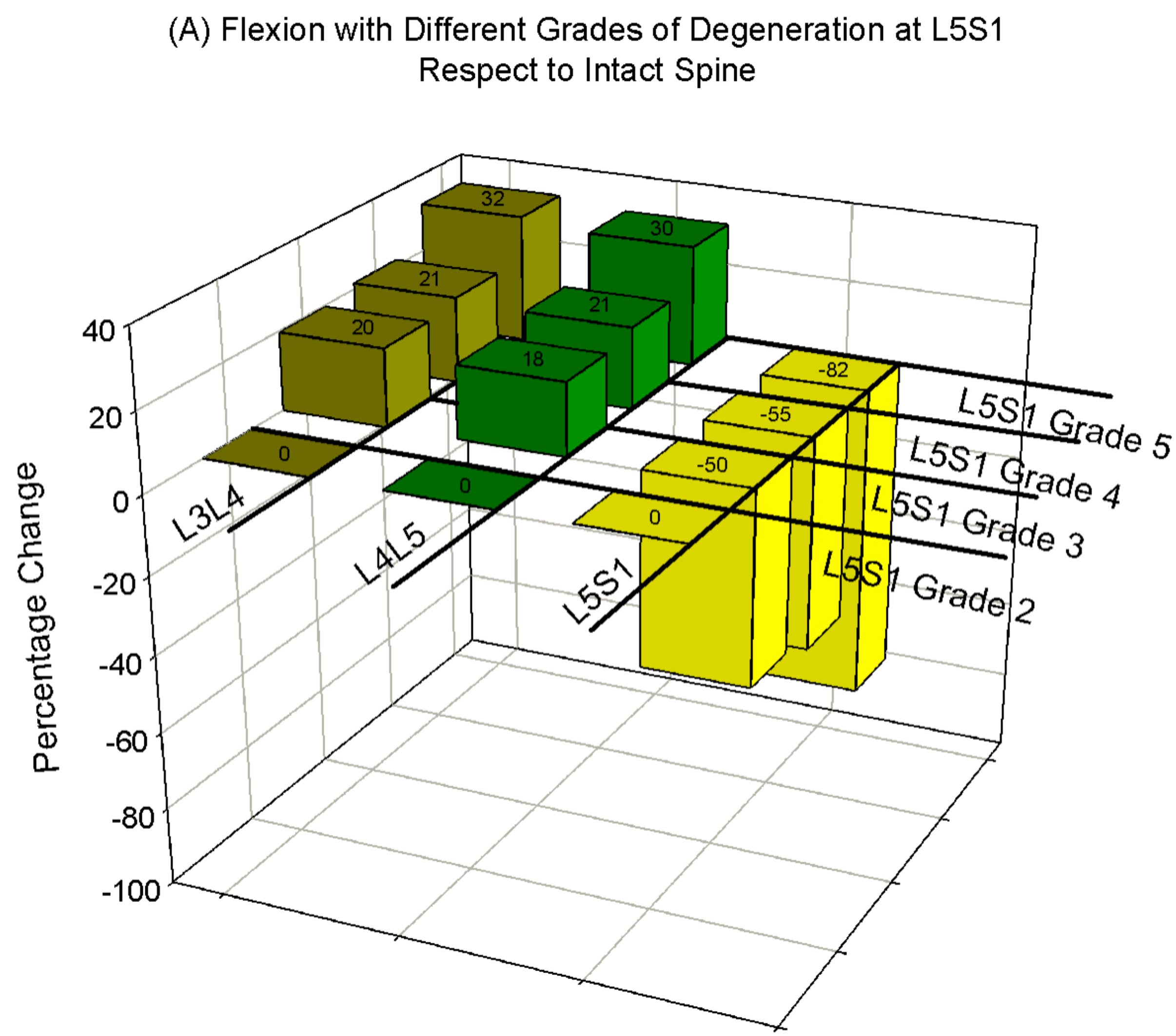

Figure 5-3 (A) illustrates percentage change under flexion moment with different grades of degeneration at L5S1.

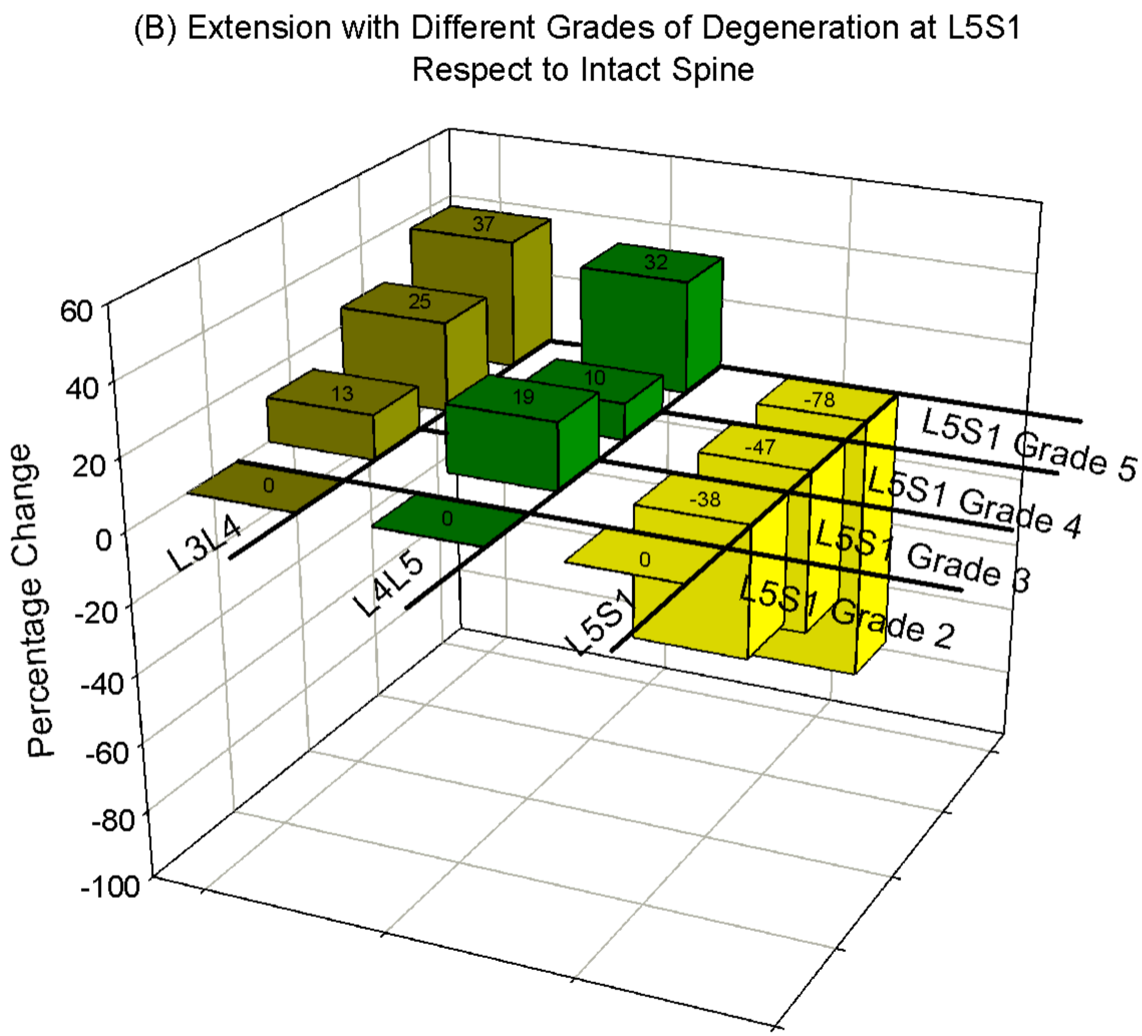

Figure 5-3 (B) shows percentage change under extension moment with different grades of degeneration at L5S1.

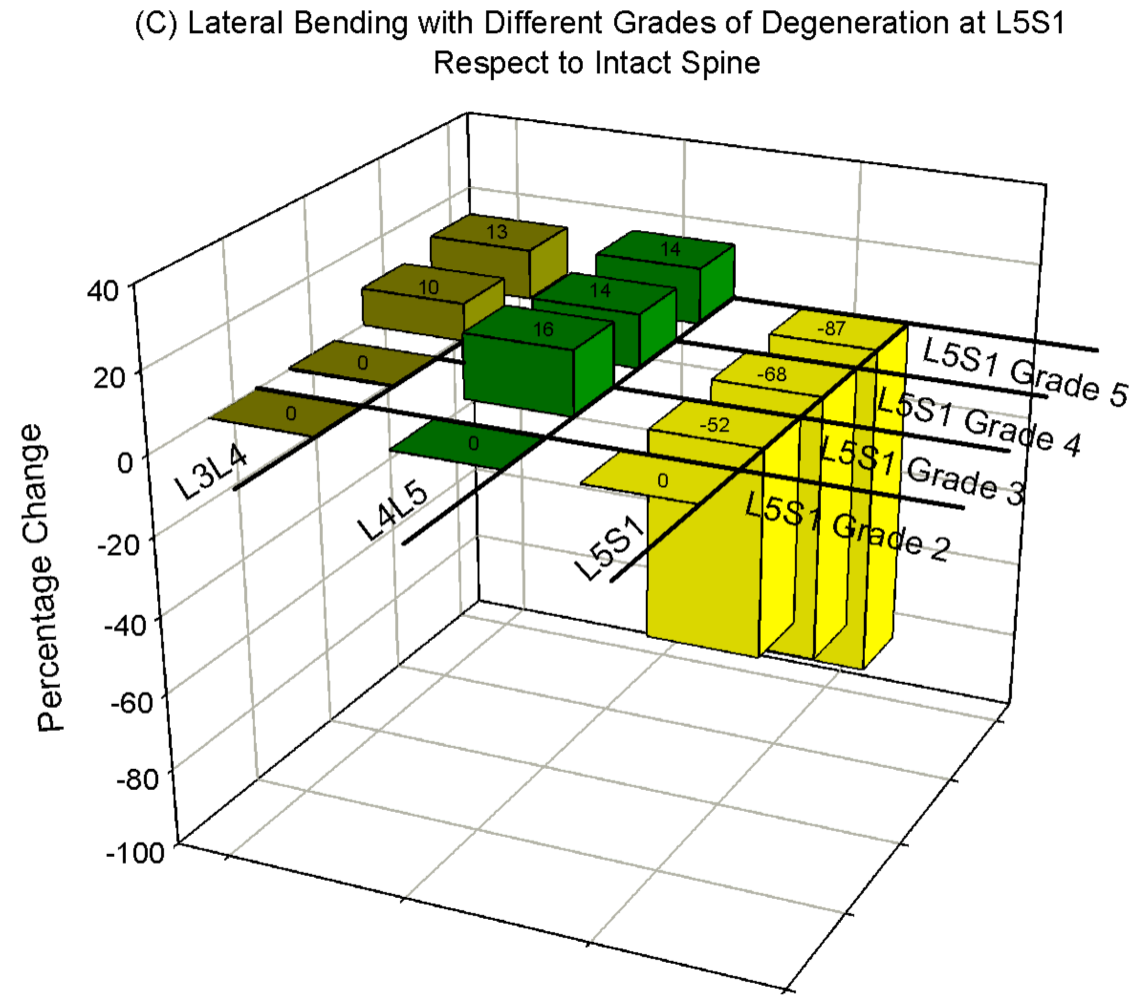

Figure 5-3 (C) illustrates percentage change under lateral moment with different grades of degeneration at L5S1.

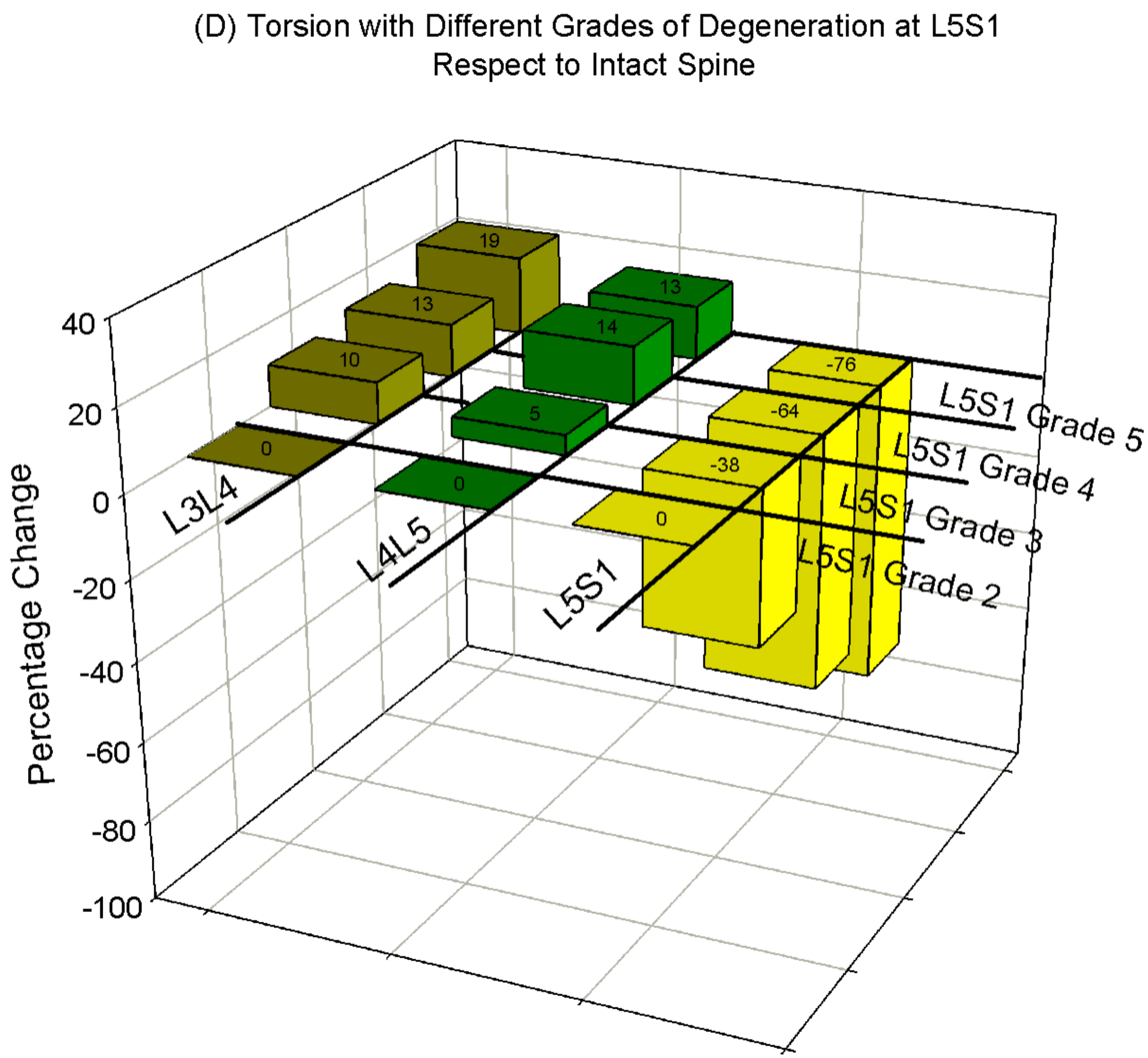

Figure 5-3 (D) shows percentage change under torsional moment with different grades of degeneration at L5S1.

Figure 5-4 represents the same information as the previous graphs Figure 5-3 but the data is arranged in a level matter. Figure 5-4 (A) shows percentage change at L3L4 between the model with degeneration at L5S1 and the intact spine. L3L4 was a skipped level of the degeneration (L5S1). The change of L3L4's motion in flexion and extension were higher than the ones in torsion and lateral bending. 10% to 40% increase in motion was observed at L3L4 in flexion and extension when the degeneration took place at L5S1. With the same condition, less increase of motion was observed under lateral bending and torsion moment (10% to 20%). Figure 5-4 (B) displays percentage change at L4L5, which was an adjacent level to the degeneration. The change of L4L5's motion in flexion and extension were still higher than the ones under the moments of lateral bending and torsion. The increase of L4L5's motion in flexion and extension in grade III of degeneration was 18% to 19% while the increase of L4L5's motion in lateral bending and torsion was 5% to 9%. With grade V of degeneration at L5S1, flexion and extension showed 33% to 36% increase in rotation. On the other hand, lateral bending and torsion showed 8% to 22% increase in rotation with grade V of degeneration at L5S1. Lastly, Figure 5-4 (C) shows the percentage change of L5S1's rotation in negative values referring to the reduction of the motion. All loading conditions present the same fashion. There were reductions at L5S1 with grade III of degeneration from -53% to -38% while grade V of degeneration from -89% to -74% of the original rotation. In this segment, decreases in motion in each loading conditions were comparable.

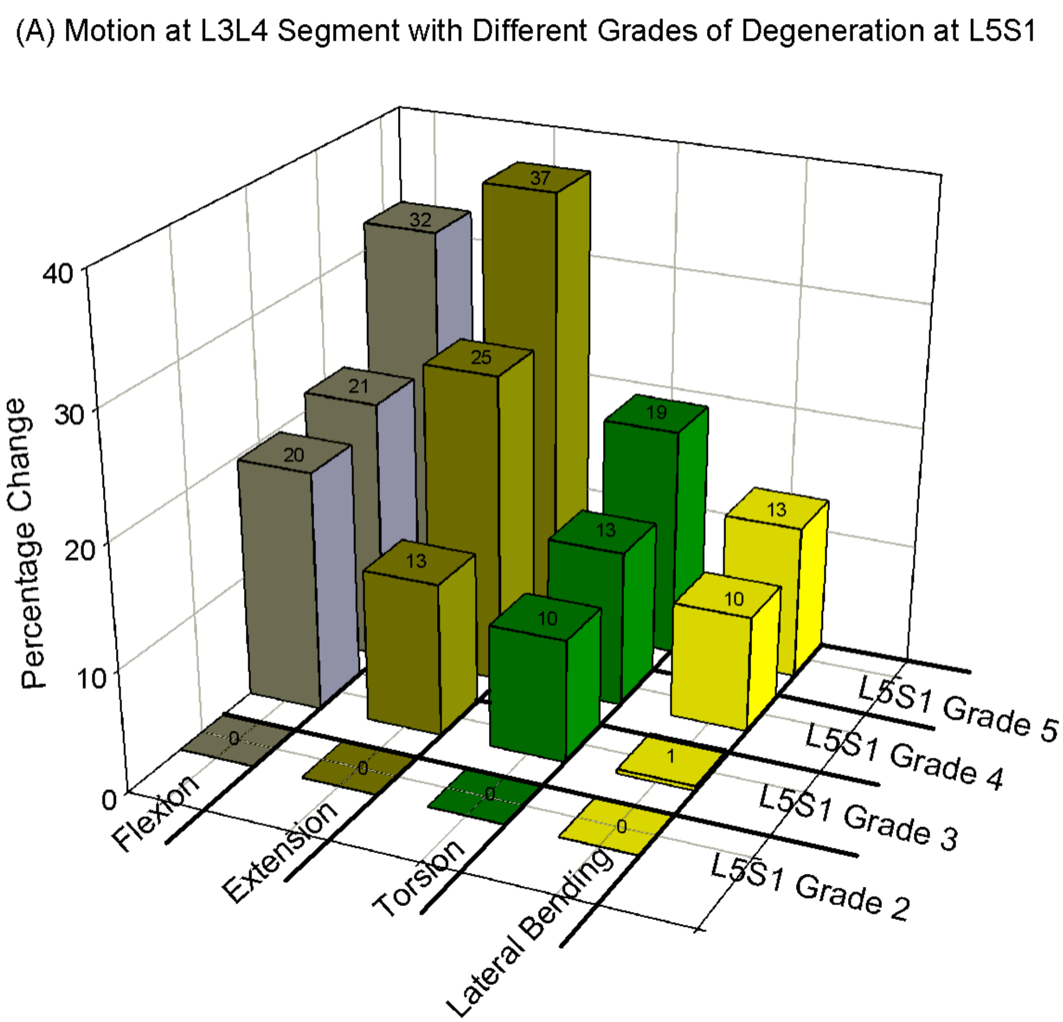

Figure 5-4 (A) shows rotation at L3L4 segment under flexion, extension, torsion and lateral bending in a spine with different grades of degeneration at L5S1.

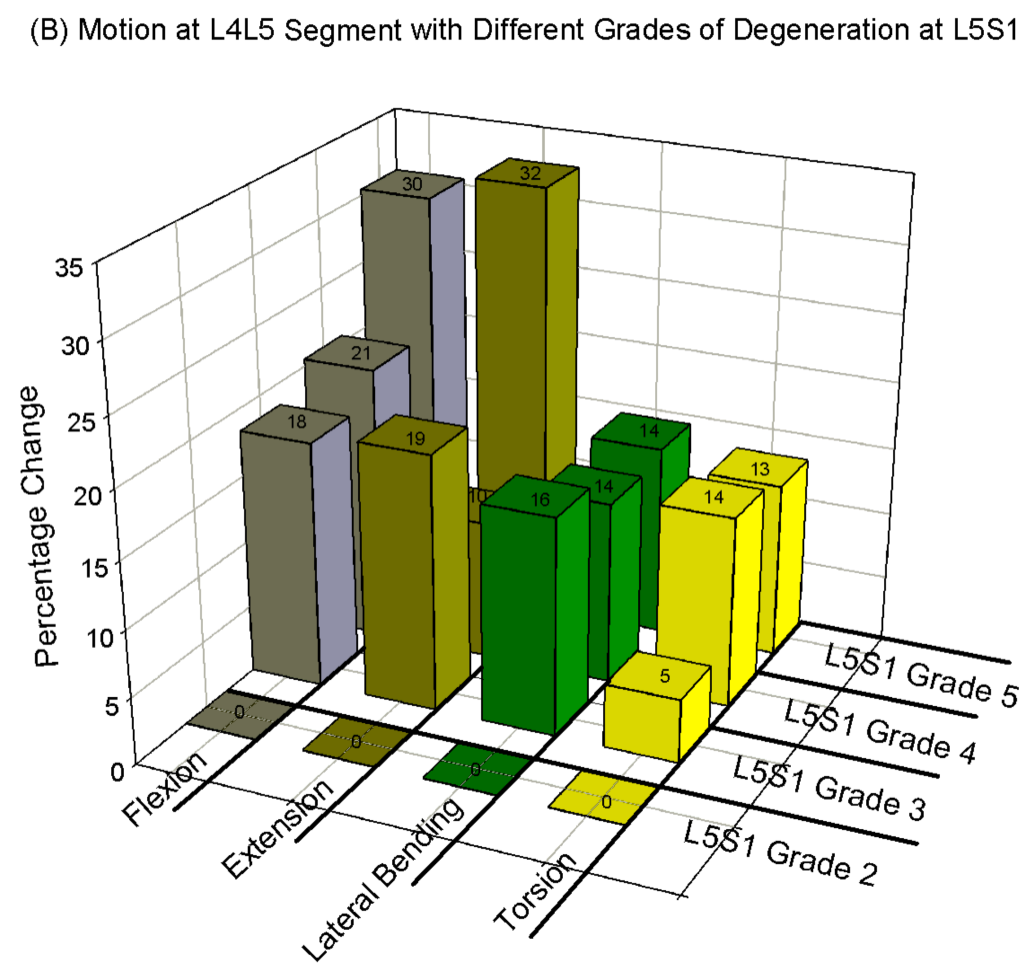

Figure 5-4 (B) shows rotation at L4L5 segment under flexion, extension, torsion and lateral bending in a spine with different grades of degeneration at L5S1.

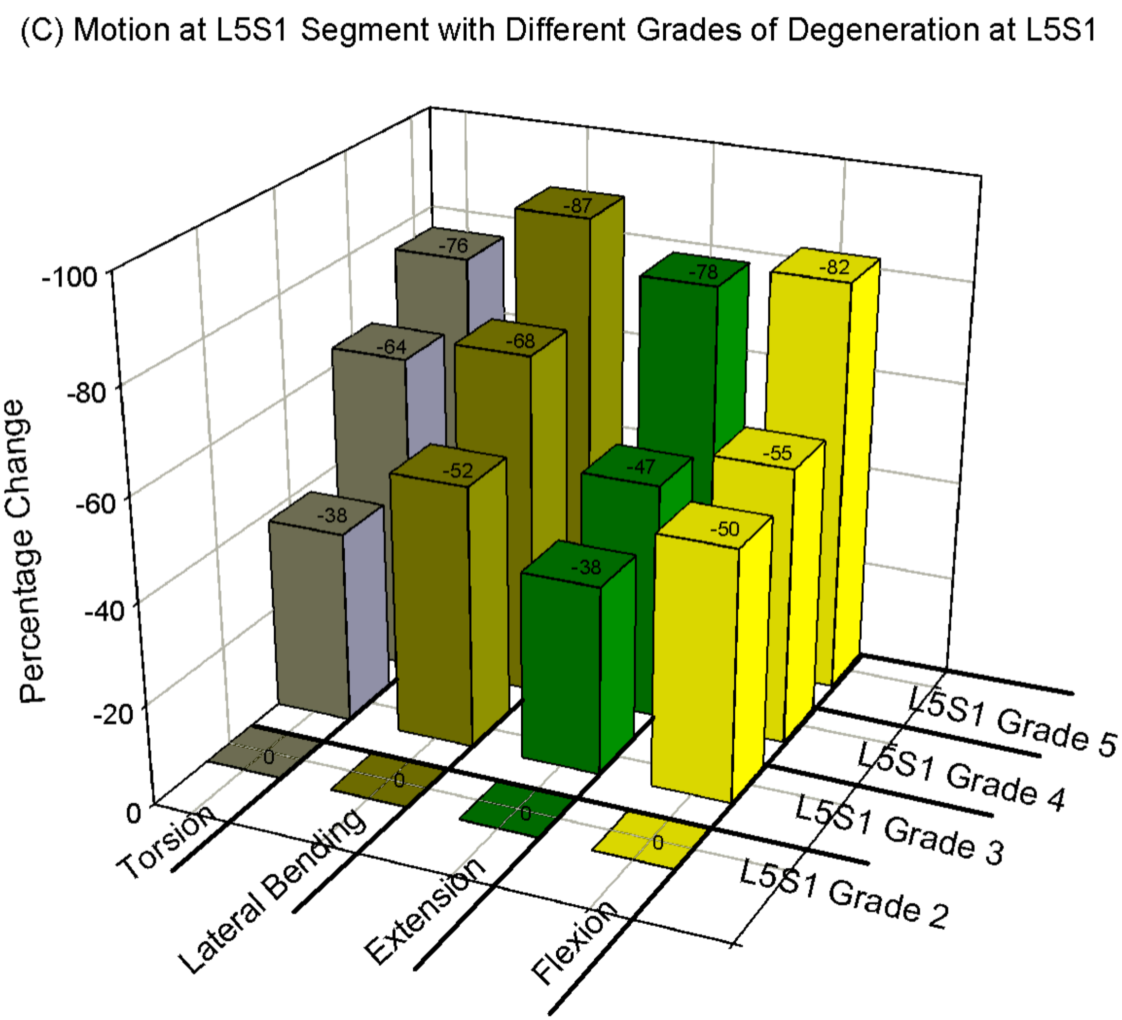

Figure 5-4 (C) shows rotation at L5S1 segment under flexion, extension, torsion and lateral bending in a spine with different grades of degeneration at L5S1.

3. Finite Element Modeling of L1 to S1 Spine with Degeneration at L5S1 Level and Disc Arthroplasty at L4L5 Level

With the same total of rotation from L1 to S1, Figure 5-5 compares models with and without an implant in different loading conditions and different grades of degeneration. There are 2D graphs where the x-axis is the segmental level and y-axis is the degree of rotation. Each loading condition presents the results separately into four graphs for each grade II, III, IV and V at the degenerated disc. Loading condition of flexion as has shown in Figure 5-5 (A), shows an increase in rotation at L4L5 in both models. The rotation at the adjacent levels conveyed less motion for all grades of degeneration. The maximum rotation was detected at the implant level with a grade V at L5S1. Likewise for flexion and extension, the models displayed similar trends as in Figure 5-5 (B). Rotation of L4L5 in the implanted model was at least twice as much as the rotation of a normal disc at L4L5. On the other hand, loading condition of torsion resulted in a loss of motion at both the implant level and degenerated level. The cephalic level to the implant counteracted and showed an increase of motion. With the implant, higher rotation was observed at L3L4 in lateral bending as degeneration worsened.

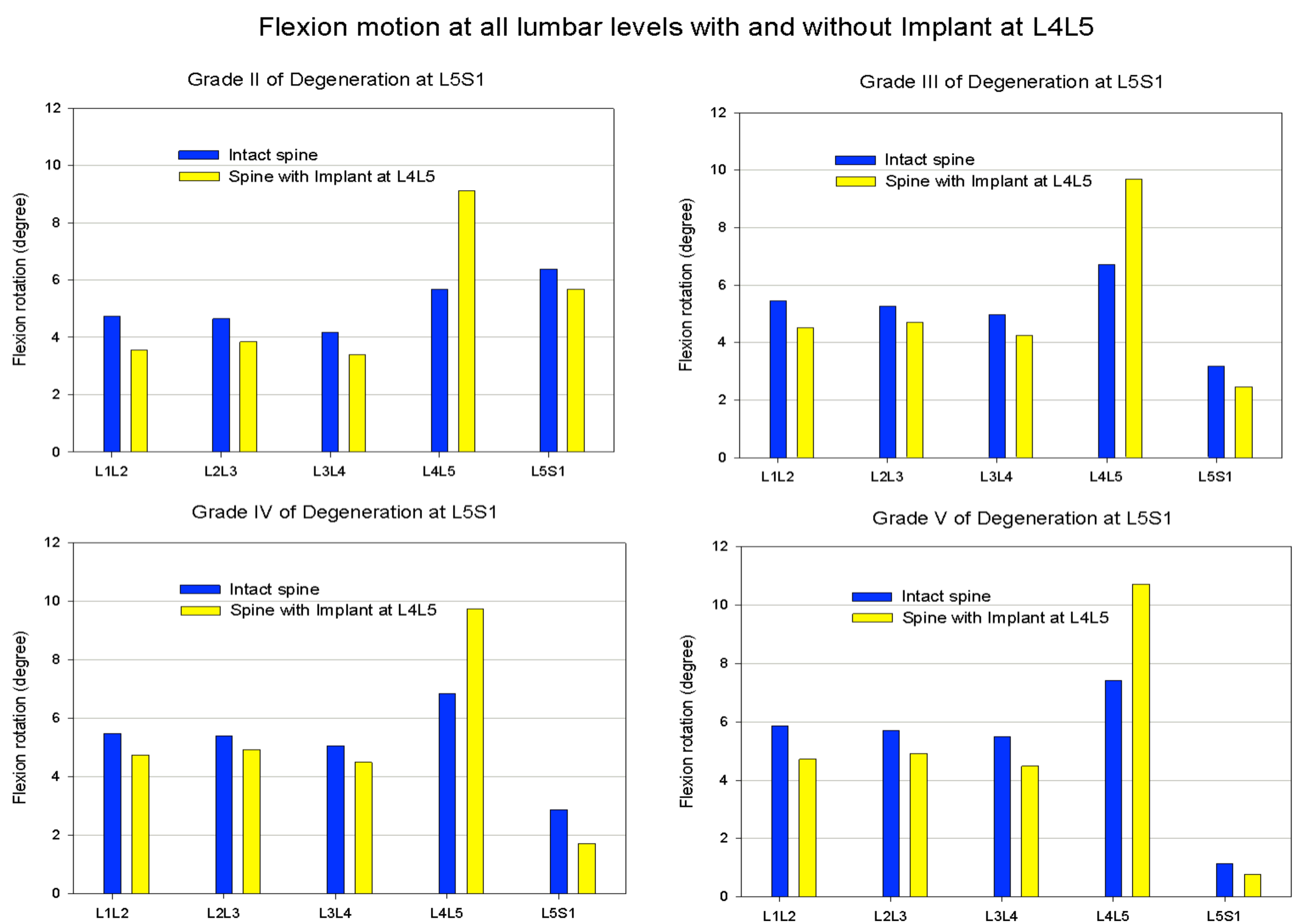

Figure 5-5 (A) shows comparisons between the rotation under flexion moment in a spine with and without implant at L4L5 with presence of disc degeneration at L5S1.

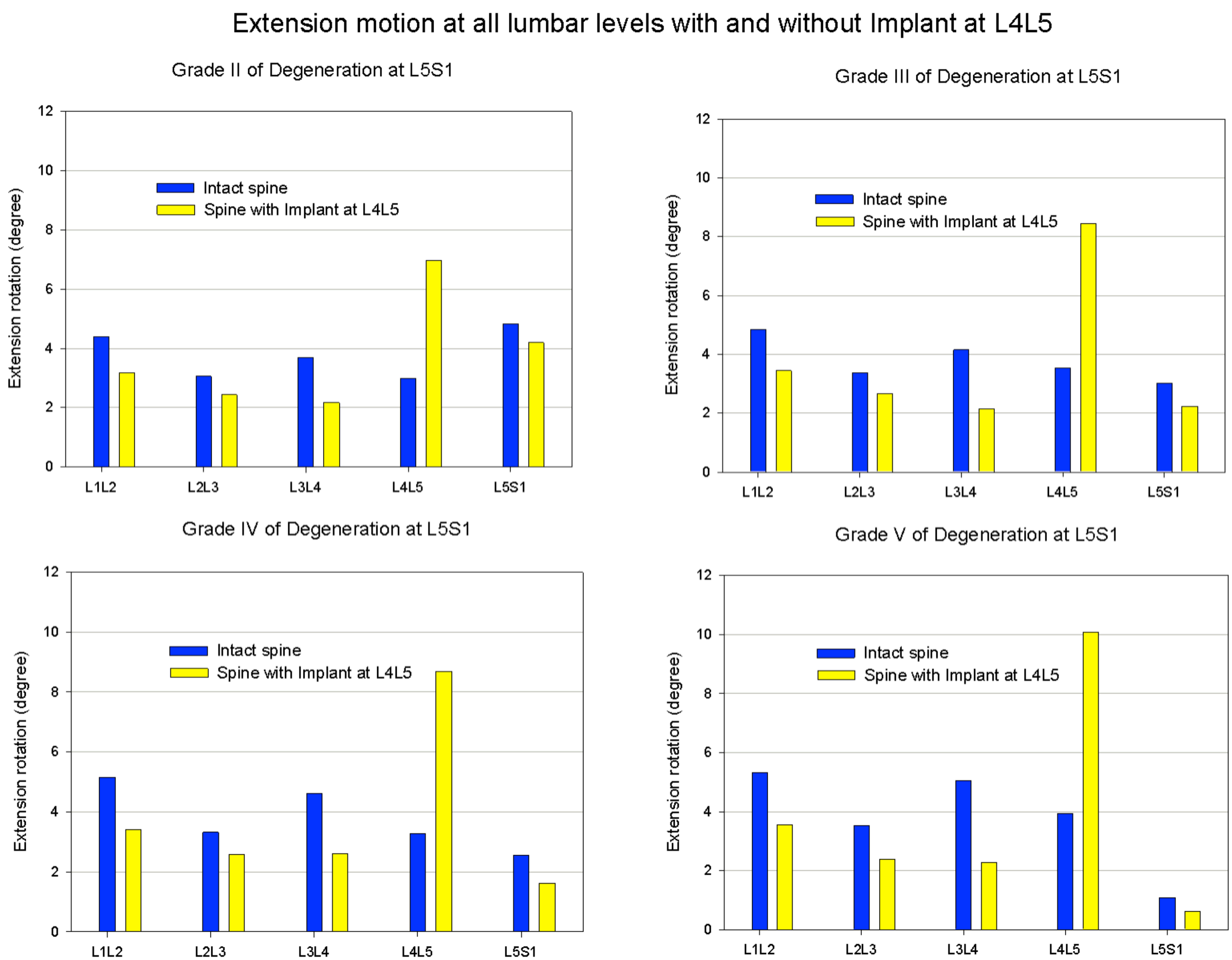

Figure 5-5 (B) shows comparisons between the rotation under extension moment in a spine with and without implant at L4L5 with presence of disc degeneration at L5S1.

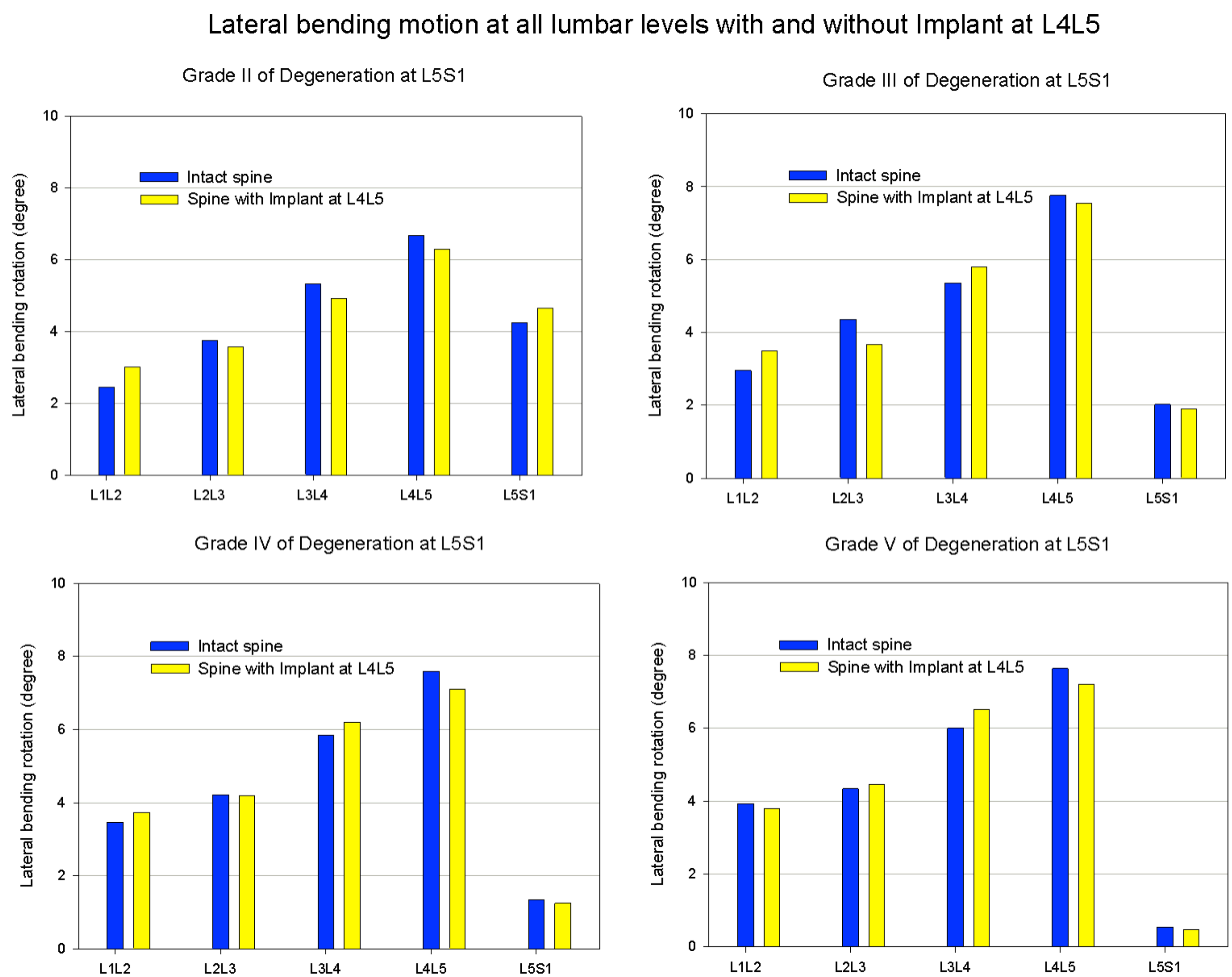

Figure 5-5 (C) shows comparisons between the rotation under lateral moment in a spine with and without implant at L4L5 with presence of disc degeneration at L5S1.

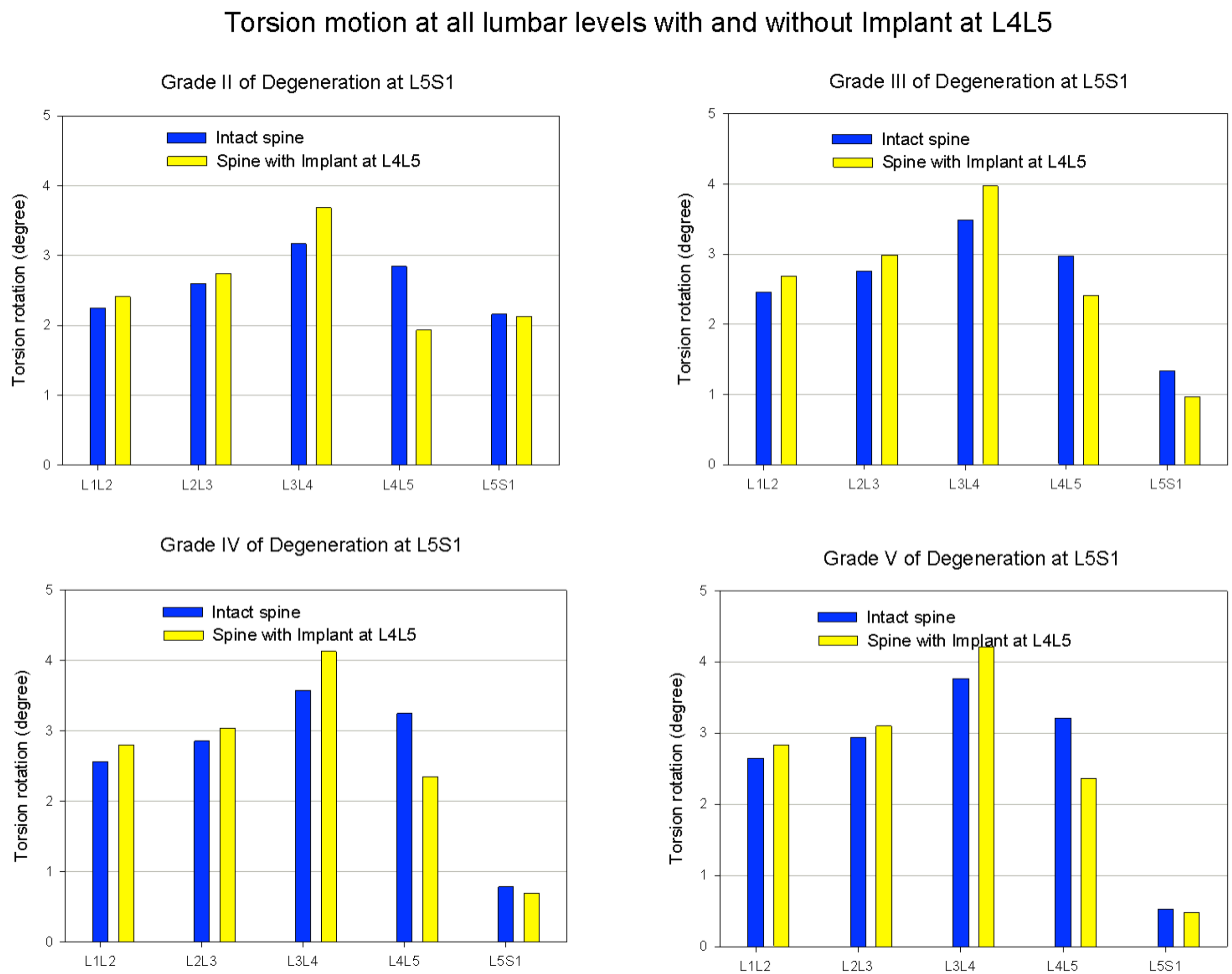

Figure 5-5 (D) shows comparisons between the rotation under torsional moment in a spine with and without implant at L4L5 with presence of disc degeneration at L5S1.

Information from Figure 5-5 was calculated and plotted in a 3D graph. Figure 5-6 illustrated percentage changes from the results of a disc arthroplasty. In this graph, a comparison between the normal disc (grade II) at L5S1 in the intact model, the model with the normal disc (grade II) at L5S1, and the implant at L4L5 was presented in a percentage. Same comparison goes with grade III, IV and V. At the implant level and in flexion; the motion increased by 42% to 60% while the adjacent levels' motion decreased by -11% to -33%. The change at the implant level was more obvious in extension. Increase in motion at the implant level ranged from 134% to 165%, but the rotation declined at the adjacent levels -13% to -55%. The cephalic level showed more reduction in motion than the degenerative level. Decrease in motion at the implant level was spotted in lateral bending and torsion from -3% to -11% and -19% to -32%, respectively. These reductions were more than the reductions of motion at L5S1, which was just -1% to -6% in lateral bending and -1% to -28% in torsion. However, the increase in motion was seen in the level above the implant (L3L4) for torsion. With grade II degeneration at L5S1, the model with implant acted dissimilar from the rest of the grades of degeneration. For grade II, in term of the adjacent levels, rotation of L5S1 increased by 9% while the rotation of L3L4 decreased by -8%. On the other hands, grades III, IV and V showed an increase at L3L4 by 6% to 11% and decrease at L5S1 by -1% to -7%.

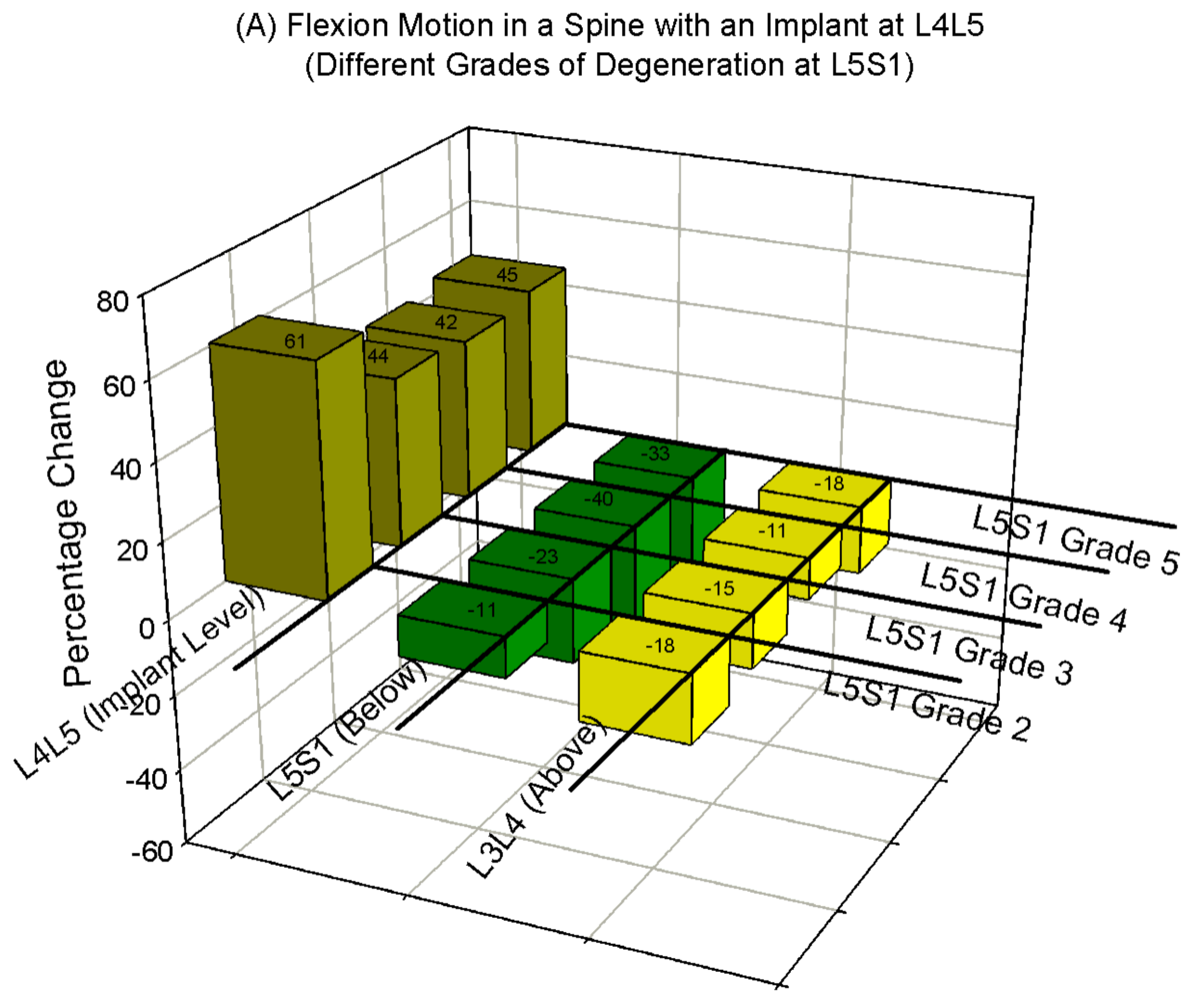

Figure 5-6 (A) shows rotation under flexion moment in a spine with an implant at L4L5.

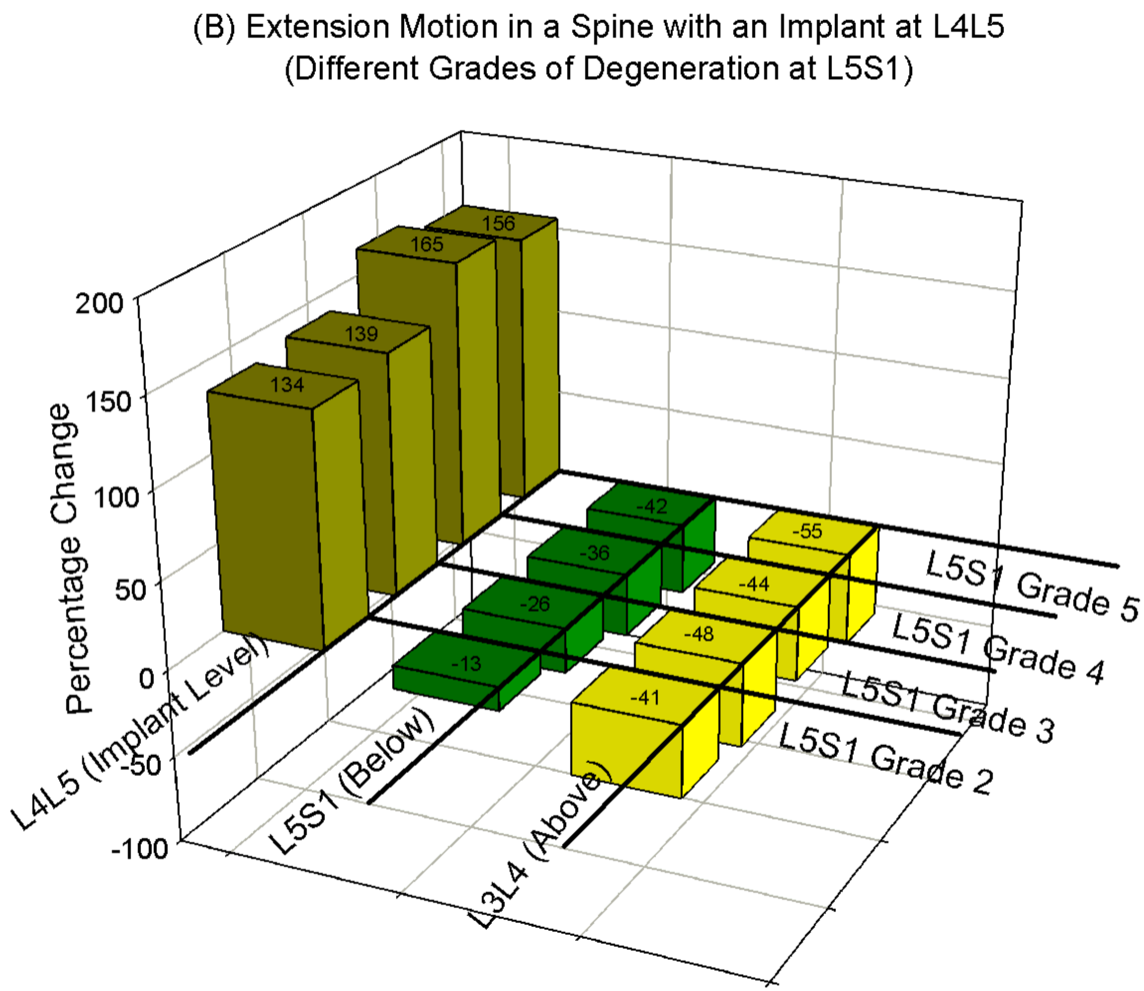

Figure 5-6 (B) shows rotation under extension moment in a spine with an implant at L4L5.

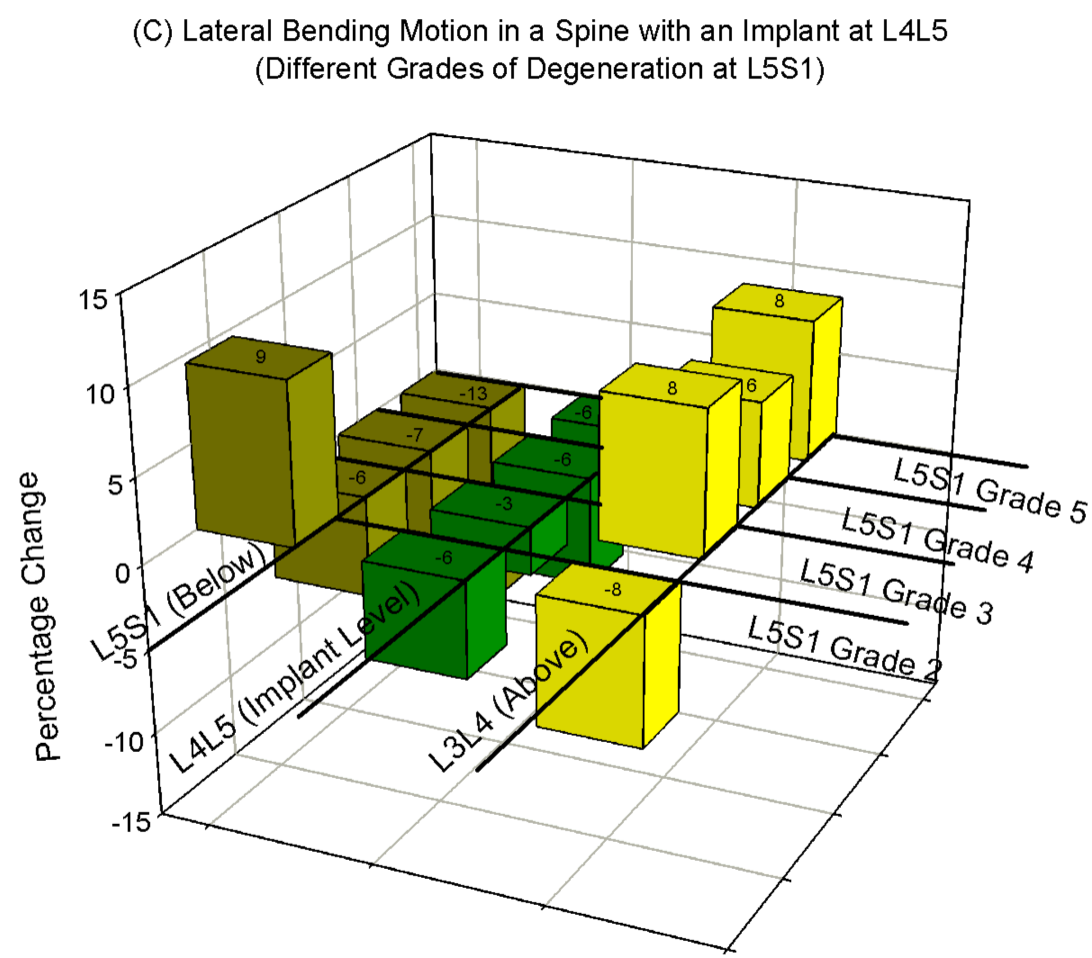

Figure 5-6 (C) shows rotation under lateral moment in a spine with an implant at L4L5.

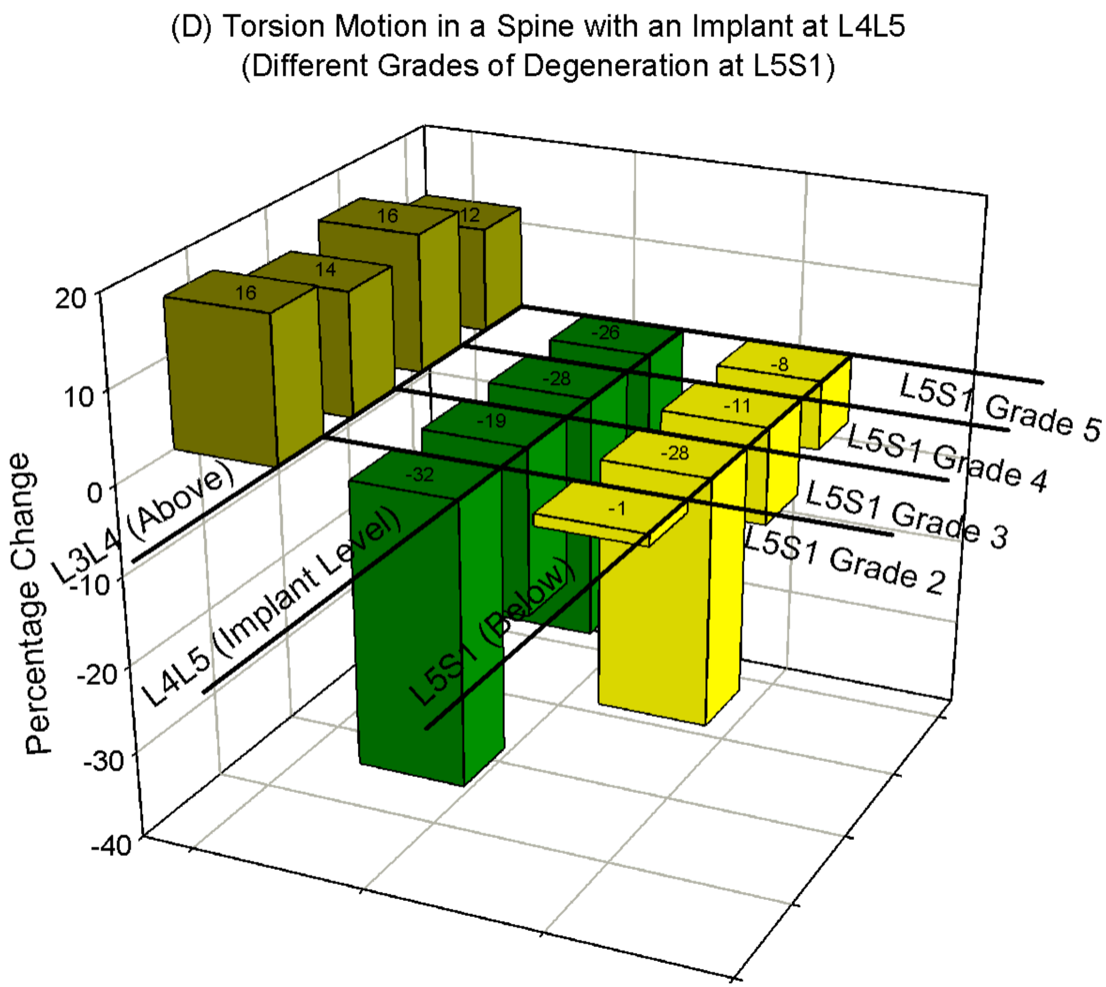

Figure 5-6 (D) shows rotation under flexion moment in a spine with an implant at L4L5

Figure 5-7 shows the same information as Figure 5-6 but in a level manner. Grade of degeneration represented in the x-axis, level of intervertebral disc was in the y-axis, and percentage change was along the z-axis. Figure 5-7 (A) presented rotations at L3L4. Under loading moment of flexion, rotation at L3L4 declined by approximately -17%, rotation under extension declined by approximately -47%. However, increased rotation in lateral bending and torsion at L3L4 was observed. Figure 5-7 (B) showed percentage change at L4L5 (implant level). An obvious increase in rotation was observed at the implant level in extension from 134% to 165%, in flexion from 42% to 61%. In contrast, this decrease was seen in lateral bending and torsion by 3% to 11% and 19% to 32%, respectively. Figure 5-7 (C) illustrates percentage change at L5S1 between the model with and without implant at L4L5 when there was degeneration at L5S1. Under all loading moments, L5S1 segment with the implant at L4L5 rotated less than the spine with a normal disc (grade II) at L4L5. The maximum change in rotation was under extension with grade V degeneration at L5S1 (-42%). This results were similar to (Knapik et al., 2012).

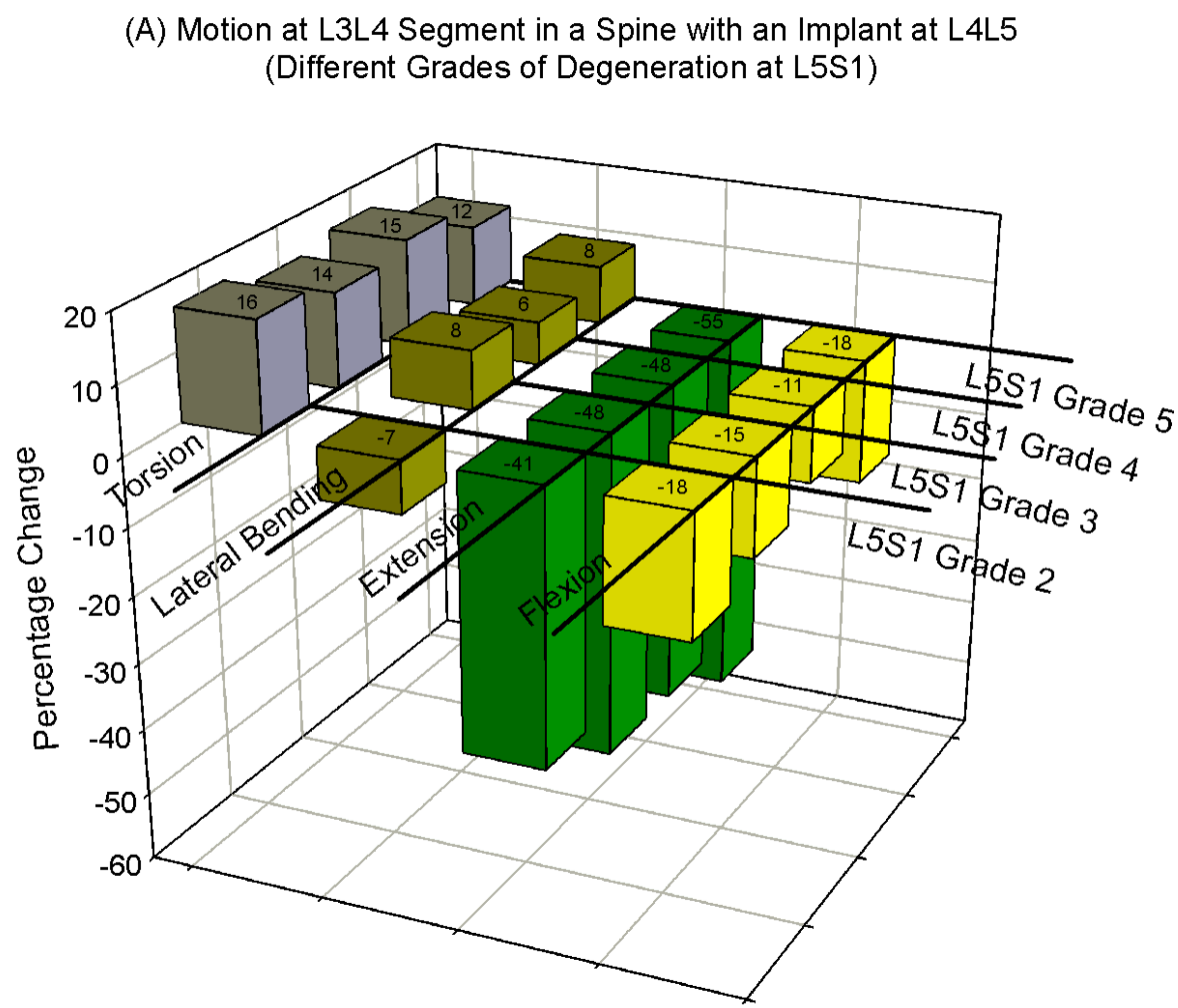

Figure 5-7 (A) shows rotation at L3L4 segment under flexion, extension, torsion and lateral bending in a spine with an implant at L4L5 and different grades of degeneration at L5S1.

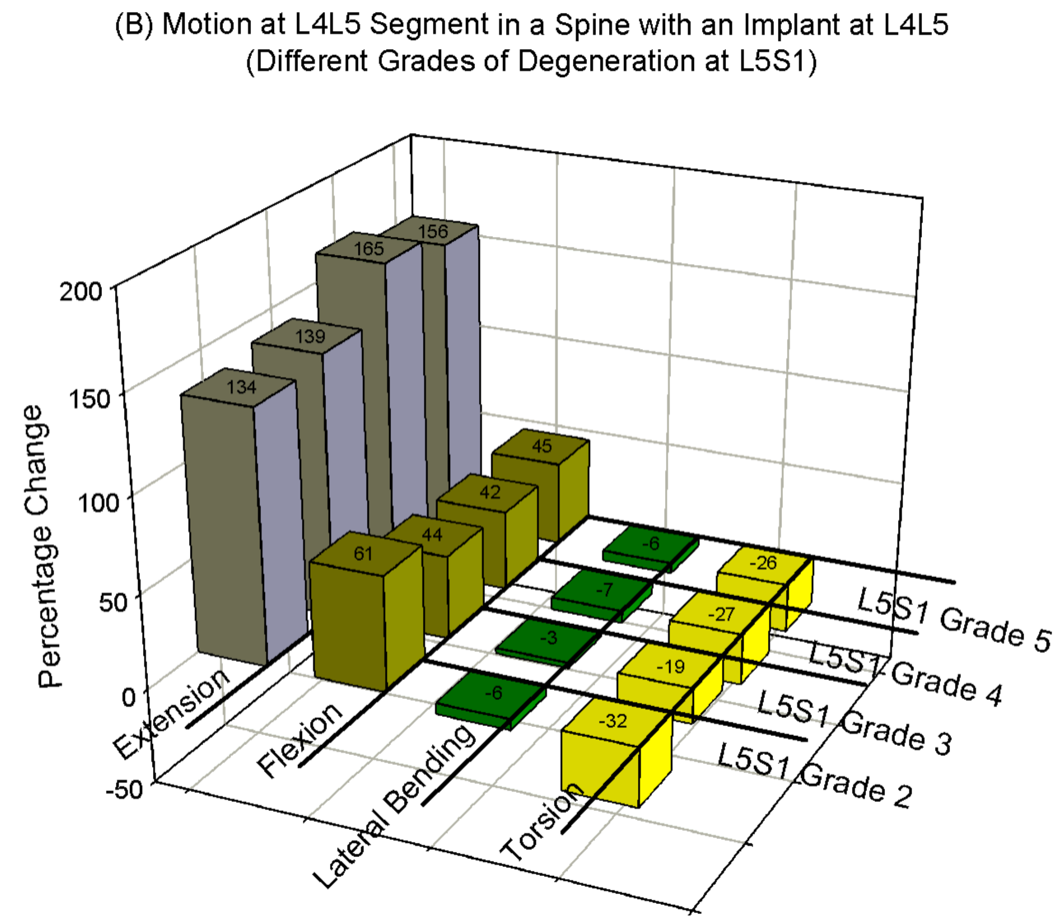

Figure 5-7 (B) shows rotation at L4L5 segment under flexion, extension, torsion and lateral bending in a spine with an implant at L4L5 and different grades of degeneration at L5S1.

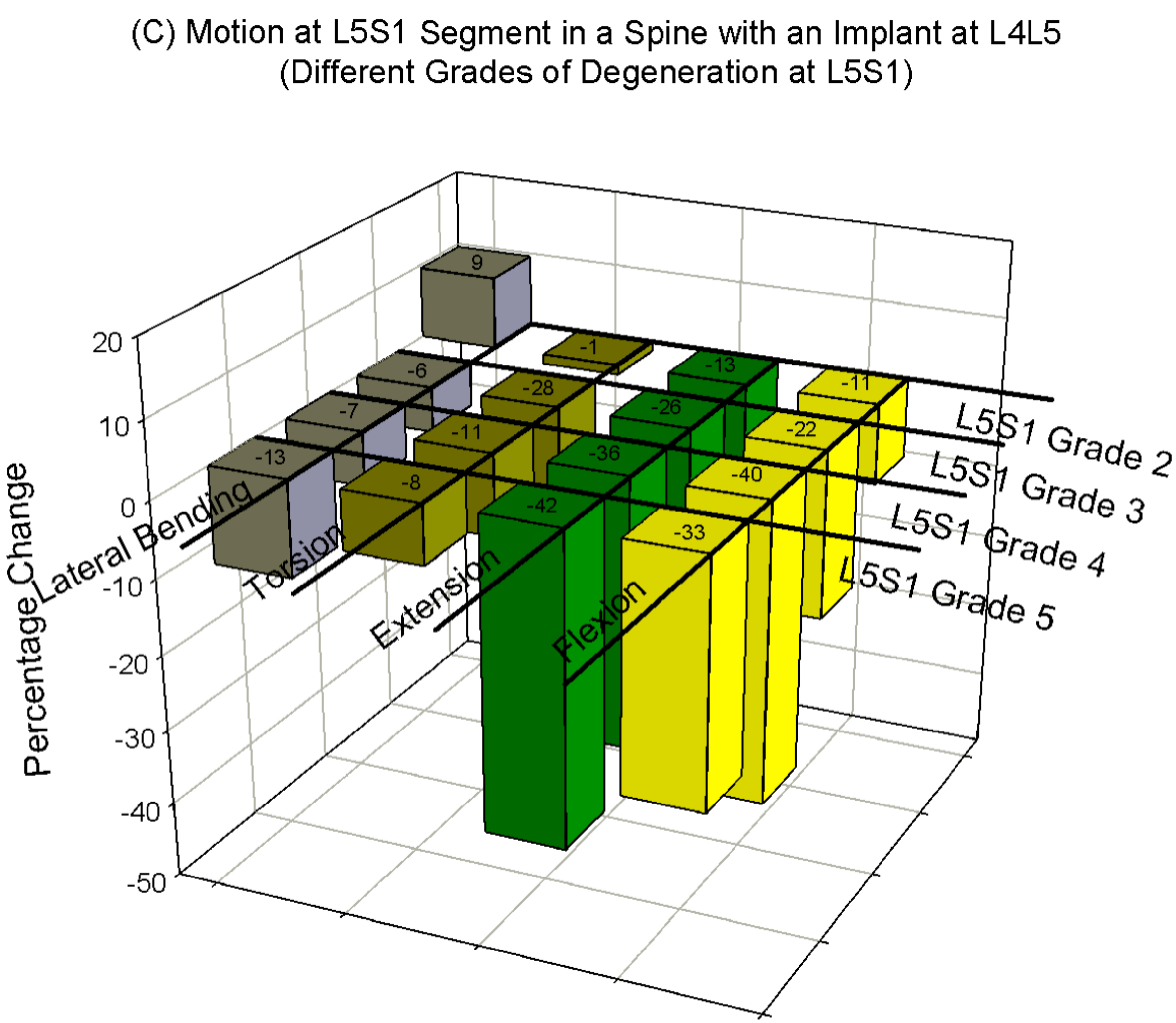

Figure 5-7 (C) shows rotation at L5S1 segment under flexion, extension, torsion and lateral bending in a spine with an implant at L4L5 and different grades of degeneration at L5S1.

Rotation of L1 to S1 spine with degeneration at L5S1 and disc arthroplasty at L4L5 was presented in Figure 5-8. This set of graphs show the effects of two factors: grade of degeneration and the implant. According to Figure 5-2, loss of motion was observed at the degenerated level (L5S1) and the adjacent level (L4L5) compensated for the loss in motion. With the implant at L4L5, the rotation at L5S1 reduced even further. For flexion and extension, the model with disc arthroplasty at L4L5 and degeneration at L5S1 showed significant increase in rotation at the implant level. The adjacent level's motion (L3L4) increased as grade increased from II- IV and became remained unchanged from IV-V. For lateral bending as presented in Figure 5-8 (C), the motion at L4L5 increased at grade III, and then dropped at grade IV and V at L5S1. Motion at L3L4, the adjacent level to the implant, increased gradually as the degeneration worsened. Under loading moment of torsion, rotation at the implant level increased and became steady at grade III, IV and V while the rotation at L5S1 decreased gradually and rotation at L3L4 increased. Rotation for both the implant levels and degenerated levels decreased. The segment that compensated for a loss in motion was torsion moment at L3L4.

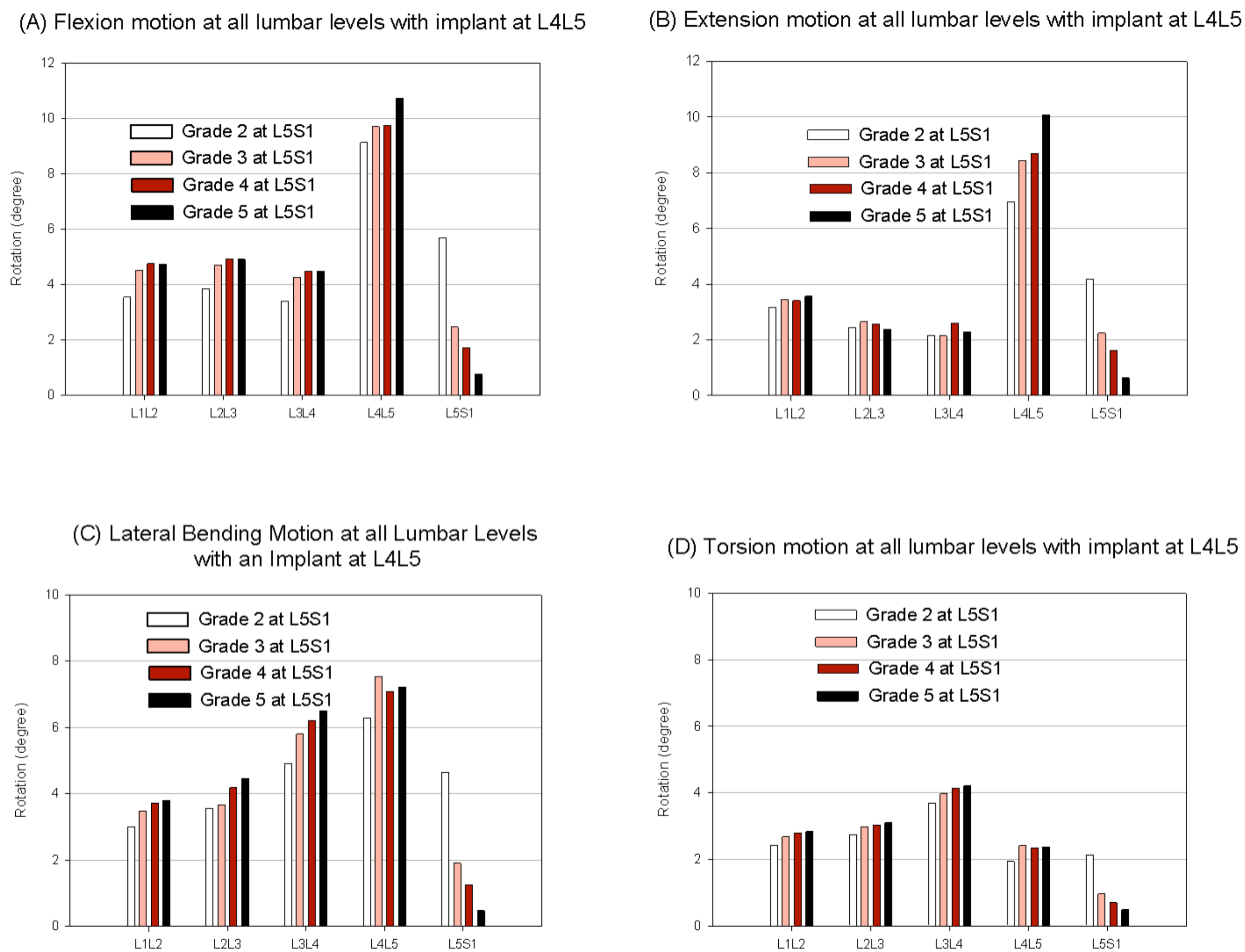

Figure 5-8 shows rotation under loading condition of (A) flexion, (B) extension, (C) lateral bending and (D) torsion in a spine with an implant at L4L5.

As said by the data from Figure 5-8, the numbers were computed and printed in 3D graph. Figure 5-9 presents percentage change of the implanted model with different levels of degeneration at L5S1. In other words, changes were observed in the implanted model as degeneration at L5S1 worsens. Figure 5-9 (A), (B), (C) and (D) show the change in flexion, extension, lateral bending and torsion, respectively. From the graph, x-axis is segmental level. Y-axis shows different grades of degeneration and z-axis expresses percentage change. As the degeneration of L5S1 on flexion and extension increases, the motion at the implant level increased and decreased the rotation at L5S1 lower than the model with degeneration alone. Loading condition of lateral bending and torsion expressed similar results; the motion at the implant level with increasing degeneration tended to be steady while the skipped level's motion increased gradually.

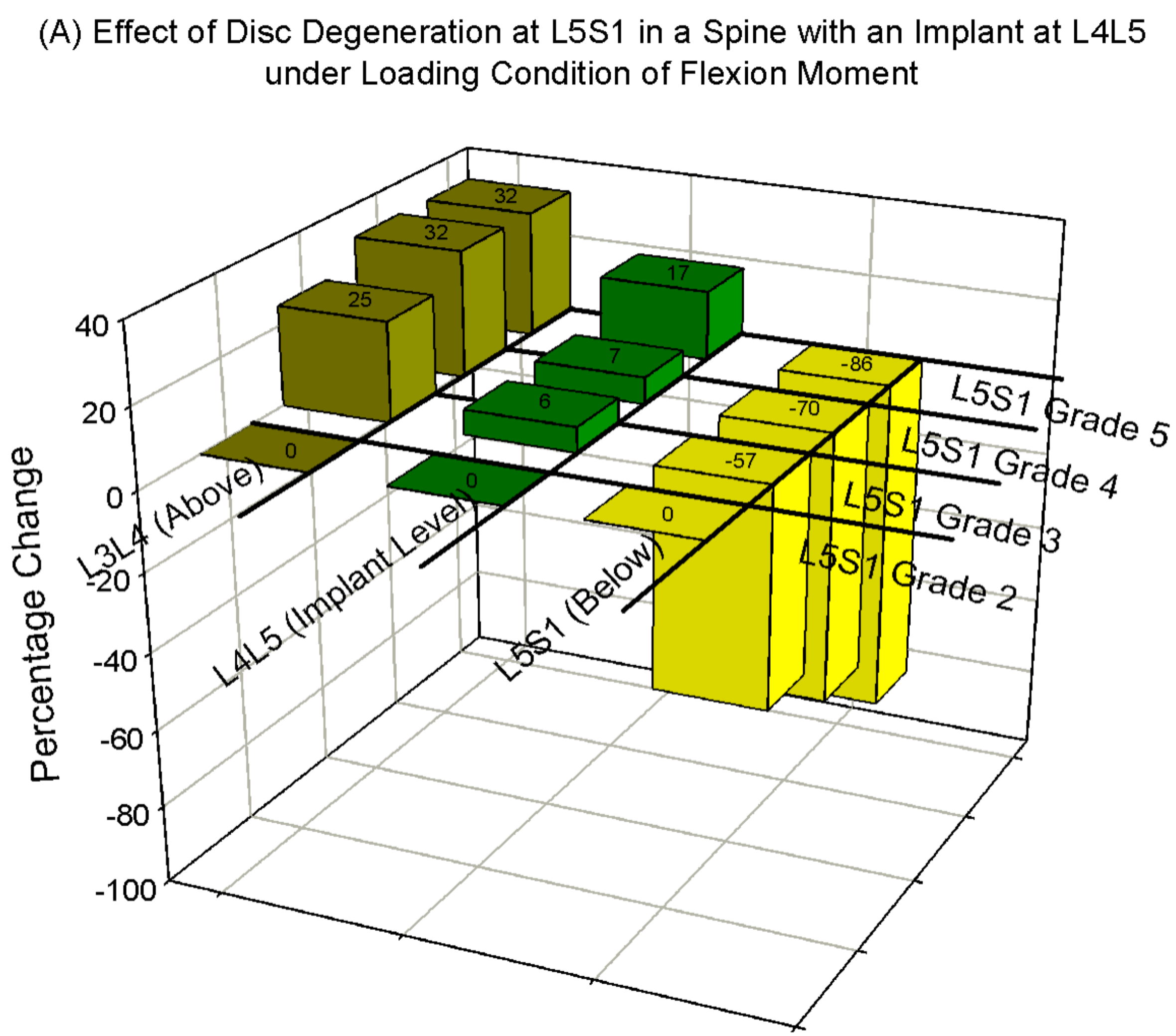

Figure 5-9 (A) shows effect of disc degeneration at L5S1 in a spine with an implant at L4L5 under loading condition of flexion moment.

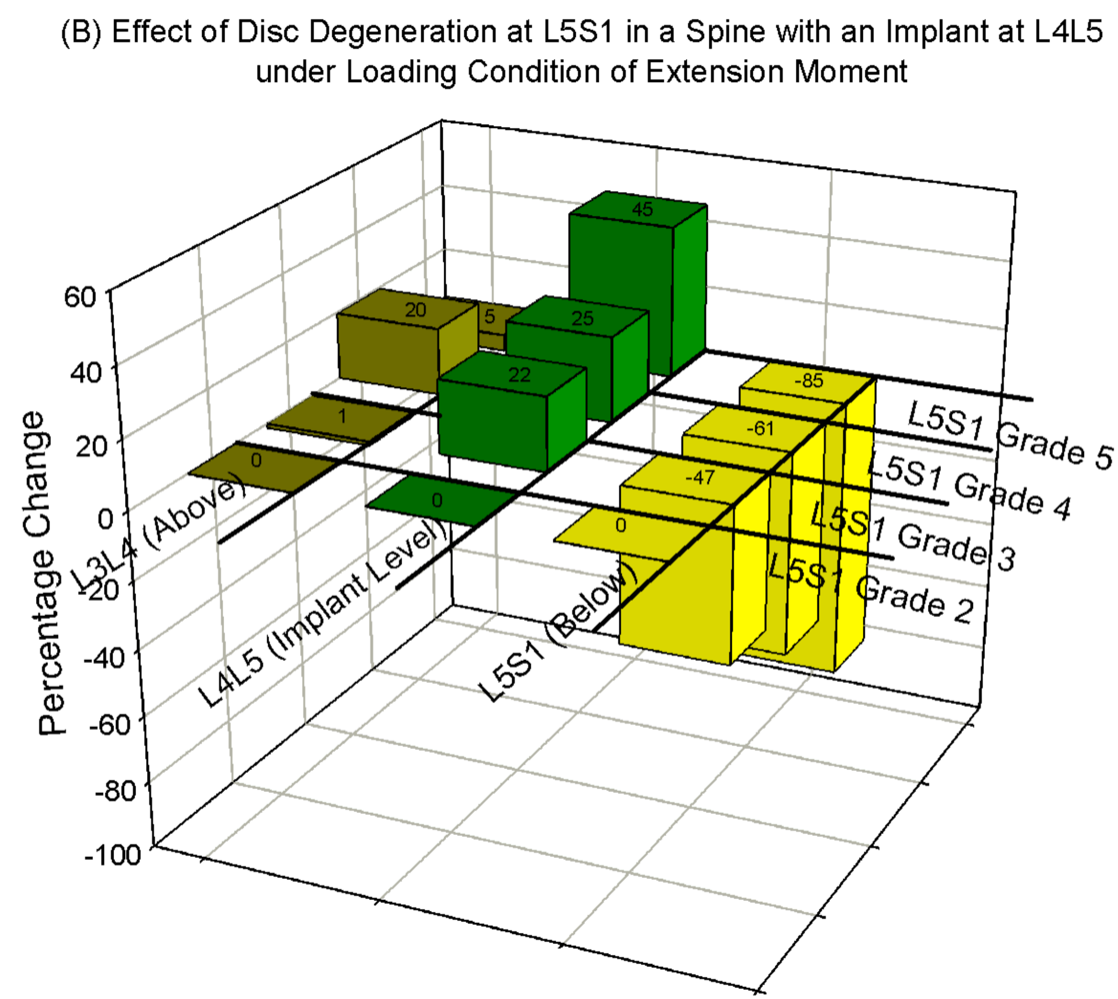

Figure 5-9 (B) shows effect of disc degeneration at L5S1 in a spine with an implant at L4L5 under loading condition of extension moment.

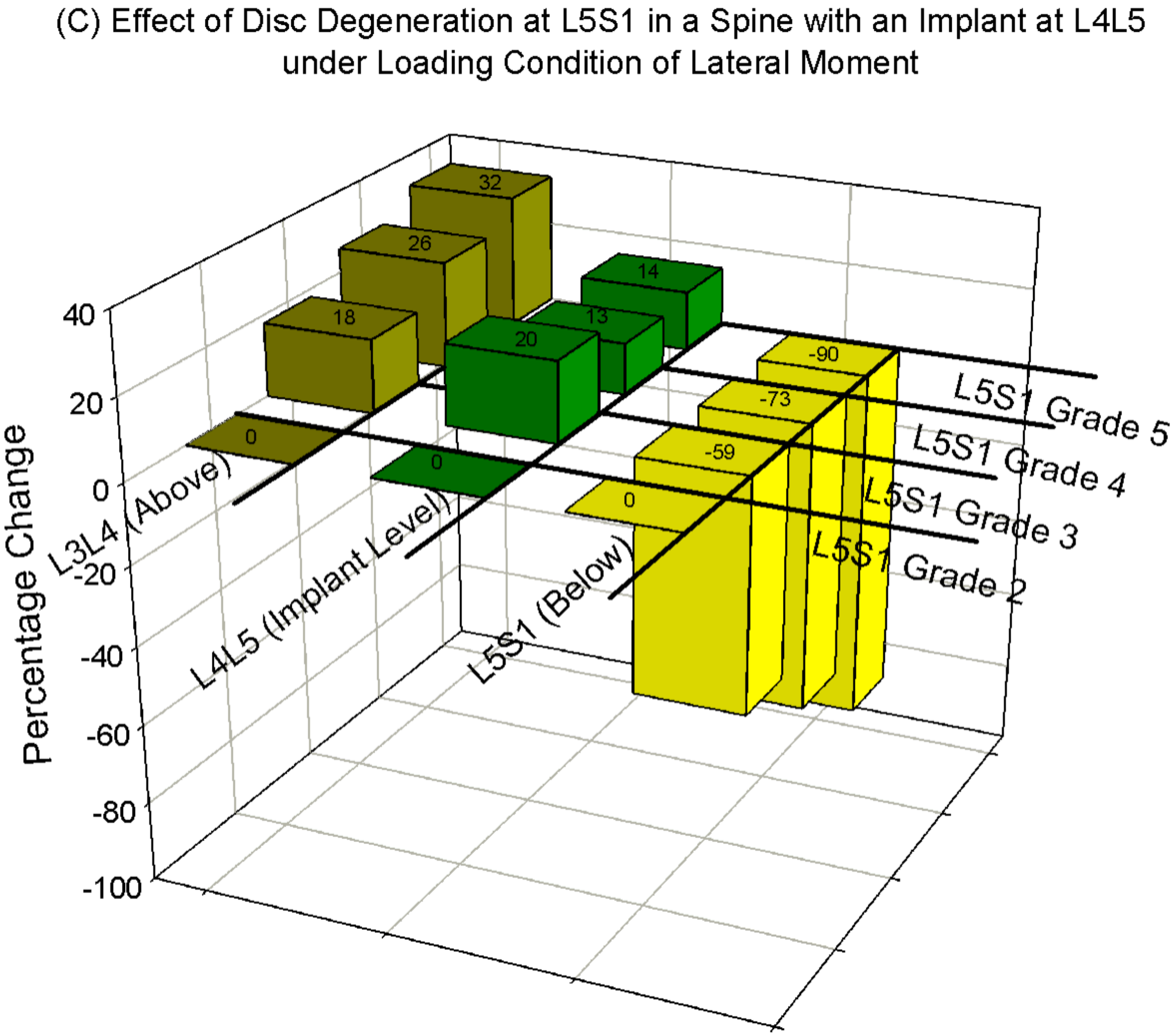

Figure 5-9 (C) shows effect of disc degeneration at L5S1 in a spine with an implant at L4L5 under loading condition of lateral moment.

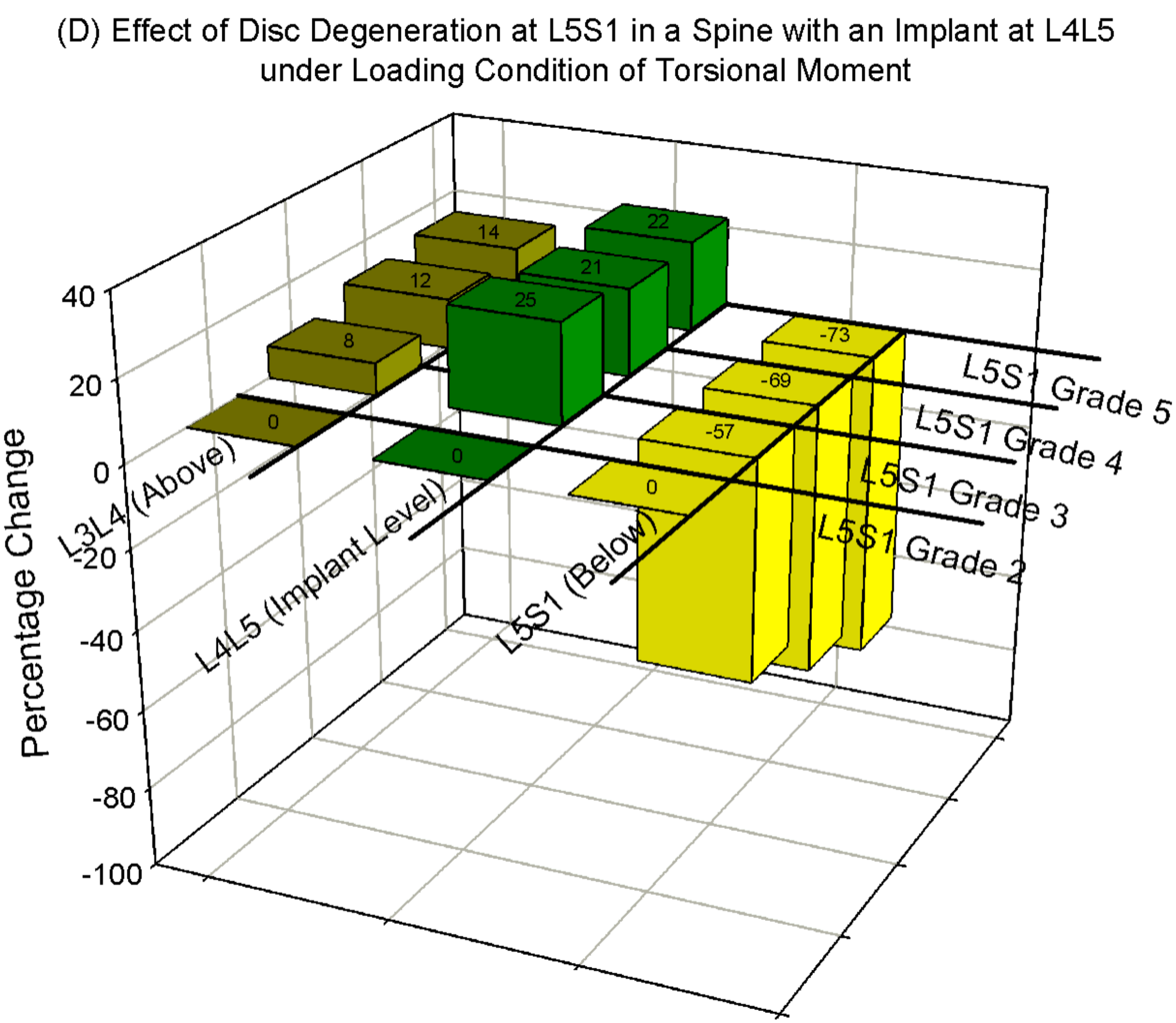

Figure 5-9 (D) shows effect of disc degeneration at L5S1 in a spine with an implant at L4L5 under loading condition of torsional moment.

4. Finite Element Modeling of L1 to S1 Spine and Fusion at L4L5 Level

Intervertebral disc at L4L5 was fused as a solid bone. The total rotation in each loading condition referred to the intact model; each model has the same amount of total rotation that the intact spine rotates from L1 to S1. Figure 5-10 demonstrates motion in all disc levels and all loading conditions. The rotations at L4L5 in all loading conditions plummeted and were close to zero. At the fused level (L4L5), the motion reduced by 86% on average. Consequently, the cephalic level (L3L4) to the fused level compensated for the loss in motion and the increase in rotation was observed by 24% on average. The increase presented again at the caudal level (L5S1), at 29%, on average. In other words, the rotation at the fused segment reduced while the rotation at the adjacent segments compensated for the lack of motion at the fused level. Therefore, the results have similar trends with (Luk et al., 1987; Strömqvist et al., 1997; Weinhoffer et al., 1995). Figure 5-11 shows the comparison between the fusion model and the intact model. Intact's motions are represented in blue bars and the implanted model' motions are shown in yellow bars. All the disc levels, in all loading condition, except the fused level increased in motion.

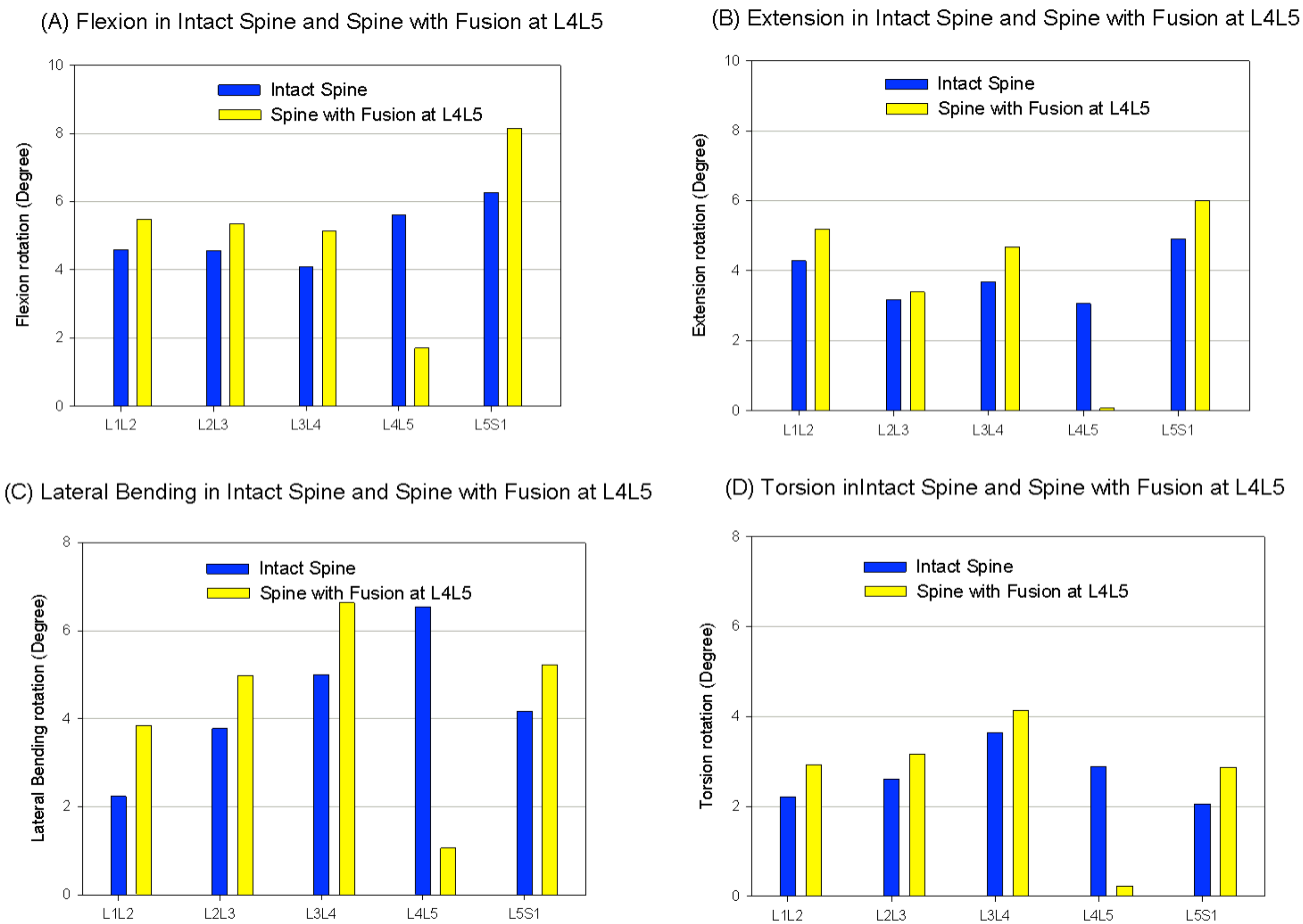

Figure 5-10 shows rotations under (A) flexion (B) extension (C) lateral bending (D) torsion in the intact spine and a spine with fusion at L4L5.

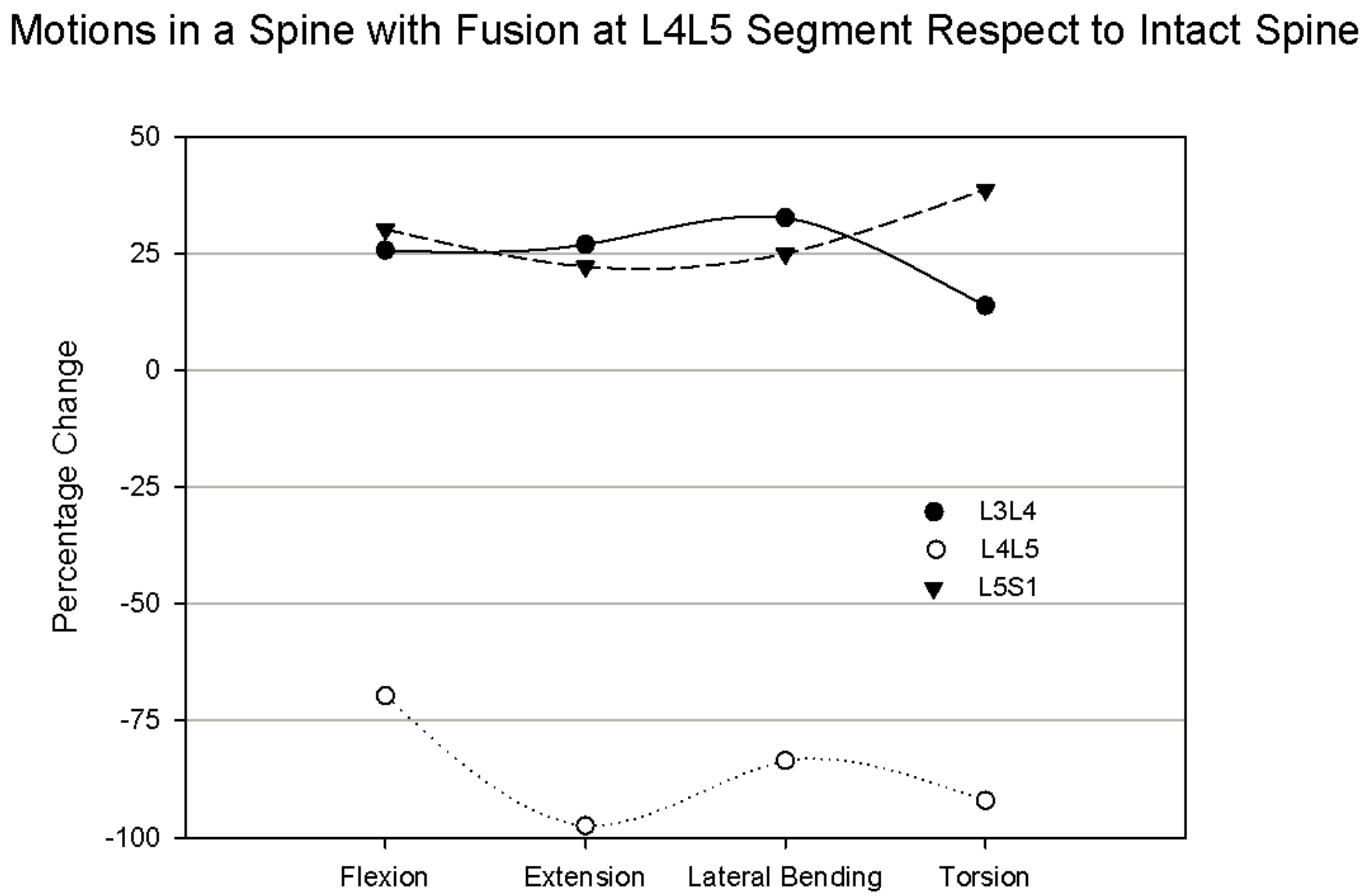

Figure 5-11 shows percentage change of motions in a spine with fusion at L4L5 segment respect to intact spine.

5. Facet Loads of the Adjacent Segments

Facet loads in the x, y, z components at the adjacent segments were calculated. Facet loads in the normal spine were compared with facet loads in the spine with a disc arthroplasty.

Figure 5-12 presents facet loads in the flexion loading condition. Figure 5-12 (A), (B) and (C) shows facet forces in a spine with a normal disc at L4L5, spine with an implant at L4L5. The graph also shows the change in facet forces between the two spine models with varying grades of degeneration at L5S1. There was no contact load at L3L4 or L4L5 in spine with a normal disc and the spine with the disc arthroplasty. Therefore, the facet forces and percentage change of the facet loads at L3L4 and L4L5 are zero (Figure 5-12(C)). However, at L5S1, a ball-and-socket implant showed a decrease in facet loads by -7% (grade II of degeneration). The trend increases from -7% to 19% as grades of degeneration increases.

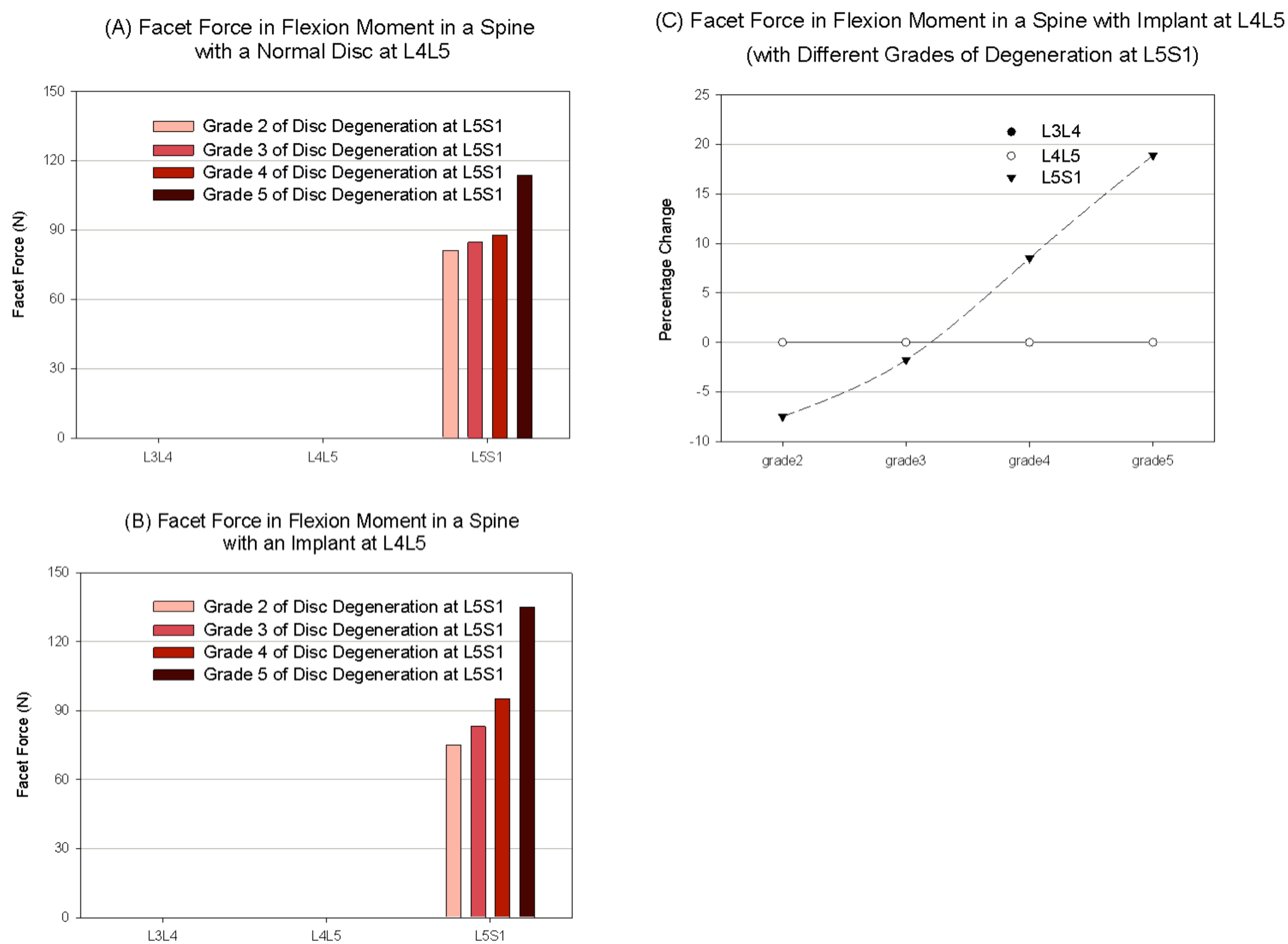

Figure 5-12 shows facet forces in flexion in a spine (A) with a normal disc at L4L5 (B) with implant at L4L5 (C) with an implant at L4L5.

Facet loads for the extension loading condition in a normal spine were observed as shown in Figure 5-13. Figure 5-13 (A), (B) and (C) show facet forces in a spine with normal disc at L4L5, implant at L4L5 and the percentage change of facet forces between the two models of spines with varying grades of degeneration at L5S1. In a spine with disc arthroplasty, facet forces decreased at the implant and adjacent levels when there was degeneration present at L5S1. In fact, the facet joints were not pressed against each other at the implant level, resulting in zero contact forces at the L4L5 segment. In other words, the percentage change of facet forces at L4L5 segment decreased by -100%. At L3L4 and L5S1, facet forces decreased by -2% and -16%, respectively. These results agree with past researchers (Goel et al., 2005).

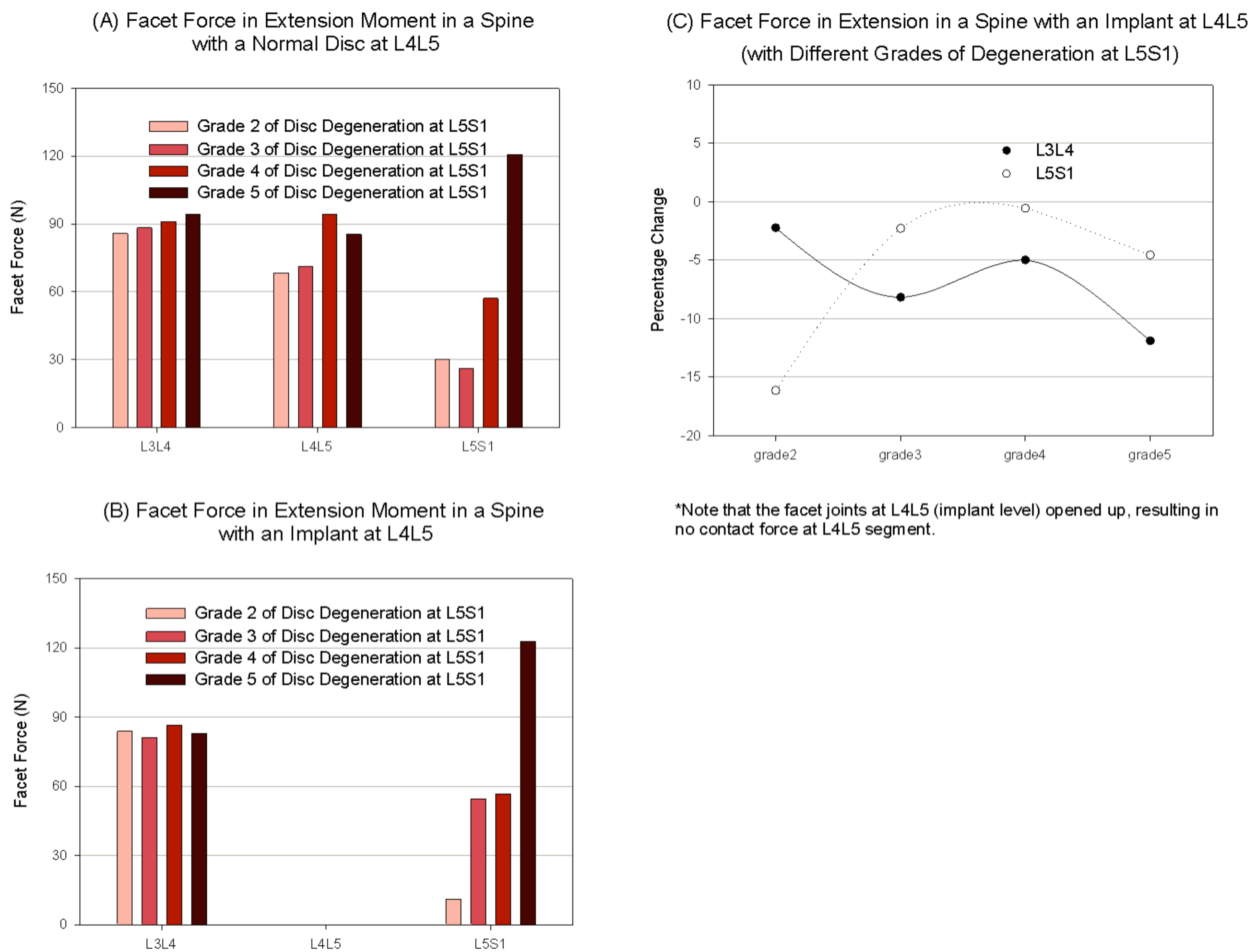

*Note that the facet joints at L4L5 (implant level) opened up, resulting in no contact force at L4L5 segment.

Figure 5-13 shows facet forces in extension in a spine (A) with a normal disc at L4L5 (B) with implant at L4L5 (C) with an implant at L4L5.

In the lumbar region, twisting motion is another movement that is restricted by the presence of facet joints. Figure 5-14(A), (B) and (C) show facet forces in a spine with normal disc at L4L5, implant at L4L5 and the percentage change of facet forces between the two models of spines with varying grades of degeneration at L5S1. In a spine with disc arthroplasty, there was a decrease in facet loads at L5S1 segment with respect to a normal spine (Figure 5-14). The trend increases as the grades of degeneration increases. At the implant and L3L4 segments, the facet loads slightly increased when the intervertebral disc was normal (grade II) at L5S1 and further increased as grades of degeneration increased. At L4L5 segment, the implant had a significant influence on the facet loads. Facet loads increased from 4% to 52% when there was degeneration at L5S1 (Figure 5-14 (C)).

During lateral bending, facet loads decreased when there was an implant at L4L5 with varying grades of degeneration at L5S1. The trends increased as grades of degeneration increased. Figure 5-15 (A), (B) and (C) show facet forces in a spine with normal disc at L4L5, implant at L4L5 and percentage change of facet forces between the two models of spines with varying grades of degeneration at L5S1. With an implant at L4L5 and grade II disc degeneration at L5S1, both adjacent and implant segments have decreased facet loads. Then, the trends increased grades of degeneration increased.

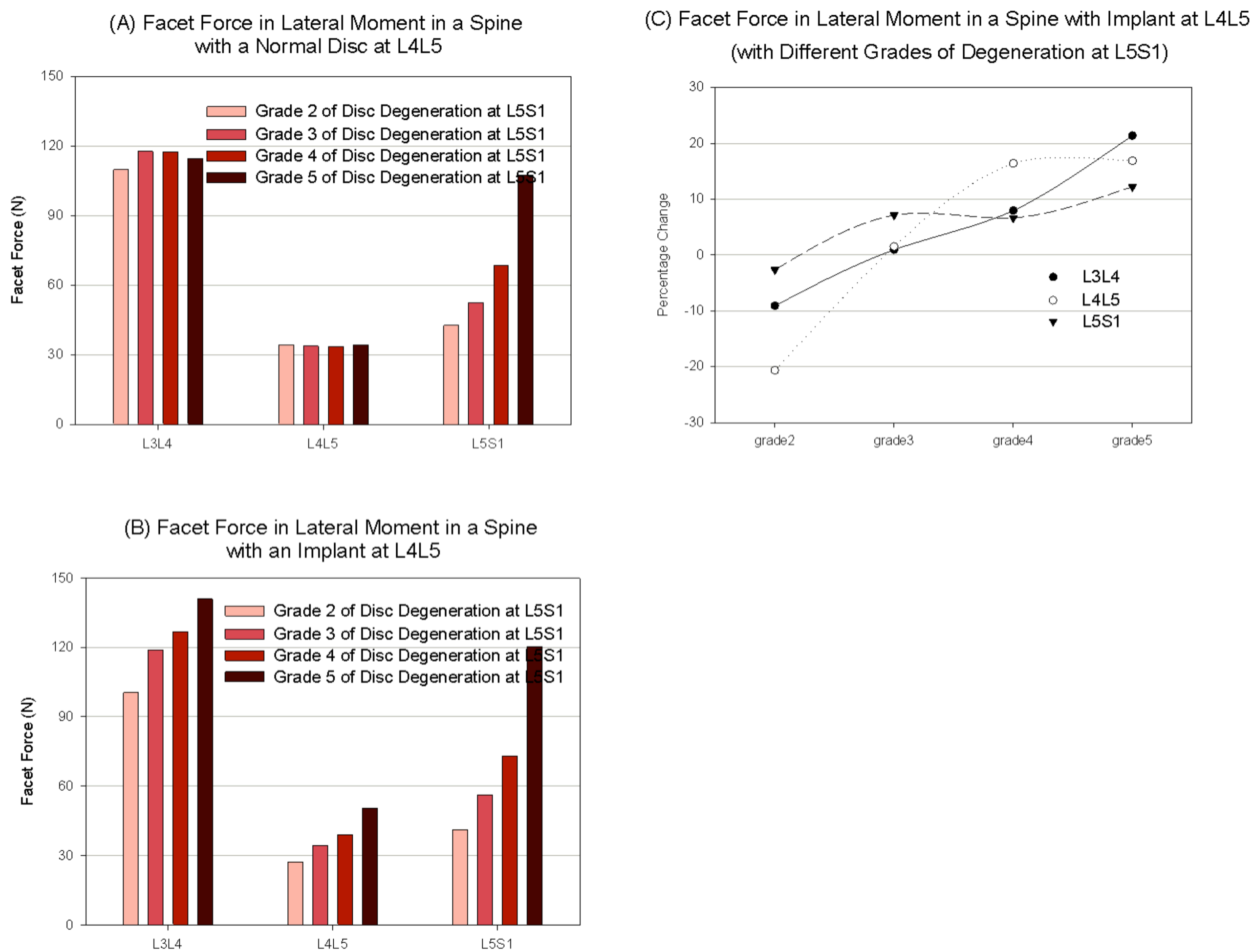

Figure 5-14 shows facet forces under lateral bending in a spine (A) with a normal disc at L4L5 (B) with implant at L4L5 (C) with an implant at L4L5.

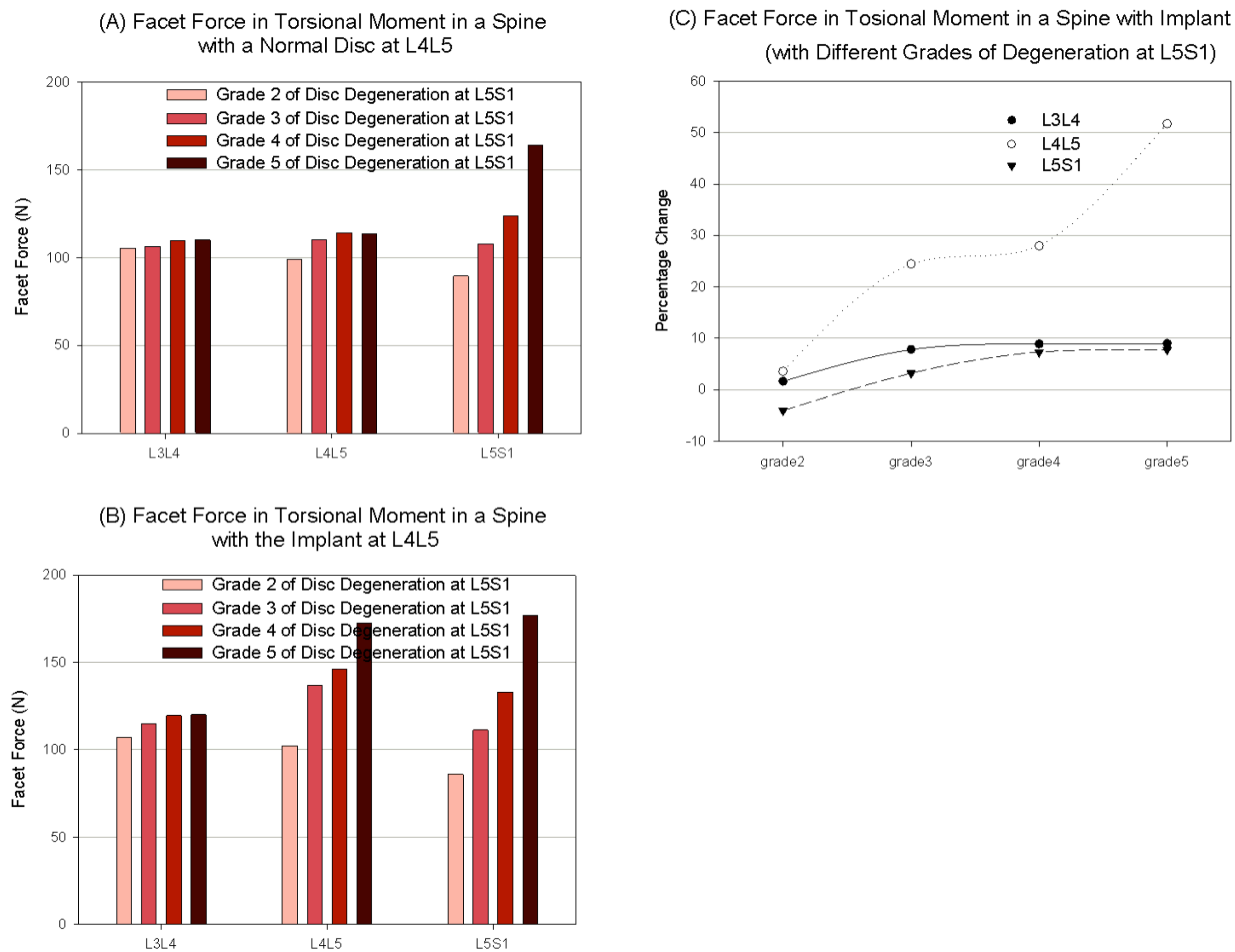

Figure 5-15 shows facet forces in torsional in a spine (A) with a normal disc at L4L5 (B) with implant at L4L5 (C) with an implant at L4L5.

6. Von Mises Stresses of the Adjacent Intervertebral Discs

Von Mises stresses on the annulus and nucleus at the adjacent segments were studied. Figure 5-16 shows a comparison of von Mises stresses of the annulus and nucleus at the adjacent segments, L3L4 and L5S1. Figure 5-16 (A), (B), (C) and (D) present the stresses in loading condition of flexion, extension, lateral bending and torsion, respectively. The curves in the graph illustrate stresses of the annulus at L3L4 and L5S1 and of the nucleus at L3L4 and L5S1 with varying grades of degeneration at L5S1. Von Mises stress decreased in flexion and extension with a total disc replacement at L4L5 with varying grades of degeneration at L5S1. In flexion, the von Mises stress at L3L4 disc decreased from -11% to -50% and at L5S1 disc they decreased from -2% to -18%. Under extension loading condition, von Mises stresses at L3L4 disc decreased from -24% to -36% and at L5S1 disc they decreased from -4% to -12%. In lateral bending and torsion rotations, von Mises stresses increased at the adjacent discs. Similar trends were observed under lateral and torsional moments. The von Mises stresses at adjacent discs increased from 4% to 23% and from 2% to 21% in lateral bending and torsion, respectively.

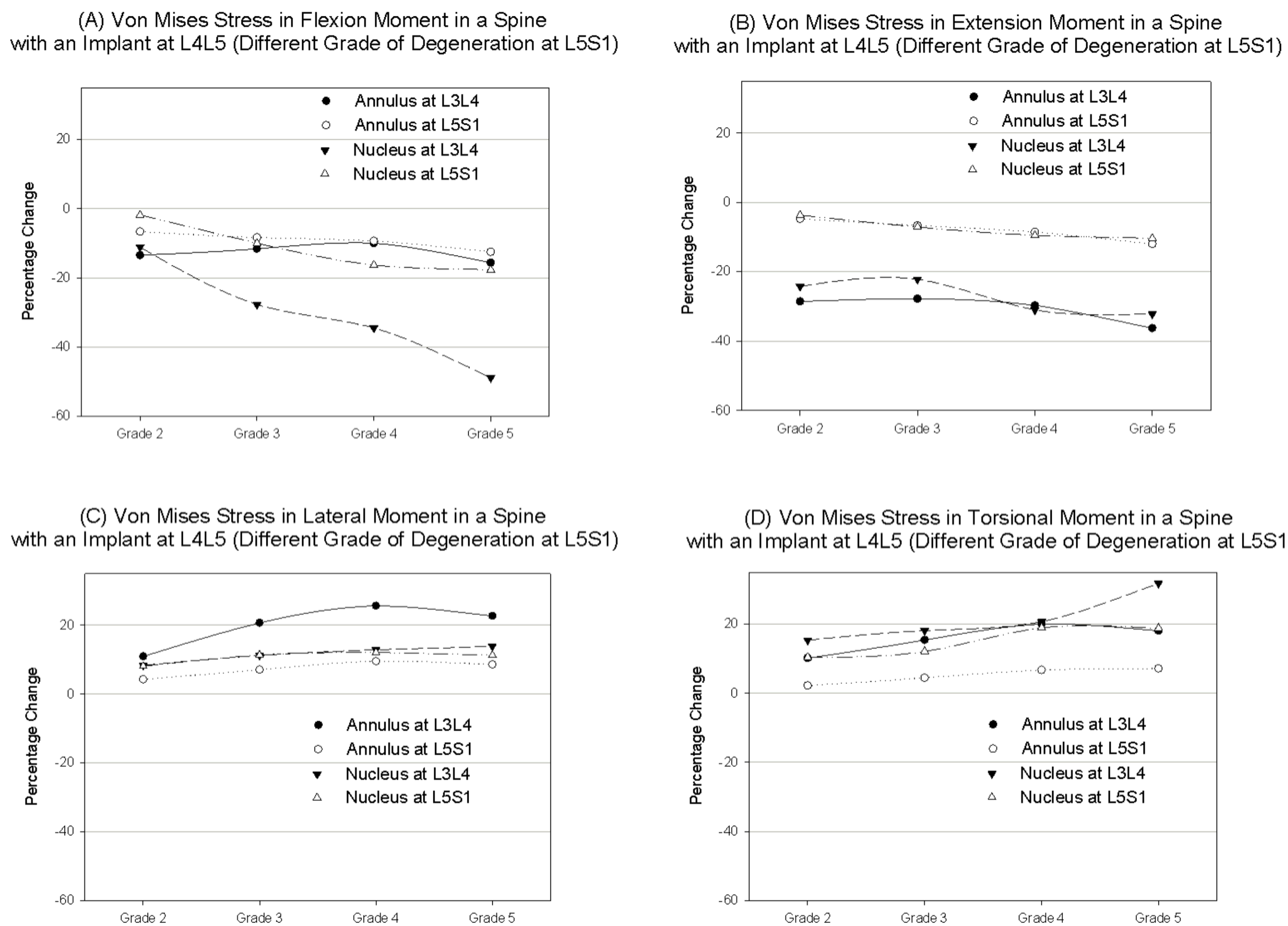

Figure 5-16 shows percentage change of Von Mises stresses at adjacent level under (A) flexion (B) extension (C) lateral bending (D) torsion.

6) Conclusion

A degenerated intervertebral disc in the human spine impacts resulting motions, facet forces, and disc stresses at the adjacent segments. The model represents a single-level disc degeneration in the lumbar region. In the lumbar spine model with disc degeneration at L5S1 segment, the motion at the adjacent segment (L4L5) increased in order to compensate for the loss in motion at the degenerated level. The maximum increase in motion was observed when L5S1 was at grade V disc degeneration while in extension. Moreover, the motion at the skipped segment (L3L4) was also impacted by the disc degeneration and it was observed that the maximum increase in motion was also seen when L5S1 was at grade V while in extension. Facet forces at the adjacent L4L5 segment increased under extension and torsional rotation as grades of degeneration also increased. With the effect of disc degeneration, von Mises stresses in the annulus and nucleus at the adjacent segment increased with the grade of degeneration in all six tested loading conditions. In contrast, the stress at the degenerated segment decreased in all six tested loading conditions. Based on the above results, degeneration at L5S1 may cause future degeneration at the adjacent segment.

One option of the surgical treatments for degenerated disc is spinal fusion. The FEM of spine with fusion presented a spinal fusion at L4L5 while other intervertebral discs were assumed to be normal (grade II). A spinal with fusion at L4L5 showed significant decrease in motion at the fused segment. Maximum decrease of motion was observed under extension moment while minimum decrease of motion was seen under flexion. Higher motions were observed at the adjacent segment. Facet forces as well as the von Mises stress at the adjacent segment increased respect to the intact spine.

Total disc replacement (TDR) is another option of the surgical treatment for degenerated disc. In the study, the model was designed to have TDR at L4L5 segment while the other intervertebral discs were normal (grade II). The method of implant insertion mimicked anterior approach, which included the removal of anterior longitudinal ligaments, nucleus as well as some part of annulus. The motion at the caudal adjacent segment decreased under all six tested loading moments. At the cephalic segment, the motion increased under lateral bending and torsion. Facet forces and von Mises stresses at the adjacent segments decreased respect to the intact spine.

Comparing fusion and TDR shows that TDR produces more favorable results on the adjacent segment. The resulting motion at the adjacent segments to the TDR segment decreased under flexion and extension. However, the motion at the segment adjacent to the fused level compensated the loss in motion under all six loading conditions. However, the motion at the TDR segment increased twice as much as without the TDR under extension moment. This may give us more reason to believe that TDR impacts the adjacent segments less and may be more beneficial in preventing future problems at the adjacent segments. Thus, to get a better understanding in long-term effects of the TDR, a model of lumbar spine with a single-level total disc replacement and a degenerated adjacent segment was studied.

In the lumbar spine with disc arthroplasty at L4L5 and disc degeneration at L5S1, the trends of the results could be separated into two groups. First group gave similar results, which were flexion and extension. The adjacent segment (L3L4) showed decrease in motion under flexion and extension. The maximum decrease in motion was observed under extension at grade V of degeneration. TDR in a spine with a single disc degeneration not only reduces motion at the adjacent segment under flexion and extension, but it also decreases the facet forces at the adjacent segment at grade II degeneration under the same loading conditions; however, these trends increase as the grades of degeneration increase. It also showed decreases of von Mises stresses at the adjacent intervertebral discs. As the grade of degeneration increases, the stresses at the adjacent segments further decreased respect to the spine with same grade of degeneration without the TDR. However, the lumbar spine with disc degeneration and TDR under lateral bending and torsional loading conditions, the stresses as well as the motion at the adjacent intervertebral discs increased and kept increasing with the increase of grades of degeneration. Facet forces under lateral bending and torsion decreased in grade II, but the trend increased as the grade of degeneration increased. The motion at the degenerated disc (L5S1) under all six loading conditions decreased and the maximum decrease was under extension moment. For the facet forces and von Mises stresses at the degeneration disc (L5S1), they have the same trends with the upper adjacent segment (L3L4).

In shorts, a single-level disc degeneration in lumbar region influences the increase in motion, facet forces and von Mises stresses at the adjacent segments. The results show similar trends to what spinal fusion does to its adjacent segments, which are going to potentially cause degeneration at its adjacent segments. In contrast, TDR reduces the motion, facet forces and von Mises stresses at the adjacent segments under flexion and extension, but increases the motion and von Mises stresses at the adjacent segments under lateral bending and torsion. The lumbar spine with both TDR and disc degeneration under all six tested loading conditions initially showed the same results as the spine with TDR alone. However, as the grade of degeneration increases, rotation, facet forces and von Mises stresses at the adjacent segments under flexion and extension decreased, but the rotation and von Mises stresses under lateral bending and torsion increased.

Reference

Blumenthal, S. L., Ohnmeiss, D. D., Guyer, R. D., & Hochschuler, S. H. (2003). Prospective study evaluating total disc replacement: preliminary results. *Journal of Spinal Disorders & Techniques*, *16*(5), 450–454.

Chazal, J., Tanguy, A., Bourges, M., Gaurel, G., Escande, G., Guillot, M., & Vanneuville, G. (1985). Biomechanical properties of spinal ligaments and a histological study of the supraspinal ligament in traction. *Journal of Biomechanics*, *18*(3), 167–176.

Chen, S.-H., Chen, C.-S., Chen, W.-J., & Zhong, Z.-C. (2009). Biomechanical comparison between lumbar disc arthroplasty and fusion. *Medical Engineering and Physics*, *31*(2), 244–253. http://doi.org/10.1016/j.medengphy.2008.07.007

Cunningham, B. W., McAfee, P. C., Geisler, F. H., Holsapple, G., Adams, K., Blumenthal, S. L., … Tortolani, P. J. (2008). Distribution of in vivo and in vitro range of motion following 1-level arthroplasty with the CHARITÉ artificial disc compared with fusion. *Journal of Neurosurgery: Spine*, *8*(1), 7–12. http://doi.org/10.3171/SPI-08/01/007

Delamarter, R. B., Fribourg, D. M., Kanim, L. E. A., & Bae, H. (2003). ProDisc artificial total lumbar disc replacement: introduction and early results from the United States clinical trial. *Spine*, *28*(20), S167–175. http://doi.org/10.1097/01.BRS.0000092220.66650.2B

Denozière, G., & Ku, D. N. (2006). Biomechanical comparison between fusion of two vertebrae and implantation of an artificial intervertebral disc. *Journal of*

Biomechanics, *39*(4), 766–775. http://doi.org/10.1016/j.jbiomech.2004.07.039

Dooris, A. P., Goel, V. K., Grosland, N. M., & Gilbertson, L. G. (2001). Load-sharing between anterior and posterior elements in a lumbar motion segment implanted with an artificial disc. *Spine*, *26*(6), E122.

Fogelholm, R. R., & (deceased), A. V. A. (2001). Smoking and intervertebral disc degeneration. *Medical Hypotheses*, *56*(4), 537–539. http://doi.org/10.1054/mehy.2000.1253

France, J. C., Yaszemski, M. J., Lauerman, W. C., & Cain, J. E. (1999). A randomized prospective study of posterolateral lumbar fusion. Outcomes with and without pedicle screw instrumentation. *Spine*, *24*(6), 553.

Freemont, A. J., Watkins, A., Le Maitre, C., & Jeziorska, M. (2002). Current understanding of cellular and molecular events in intervertebral disc degeneration: implications for therapy. *The Journal of Pathology*, *196*(4), 374–379. http://doi.org/10.1002/path.1050

Ghosh, P. (Ed.). (1988). *The Biology of the intervertebral disc* (Vol. 1). Boca Raton, FL: CRC Press.

Goel, V. K., Grauer, J. N., Patel, T. C., & Biyani, A. (2005). Effects of charité artificial disc on the implanted and adjacent spinal segments mechanics using a hybrid testing protocol. *Spine*, *30*(24), 2755.

Grauer, J. N., Biyani, A., Faizan, A., & Kiapour, A. (2006). Biomechanics of two-level Charité artificial disc placement in comparison to fusion plus single-level disc placement combination. *The Spine Journal*, *6*(6), 659–666. http://doi.org/10.1016/j.spinee.2006.03.011

Ha, K. Y., Schendel, M. J., Lewis, J. L., & Ogilvie, J. W. (1993). Effect of immobilization and configuration on lumbar adjacent-segment biomechanics. *Journal of Spinal Disorders*, *6*(2), 99.

Hamill, J., & Knutzen, K. (2009). *Biomechanical basis of human movement*. Wolters Kluwer Health/Lippincott Williams and Wilkins.

Ha, S.-K., Kim, S.-H., Kim, D. H., & Park, J.-Y. (2009). Biomechanical Study of Lumbar Spinal Arthroplasty with a Semi-Constrained Artificial Disc (Activ L) in the Human Cadaveric Spine. *Journal of Korean Neurosurgical Society*, *45*(3), 169. http://doi.org/10.3340/jkns.2009.45.3.169

Hilibrand, A. S., & Robbins, M. (2004). Adjacent segment degeneration and adjacent segment disease: the consequences of spinal fusion? *The Spine Journal*, *4*(6), S190–S194. http://doi.org/10.1016/j.spinee.2004.07.007

Hitchon, P. W., Eichholz, K., Barry, C., & Rubenbauer, P. (2005). Biomechanical studies of an artificial disc implant in the human cadaveric spine. *Journal of Neurosurgery: Spine*, *2*(3), 339–343. http://doi.org/10.3171/spi.2005.2.3.0339

Knapik, G. G., Mendel, E., & Marras, W. S. (2012). Use of a personalized hybrid biomechanical model to assess change in lumbar spine function with a TDR compared to an intact spine. *European Spine Journal*, *21*(S5), 641–652. http://doi.org/10.1007/s00586-011-1743-4

Lee, C. K. (1988). Accelerated degeneration of the segment adjacent to a lumbar fusion. *Spine*, *13*(3), 375.

Lee, C., & Langrana, N. (1984). Lumbosacral spinal fusion: a biomechanical study. *Spine*, *9*(6), 574–581.

Lehmann, T., Spratt, K., & Tozzi, J. (1987). Long-term follow-up of lower lumbar fusion patients. *Spine*, *12*(2), 97–104.

Lemaire, J. P., Skalli, W., Lavaste, F., Templier, A., Mendes, F., Diop, A., … Laloux, E. (1997). Intervertebral disc prosthesis. Results and prospects for the year 2000. *Clinical Orthopaedics and Related Research*, (337), 64–76.

Li, H., & Wang, Z. (2006). Intervertebral disc biomechanical analysis using the finite element modeling based on medical images. *Computerized Medical Imaging and Graphics*, *30*(6), 363–370. http://doi.org/10.1016/j.compmedimag.2006.09.004

Luk, K., Lee, F., & Leong, J. (1987). The effect on the lumbosacral spine of long spinal fusion for idiopathic scoliosis: a minimum 10-year follow-up. *Spine*, *12*, 996–1000.

Moore, K. L. (2011). *Essential clinical anatomy*.

Moumene, M., & Geisler, F. H. (2007). Comparison of biomechanical function at ideal and varied surgical placement for two lumbar artificial disc implant designs: mobile-core versus fixed-core. *Spine*, *32*(17), 1840.

Naidich, T. P. (2011). *Imaging of the spine*. Saunders/Elsevier.

Natarajan, R. N., Williams, J. R., & Andersson, G. B. J. (2004). Recent advances in analytical modeling of lumbar disc degeneration. *Spine*, *29*(23), 2733–2741.

Natarajan, R. N., Williams, J. R., & Andersson, G. B. J. (2006). Modeling Changes in Intervertebral Disc Mechanics with Degeneration. *Journal of Bone and Joint Surgery*, *88*(Supplement 2), 36.

Noailly, J., Lacroix, D., & Planell, J. A. (2005). Finite Element Study of a Novel Intervertebral Disc Substitute. *Spine*, *30*(20), 2257–2264. http://doi.org/10.1097/01.brs.0000182319.81795.72

Oda, H., Matsuzaki, H., Tokuhashi, Y., & Wakabayashi, K. (2004). Degeneration of intervertebral discs due to smoking: experimental assessment in a rat-smoking model. *Journal of Orthopaedic Science : Official Journal of the Japanese Orthopaedic Association*, *9*(2), 135.

Panjabi, M., Henderson, G., Abjornson, C., & Yue, J. (2007). Multidirectional testing of one- and two-level ProDisc-L versus simulated fusions. *Spine*, *32*(12), 1311.

Panjabi, M. M. (2007). Hybrid multidirectional test method to evaluate spinal adjacent-level effects. *Clinical Biomechanics*, *22*(3), 257–265. http://doi.org/10.1016/j.clinbiomech.2006.08.006

Park, P., Garton, H. J., Gala, V. C., & Hoff, J. T. (2004). Adjacent Segment Disease after Lumbar or Lumbosacral Fusion: Review of the Literature. *Spine*, *29*(17), 1938–1944. http://doi.org/10.1097/01.brs.0000137069.88904.03

Pellise Ferran, F., Hernandez, A., Vidal, X., & Minguell, J. (2007). Radiologic Assessment of All Unfused Lumbar Segments 7.5 Years After Instrumented Posterior Spinal Fusion. *Spine*, *32*(5), 574–579. http://doi.org/10.1097/01.brs.0000256875.17765.e6

Per, E., Hans, M., Adel, S., Yiang Xiao, Y., & Rune, H. (2009). A prospective randomised study on the long-term effect of lumbar fusion on adjacent disc degeneration. *Eur Spine J*, *18*, 1175–1186.

Putzier, M., Funk, J. F., Schneider, S. V., Gross, C., Tohtz, S. W., Khodadadyan-Klostermann, C., … Kandziora, F. (2006). Charité total disc replacement--clinical and radiographical results after an average follow-up of 17 years. *European Spine Journal: Official Publication of the European Spine Society, the European Spinal Deformity Society, and the European Section of the Cervical Spine Research Society*, *15*(2), 183–195. http://doi.org/10.1007/s00586-005-1022-3

Rohlmann, A., Zander, T., & Bergmann, G. (2005). Effect of Total Disc Replacement with ProDisc on Intersegmental Rotation of the Lumbar Spine. *Spine*, *30*(7), 738–743. http://doi.org/10.1097/01.brs.0000157413.72276.c4

Ross, R., Mirza, A. H., Norris, H. E., & Khatri, M. (2007). Survival and clinical outcome of SB Charite III disc replacement for back pain. *The Journal of Bone and Joint Surgery. British Volume*, *89*(6), 785–789. http://doi.org/10.1302/0301-620X.89B6.18806

Shim, C. S., Lee, S.-H., Shin, H.-D., & Kang, H. S. (2007). CHARITE versus ProDisc: a comparative study of a minimum 3-year follow-up. *Spine*, *32*(9), 1012.

Shirazi-Adl, A., & M, P. (2000). Load-bearing and stress analysis of the human spine under a novel wrapping compression loading. *Clinical Biomechanics*, *15*(10), 718–725. http://doi.org/10.1016/S0268-0033(00)00045-0

Shono, Y., Kaneda, K., Abumi, K., & McAfee, P. C. (1998). Stability of Posterior Spinal Instrumentation and Its Effects on Adjacent Motion Segments in the Lumbosacral Spine. *Spine*, *23*(14), 1550–1558. http://doi.org/10.1097/00007632-199807150-00009

Strömqvist, B., Johnsson, R., & Axelsson, P. (1997). The spondylolytic vertebra and its adjacent segment. Mobility measured before and after posterolateral fusion. *Spine*, *22*(4), 414.

Tropiano, P., Huang, R. C., Girardi, F. P., Cammisa, F. P., & Marnay, T. (2006). Lumbar Total Disc Replacement. *The Journal of Bone & Joint Surgery*, *88*(1 suppl 1), 50–64. http://doi.org/10.2106/JBJS.E.01066

Wang, W., Zhang, H., Sadeghipour, K., & Baran, G. (2013). Effect of posterolateral disc replacement on kinematics and stress distribution in the lumbar spine: A finite element study. *Medical Engineering & Physics*, *35*(3), 357–364. http://doi.org/10.1016/j.medengphy.2012.05.013

Weinhoffer, S., Guyer, R., & Herbert, M. (1995). Intradiscal pressure measurements above an instrumented fusion. *Spine*, *20*(5), 526–531.

VITA

NAME:	Sithichai Chaichanavitchakij
EDUCATION:	B.S., Nano-Engineering, Chulalongkorn University, Bangkok, Thailand, 2011
	M.S., Bioengineering, University of Illinois at Chicago, Chicago, Illinois, 2015
HONORS:	Board of Trustees Tuition and Service Fee waiver, University of Illinois at Chicago, Spring 2014
	Teaching Assistant, Department of Physical Therapy, University of Illinois at Chicago, Fall 2015